Glucocorticoids recruit Tgfbr3 and Smad1 to shift transforming growth factor-β signaling from the Tgfbr1/Smad2/3 axis to the Acvrl1/Smad1 axis in lung fibroblasts

Inauguraldissertation
zur Erlangung des Grades eines
Doktors der Medizin des
Fachbereichs Medizin der

Justus-Liebig-Universität Gießen

vorgelegt von

Schwartze, Julian Tristan
aus Langen (Hessen), Deutschland

Gießen (2014)

Aus dem Department of Lung Development and Remodelling, Max Planck Institute for Heart and Lung Research, Bad Nauheim, Germany; Department of Internal Medicine (Pulmonology), University of Giessen and Marburg Lung Center, German Center for Lung Research, Giessen, Germany.

Leiter/Direktor: Prof. Dr. med. Werner Seeger

Gutachter: Prof. Dr. med. Werner Seeger

Gutachter: Prof. Dr. Klaus T. Preissner

Tag der Disputation: 31.07.2015

I. Table of contents

II. List of figures

III. List of tables

IV. List of abbreviations

ACTH	adrenocorticotropic hormone
ACTA2	α-smooth muscle actin (protein, human)
ALK1/Acvrl1	activin receptor-like kinase 1
ALK5/Tgfbr1	activin receptor-like kinase 5, transforming growth factor-β receptor 1
ALL	acute lymphoblastic leukemia
APS	ammonium persulfate
ARDS	acute respiratory distress syndrome
BALF	bronchoalveolar lavage fluid
BMP	bone morphogenetic protein
BPD	bronchopulmonary dysplasia
bud	budesonide
CCN2 (gene)	encodes connective tissue growth factor (CTGF)
CBP	cAMP-response-element-binding-protein
CLD	chronic lung disease
CRF	corticotropin-releasing factor
CRH	corticotropin-releasing hormone
COL1A1 (gene)	pro-collagen 1
COL3A1 (gene)	pro-collagen 3
COPD	chronic obstructive pulmonary disease
dex	dexamethasone
DLR	dual luciferase ratio
D-MEM	Dulbecco's modified Eagle's medium
DMSO	dimethyl sulfoxide
DNA	deoxyribonucleic acid
DTT	dithiothreitol
ECM	extracellular matrix
ECMO	extracorporeal membrane oxygenation
EDTA	ethylendinitrilo-N, N, *N*, *N*′-tetra-acetic-acid
ENG	endoglin
EGTA	ethylene glycol-bis (2-amino-ethylether)-N, N, *N*′, *N*′-tetraacetic-acid
FCS	fetal calf serum
flu	fluticasone
GILZ	glucocorticoid-induced leucine zipper protein

GR	glucocorticoid receptor
GRE	glucocorticoid-responsive element
HEPES	2-(4-2-hydroxyethyl)-piperazinyl-1-ethansulfonate
HHT	hereditary hemorrhagic telangiectasia
HRP	horseradish peroxidase
ICS	inhaled corticosteroids
ID1 (gene)	inhibitor of differentiation-1
IL-13	interleukin-13
IPF	idiopathic pulmonary fibrosis
LAP	latency associated protein
LTBP	latency TGF-β-binding protein
met	methylprednisolone
MKP-1	mitogen-activated protein kinase phosphatase-1
MMP	matrix metalloproteinase
mRNA	messenger ribonucleic acid
MYH11	smooth muscle myosin heavy chain (protein, human)
PBS	phosphate buffered saline
POMC	pro-opiomelanocorticotropin
RT-PCR	real-time polymerase chain reaction
SAD	small airway disease
SBE	Smad-binding element
SDS	sodium dodecyl sulfate
SLPI	secretory leukoprotease inhibitor
Smad	transcriptional regulator: fusion of two gene names, *Drosophila mothers against dpp* (*Mad*) and *C. elegans Sma*
TEMED	N, N, *N′*, *N′*-tetra-methyl-ethylendiamine
TGF-β	transforming growth factor-β
TβR-I/Tgfbr1	transforming growth factor-β receptor 1
TβR-II/Tgfbr2	transforming growth factor-β receptor 2
TβR-III/Tgfbr3	transforming growth factor-β receptor 3

V. Summary

Glucocorticoids are regarded as the main therapeutic option for many pulmonary diseases, performing outstandingly well in asthmatic patients, however, failing to benefit patients suffering from the acute respiratory distress syndrome (ARDS), idiopathic pulmonary fibrosis (IPF), chronic obstructive pulmonary disease (COPD), and impaired lung development associated with bronchopulmonary dysplasia (BPD), often seen in pre-term infants. The transforming growth factor (TGF)-β polypeptide has been implicated as a pathogenic mediator of all of these pulmonary pathologies, which prompted us to investigate the crosstalk between glucocorticoid and TGF-β signaling. The glucocorticoid dexamethasone potentiated the TGF-β Acvrl1/Smad1/5/8 signaling axis, and inhibited the TGF-β Tgfbr1/Smad2/3 signaling axis in NIH/3T3 fibroblast-like mouse cells, in smooth muscle cells, primary lung fibroblasts, and endothelial cells. The accessory type III TGF-β receptor (Tgfbr3), which is also called betaglycan, was increased by dexamethasone. Betaglycan acted as a redirecting “switch” which increased Acvrl1/Smad1 and inhibited Tgfbr1/Smad2/3 signaling in lung fibroblasts. Dexamethasone activated Acvrl1/Smad1 signaling in several constituent pulmonary cell types. Furthermore, this study demonstrated that this axis was active in lung fibroblasts, and also inhibited Tgfbr1/Smad2/3 signaling. Fibroblast-to-myofibroblast differentiation of primary lung fibroblasts synergistically increased during treatment with dexamethasone and TGF-β_1. This was evident by an accumulation of smooth muscle myosin and smooth muscle actin. Previous studies have demonstrated that myofibroblast differentiation is exclusively Smad1-dependent. Intraperitoneal application of dexamethasone to live C57BL/6J mice resulted in increased *in vivo* pulmonary Tgfbr3 expression and phospho-Smad1 levels. Interestingly, this effect was lung-specific. Overall, in this study we demonstrate that glucocorticoids impact TGF-β signaling in pulmonary cell types as well as *in vivo* in mice lungs. This may be relevant for normal lung physiology and pulmonary pathology.

VI. Zusammenfassung

Glukokortikoide sind die Therapie der Wahl für viele Erkrankungen der Lunge. Während sie erfolgreich in der Therapie des Asthma bronchiale eingesetzt werden, scheinen sie kaum einen Nutzen für Patienten zu haben, die an dem akuten Atemnotsyndrom (ARDS), der chronisch obstruktiven Lungenerkrankung (COPD), der Lungenfibrose sowie an einer Lungenentwicklungsstörung, die eine starke Assoziation mit der bronchopulmonalen Dysplasie bei frühgeborenen Kindern aufweist, erkranken. Der transforming growth factor (TGF)-β ist ein pathogener Mediator in all diesen genannten Lungenerkrankungen, was uns veranlasste, die Interaktion der Glukokortikoid – und TGF-β Signalkaskaden zu untersuchen. Das Glukokortikoid Dexamethason verstärkte die Acvrl1/Smad1/5/8 TGF-β Signalachse in NIH/3T3 Zellen, primären Lungenfibroblasten, glatten Muskel – sowie Endothelzellen, während es die Tgfbr1/Smad2/3 Signalachse inhibierte. Dexamethasone erhöhte die Expression des akzessorischen Typ III TGF-β Rezeptors Tgfbr3, der auch „betaglycan“ genannt wird. Es wurde gezeigt, dass Tgfbr3 als „Schalter“ agierte, der die Tgfbr1/Smad2/3 Signalachse in Lungenfibroblasten inhibierte sowie die Acvrl1/Smad1/5/8 Signalachse potenzierte. Dexamethason stimulierte die Acvrl1/Smad1/5/8 Signalachse in Lungenfibroblasten, die antagonistisch zur Tgfbr1/Smad2/3 Signalachse wirkte. Weiterhin wirkte Dexamethason synergistisch mit TGF-β auf die Differenzierung von primären Lungenfibroblasten zu Myofibroblasten, was durch eine Akkulmulation von „smooth muscle actin“ und „smooth muscle myosin“ gezeigt werden konnte. Dieser Prozess ist in Fibroblasten ausschließlich Smad1 abhängig. Das Verabreichen von Dexamethason an lebende Mäuse zeigte *in vivo* einen Lungen spezifischen Einfluss von Dexamethason auf die Expressionslevel von Tgfbr3 sowie phospho-Smad1 Level. Diese Daten weisen auf einen interessanten und bisher unbekannten Einfluss von Dexamethason auf die TGF-β Signalachsen in Lungenfibroblasten hin. Wir glauben, dass dies für die normale Lungenphysio- und pathophysiologie relevant sein könnte.

1. Introduction

1.1 Background

Glucocorticoids are a class of steroid hormones which bind to the glucocorticoid receptor, and thereby impact gene expression in almost every cell type in the body [7, 10]. The body produces a natural glucocorticoid called cortisol (or hydrocortisone). However, a number of synthetic glucocorticoids have been developed, which are far more powerful than cortisol, and which are now widely used as drugs, including dexamethasone (dex), methylprednisolone (met), budesonide (bud), and fluticasone (flu) [7]. All of these agents have potent anti-inflammatory properties, and have thus found application in many acute and chronic lung diseases which have an inflammatory component [10]. In some instances, glucocorticoids have demonstrable positive effects, and are very successfully used, for example, in asthma and chronic obstructive pulmonary disease (COPD) [11, 12]. Surprisingly, however, glucocorticoids are without any beneficial effect, or may indeed have a negative impact on many other lung diseases which have a pronounced inflammatory component, including idiopathic pulmonary fibrosis (IPF), acute respiratory distress syndrome (ARDS), and bronchopulmonary dysplasia (BPD) [13-17]. It is currently unclear why glucocorticoids do not successfully treat these diseases. The TGF-β signaling system is a signaling system that plays an important role in the onset and progression of many lung diseases, including IPF, ARDS, and BPD. Increased TGF-β signaling has been associated with the increased production of fibrotic components in IPF and BPD, and also has been associated with increased pulmonary edema in ARDS [18-22]. Studying the interaction of these two major signaling pathways may provide new insights into why glucocorticoids, despite their pronounced anti-inflammatory activity, have not helped patients who suffer from these devastating pulmonary diseases.

1.2 Transforming growth factor-β

The TGF-β superfamily is a family of growth factors and consists of 33 ligands controlling a wide range of cellular processes during embryogenesis and later on in adult homeostasis [23]. These physiological processes include regulation of cell proliferation, migration, differentiation, apoptosis, extracellular matrix (ECM) production and maintenance, as well as of the immune system [24-30]. The three TGF-β isoforms and the ten isoforms of the bone morphogenetic protein (BMP) family are well-known ligands of this family [23].

1.2.1 TGF-β ligands

Three TGF-β isoforms have been described, TGF-β_1, TGF-β_2, and TGF-β_3. Each isoform is encoded on a different gene [31-33]. Then TGF-β_1 is secreted from cells in a latent dimeric complex which contains an amino-terminal pro-domain, also called TGF-β latency-associated protein (LAP), and a carboxy-terminal domain containing the mature TGF-β [2, 34, 35]. Then, two pro-polypeptide chains form a disulfide-bonded homodimer [2, 35, 36]. Next, TGF-β is cleaved from the propeptide by furin convertase [2, 37]. However, after cleavage the TGF-β dimer and the LAP propeptide remain associated by non-covalent interactions and form the so-called small latent TGF-β complex [2]. This complex is then non-covalently linked with a latent TGF-β binding protein (LTBP) and forms the large latent TGF-β complex [2].

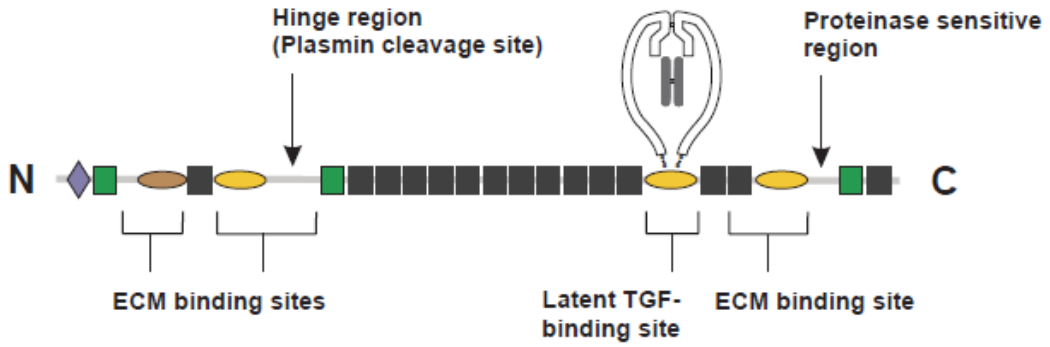

Fig. 1.1 Organization of the functional region of the latent transforming growth factor-β-binding protein-1S. Extracellular matrix is abbreviated as ECM. N represents the N-terminal end of the protein. C represents the C-terminal end of the protein. This image was taken from Unsöld *et al.* (2001) [1].

1.2.2 Activation of TGF-β

The release of active TGF-β from matrix-associated latent complexes requires two steps [2] (Fig. 1.2). First the complex has to be released from the ECM by proteolysis, and secondly inactive TGF-β has to be activated, which can take place via various mechanisms [2]. Multiple proteinases including plasmin are able to release TGF-β from the ECM by cleavage of the protease-sensitive hinge region of the LTBP [2, 38]. A proteolytic step is then needed to release TGF-β from the LAP [2]. This can be achieved by several mechanisms [2].

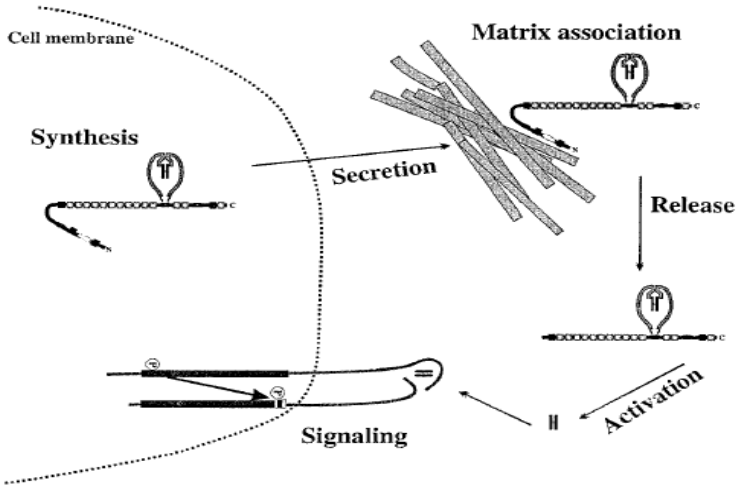

Fig. 1.2 From synthesis to activation. After synthesis inactive TGF-β is secreted from the cell and associates with extracellular matrix components. After release inactive TGF-β can be transformed into the active form by several mechanisms. This image was taken from Koli *et al*. (2001) [2].

These mechanisms can be physiochemical or enzymatic reactions which include an acidic cellular microenvironment, reactive oxygen species, matrix metalloproteinase (MMP)-2, MMP-9, and integrin alpha v beta 6 (αvβ6) [2, 39-42]. Interestingly, TGF-β activation can also be induced by certain drugs including retinoids and glucocorticoids [2, 43, 44].

1.2.3 TGF-β receptors

Members of the TGF-β family are able to signal through a family of transmembrane protein serine/threonine kinases consisting of type I and type II receptors [47, 48] (Fig. 1.3).

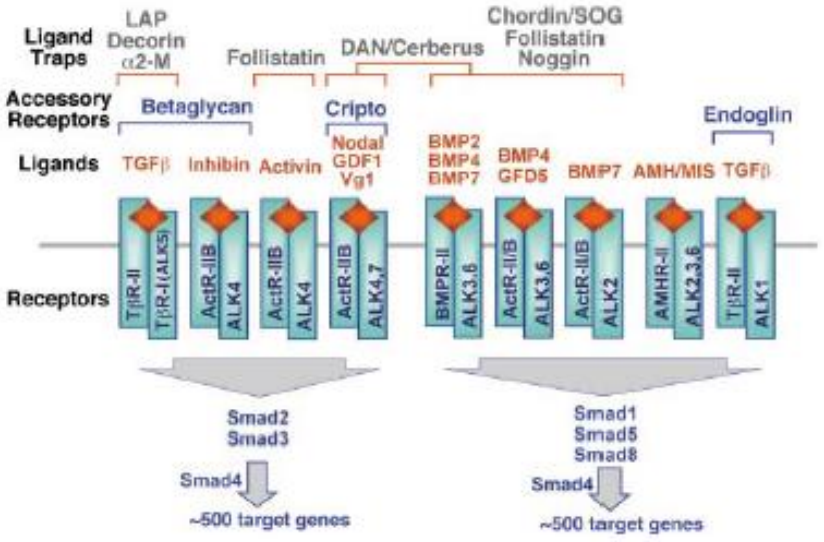

Fig. 1.3. Schematic representation of transforming growth factor-β receptors. This representation also demonstrates the relationship of TGF-β ligands with ligand-binding traps, accessory receptors, and type I and type II receptors in vertebrates. Following abbreviations are used in this image, α2-M (α2-macroglobulin), GDF1 (growth differentiation factor-1), Vg1 (vegetalising factor-1), GFD5 (growth and differentiation factor-5), AMH (Anti-Müllerian hormone), MIS (Müllerian-inhibitory substance), TβR-I and II (transforming growth factor-β receptor I and II), ActR-IIb (activin A receptor type IIb), ALK (activin receptor-like kinase), BMPR-II (bone morphogenetic protein receptor type II), AMHR-II (Anti-Müllerian hormone receptor II). This image was taken from Shi *et al*. (2003) [45].

Each receptor type is made up of approximately 500 amino acids organized into an extracellular ligand-binding domain, a transmembrane domain, and an intracellular signaling serine/threonine kinase domain [45, 49-52]. In the human genome this receptor family consists of seven type I and five type II receptors [45, 46].

1.2.4 Signal transduction mechanism and Smad proteins

Both type I Tgfbr1 and type II Tgfbr2 receptors are crucial for TGF-β-mediated signal transduction [48, 53, 54] (Fig. 1.4). Activated TGF-β binds to the Tgfbr2 with high affinity [47, 55]. Upon activation the Tgfbr2 activates the Tgfbr1 by phosphorylation and both receptors form a heteromeric complex [47, 53, 56-59]. Transforming growth factor-β preferably signals through the type I activin receptor-like kinase 5 receptor (ALK5, Tgfbr1) [60]. However, it has also been demonstrated that TGF-β can signal through the type I activin receptor-like kinase 1 receptor (ALK1, Acvrl1) [61].

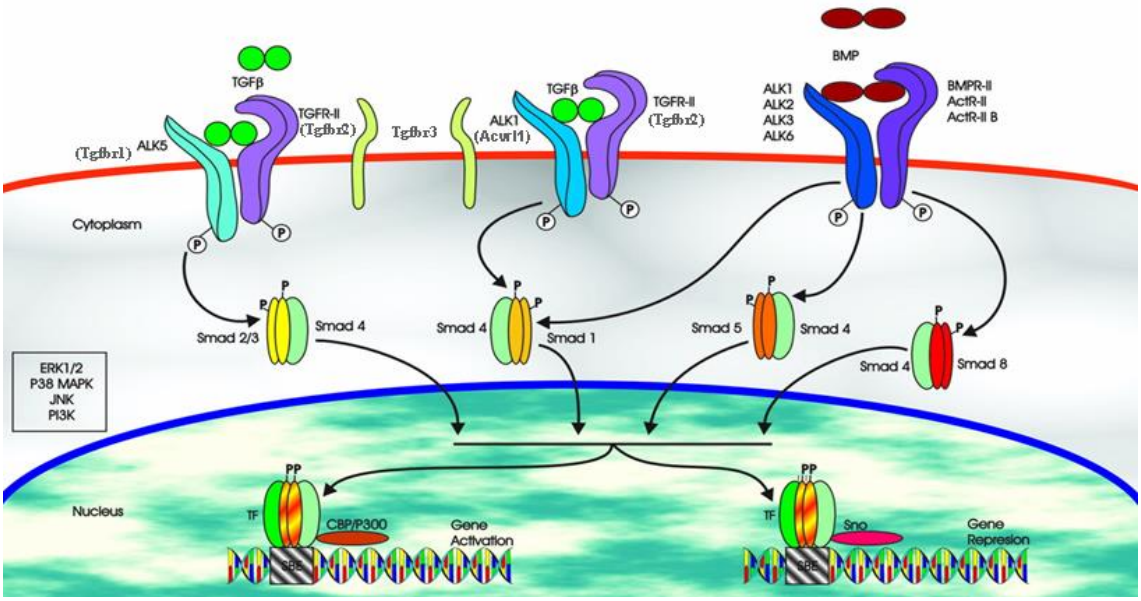

Fig. 1.4 Schematic representation of the downstream transforming growth factor-β signaling system. Following abbreviations are used in this image, Tgfbr1, 2, and 3 (transforming growth factor-β receptor 1, 2, and 3), Acvrl1 (activin A receptor type II-like 1), ALK (activin receptor-like kinase), ActR-II (activin A receptor type IIb), BMPR-II (bone morphogenetic protein receptor type II), ERK1/2 (extracellular regulatory kinase 1/2), MAPK (mitogen-activated protein kinase), JNK (c-Jun N-terminal-kinase), PI3K (phosphoinositide 3-kinase), CBP/P300 (CREB-binding protein/adenovirus early region 1A-binding protein), SBE (Smad-binding element), Sno (Sno oncogene). This image was taken from Bobik (2006) [3] and modified.

The Smad proteins carry TGF-β superfamily member-mediated signals from the cell surface to the nucleus [4]. There are eight known proteins that belong to this family [4] (Table 1.1). They can be classified into three groups: firstly, receptor-regulated Smads (R-Smads; Smad1, Smad2, Smad3, Smad5 and Smad8), secondly, the common-mediator Smad (co-Smad; Smad4), and thirdly, the inhibitory Smads (I-Smads; Smad6 and Smad7) [4].

Table 1.1 Conservation of Smad proteins in vertebrates, *Drosophila*, and *C. elegans*

Species	Receptor-regulated	Common	Inhibitory
Vertebrates	Smad1, Smad5, Smad8 (BMP) Smad2, Smad3 (TGF-β)	Smad4	Smad6 Smad7
Drosophila	Mad	Medea	Dad
C. elegans	Sma2 Sma3	Sma4	Daf-3

Following abbreviations were used in this table, Mad (*Drosophila mothers against dpp*), Dad (diaphanous autoregulatory domain), Daf-3 (gene that encodes an inhibitory Smad). This image was taken from Attisano *et al.* (1998) [4] and modified.

Smad2 and Smad3 induce TGF-β/Activin responses, whereas Smad1, Smad5, and Smad8 induce BMP responses [4, 62-66]. Smad activation relies on phosphorylation [4]. Smad2 and Smad3 are specifically phosphorylated by the activated Tgfbr1 [4, 67, 68]. After activation, phospho-Smad2 and phospho-Smad3 form a heteromeric complex with Smad4 in order to translocate to the nucleus [4, 69, 70].

Phospho-Smad1, phospho-Smad8, and possibly phospho-Smad5 form a complex with Smad4 after activation by BMP [4, 63, 70]. The inhibitory Smad6 and Smad7 proteins act as negative regulators of BMP and TGF-β signaling, due to the ability to prevent phosphorylation and association of R-Smads [4, 71-73]. Furthermore, Smad7 specifically antagonizes TGF-β signaling, whereas Smad6 antagonizes BMP signaling [4, 71-73].

1.2.5 Gene regulation

Activated R-Smad/co-Smad complexes translocate to the nucleus influencing a wide spectrum of transcriptional regulation [4]. These complexes bind to the so-called Smad-binding element (SBE), which are formed by certain nucleotide repeat sequences and are situated in promoter or suppressor regions of certain genes [45, 74, 75]. The minimal SBE consists of four base pairs, 5′-AGAC-3′ [45, 76]. In most natural DNA sequences an extra C base pair is additionally situated at the 5′ end [45]. TGF-β-mediated signaling influences multiple cellular functions by transcriptional regulation of target genes [23-30].

Well-known target genes of downstream TGF-β induction are the profibrotic factors *SERPINE1* (encodes plasminogen activator inhibitor-1) and *CCN2* (encodes connective tissue growth factor), as well as *COL1A1* (encodes pro-collagen 1), *COL3A1* (encodes pro-collagen 3), *ACTA2* (encodes α-smooth muscle actin), and *SMAD7* [25, 27, 74, 76, 77]. Known target genes of downstream BMP signaling include *ID1* (encodes inhibitor of differentiation-1) and *SMAD6* [78-80].

1.2.6 TGF-β co-receptors

In addition to type I and type II receptors a third family of type III receptors exists [47]. This family consists of the two related proteins, namely Tgfbr3 or betaglycan; and endoglin [47, 81, 82]. It has been demonstrated that these two receptors are capable of binding TGF-β ligands and forming complexes with type I and type II receptors and are, therefore, able to modulate TGF-β signaling [47, 83-85].

1.2.7 Betaglycan: an accessory TGF-β receptor

Betaglycan is a membrane-anchored proteoglycan which consists of 853 amino acids and belongs to the family of type III receptors [47, 81, 83, 86] (Fig. 1.5). Compared with type I and type II receptors, betaglycan does not have an intrinsic cytoplasmic signaling function [47, 81, 87]. The extracellular domain binds TGF-β isoforms with high affinity and also facilitates TGF-β ligand-binding to the type II receptor [47, 83, 87-89]. It has also been demonstrated that betaglycan binds BMP extracellularly, enhancing ligand-binding to BMP type I receptors, and is, therefore, also capable of modulating downstream BMP signaling [80, 90].

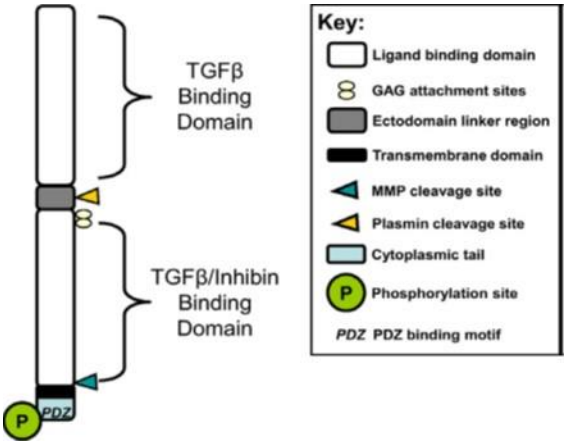

Fig. 1.5 Schematic structure of betaglycan. Following abbreviations were used in this image, MMP (matrix metalloproteinase), PDZ (**p**ost synaptic density protein, **D**rosophila disc large tumor suppressor, **z**onula occludens protein-1). This image was taken from Bilandzic *et al.* (2011) [5].

As betaglycan is able to directly interact with type I and type II receptors, it is a major determinant of cellular responsiveness to TGF-β superfamily members [5]. Depending on cell type and context-dependent mechanisms, betaglycan can either inhibit or enhance signaling properties of certain TGF-β superfamily members [5]. Stenvers and colleagues revealed that betaglycan-deficient mice developed lethal proliferative effects in the heart and apoptosis in the liver, which suggests a crucial role of betaglycan for normal organ development [91].

1.2.8 Tgfbr1 versus Acvrl1 signaling

TGF-β is capable of signaling via the Tgfbr1/Smad2/Smad3 as well as via the Acvrl1/Smad1/Smad5/Smad8 axis [92]. This may at least be partly dependent on TGF-β receptor expression levels [93].

In most cell types TGF-β favors the Tgfbr1/Smad2/Smad3 axis [92]. This pathway is known to drive profibrotic and fibrotic factors such as *SERPINE1*, *CCN2*, *ACTA2*, *COL1A1*, or *COL3A3* [25, 27, 76, 77]. Dysregulation of the Tgfr1/Smad2/Smad3 axis has been implicated in many lung pathologies in which fibrosis and inflammation are the underlying causes in the pathogenesis of disease development and progression [18-22, 94-97].

However, in endothelial cells it was documented that the other type I receptor, Acvrl1, was predominantly expressed, thereby, favoring TGF-β signaling via the Acvrl1/Smad1/5/8 axis in this cell type [92, 98]. Further investigation into this phenomenon revealed that both signaling pathways were active in this cell type and that both revealed opposite effects in terms of cellular responses to TGF-β stimulation [92]. While stimulation of the Tgfbr1/Smad2/Smad3 axis increased *serpine1* expression levels and inhibited endothelial cell proliferation and migration, the Acvrl1/Smad1/5/8 axis promoted proliferation and migration [92]. Mutations in Acvrl1 and endoglin, a TGF-β accessory receptor, have been linked to the human vascular disorder, hereditary hemorrhagic telangiectasia (HHT) [92, 99]. Interestingly, TGF-β-induced Smad1/Smad5 signaling has also recently been reported in epithelial cells, epithelium-derived tumor cells, and fibroblasts [100-102].

Furthermore, it has been found that fibroblasts from patients suffering from systemic sclerosis revealed increased SMAD1 phosphorylation and that this correlated with increased amounts of the profibrotic CTGF protein [103]. A further study demonstrated that *id1*, a target gene of the Acvrl1/Smad1/5/8 axis, and Smad1 phosphorylation levels were co-induced during a model of fibrogenesis in rats, concluding that these components might be involved in hepatic fibrosis [104].

1.2.9 TGF-β signaling in lung development

Transforming growth factor-β is widely implicated in early and postnatal lung development [105]. In general, lung development can be divided into six stages: the embryonic, pseudoglandular, canalicular, saccular, and alveolar stages, as well as the stage of vascular maturation [106]. During development the lung strives to maximize the surface area for gas exchange while minimizing the thickness of the alveolocapillary barrier [105-107].

Experimentally, it was demonstrated that between postnatal days 7 and 14, conditional TGF-β_1 overexpression in fetal monkey lungs severely impaired postnatal lung development [108]. This resulted in disrupted alveolarization, a key feature observed in BPD, suggesting that increased TGF-β signaling during this period of lung development inhibits alveolarization [105, 108]. Paradoxically, the inhibition of TGF-β signaling achieved in Smad3-deficient mice between postnatal days 14 and 28 resulted in airspace enlargement, indicating that during this period of lung maturation TGF-β signaling has a positive regulatory effect on alveolarization [21, 105, 109]. This leads to the so-called “Goldilocks” hypothesis, meaning that at certain points in time during lung maturation TGF-β signaling has to be “just right” for normal pre- and postnatal lung development [110].

During lung maturation in mice and humans, TGF-β receptor expression levels vary [111]. Alejandre-Alcázar *et al*. revealed that *tgfbr1* expression levels steadily decreased and *acvrl1* expression levels steadily increased in developing mouse lungs [111]. The TGF-β receptor 1 is known to control ECM deposition and remodeling while Acvrl1 is believed to play a key role in the endothelium during the phase of vessel maturation [47, 111, 112]. However, Alejandre-Alcázar’s study also demonstrated that Acvrl1 was expressed in vascular smooth muscle as well as in airway epithelium where the function remains unclear [111]. The same study also revealed that expression levels of the type III receptor betaglycan increased during the late phase of postnatal lung development [111].

1.2.10 TGF-β signaling in lung disease

It is thought that dysregulation of the TGF-β signaling pathway contributes to disease development and progression in fibrotic and inflammatory lung diseases such as BPD, IPF, ARDS, asthma, and COPD [19, 22, 113-120]. In the following chapter, these lung pathologies and the role of TGF-β in disease pathogenesis will be briefly discussed.

Bronchopulmonary dysplasia is characterized by diffuse pulmonary inflammation with alveolar and vascular simplification and an arrest of lung development, resulting in a reduced surface area for gas exchange and chronic pulmonary disease [121]. It affects prematurely born babies [94].

The multifactorial pathogenesis of BPD is complex and includes infection, inflammation, ventilator-induced lung injury, oxidant stress, abnormal growth factor signaling, and genetic factors [94]. Increased active and total TGF-β_1 levels were found in bronchoalveolar lavage fluid (BALF) obtained from infants suffering from chronic lung disease (CLD) [113]. Experiments in animals have revealed that inflammation increased total TGF-β_1 levels and that excessive TGF-β signaling in the developing lung led to interstitial fibrosis and inhibition of alveolar septation, both key features of BPD [19, 122].

Further experiments which gave insights into the involvement of TGF-β signaling in BPD pathogenesis have also demonstrated that high tidal ventilation and hyperoxia resulted in increased TGF-β signaling, and also in increased myofibroblast differentiation, and that this again was associated with arrested alveolar development [123, 124].

Idiopathic pulmonary fibrosis is defined as a specific form of chronic, progressive fibrosing interstitial pneumonia, is characterized by progressive worsening of dyspnea and deterioration of lung function, and is associated with a poor prognosis [13]. Key histopathological features include alveolar destruction, excess collagen deposition and remodeling, which is thought to be the result of excessive interstitial inflammation triggered by an initial inflammatory lesion within an alveolus [114, 125].

As IPF patients respond poorly to anti-inflammatory therapy, especially corticosteroids, inflammation does not seem to feature prominently in the pathogenesis of disease progression [13, 14, 18, 20, 126]. Transforming growth factor-β is a major contributor to fibrogenesis and, therefore, believed to play a key role in the progression of IPF [18]. In several studies, Khalil and co-workers revealed that IPF patients produced significantly more TGF-β and that this resulted in higher pulmonary TGF-β_1 levels [114, 115, 127]. Experimental studies demonstrated that Smad3-deficient mouse lungs developed only little evidence of fibrosis and no upregulation of fibrogenesis-associated genes, suggesting a key role for Smad3 as an intracellular mediator of TGF-β signaling in the pathogenesis of progression in IPF [18, 21].

Acute respiratory distress syndrome, according to the new “Berlin Definition”, is clinically characterized by hypoxemia and bilateral radiographic opacities,

associated with increased venous admixture, increased physiological dead space, and decreased lung compliance [128]. This syndrome is defined by diffuse bilateral inflammation leading to increased pulmonary vascular permeability, increased lung weight, and loss of aerated lung tissue [128].

Acute respiratory distress syndrome can be the result of multiple etiologies causing acute lung injury and tissue inflammation such as sepsis, pancreatitis, hemorrhagic shock, or toxic inhalation [22]. As far as the pathogenesis is concerned, TGF-β is seen as a key mediator of ARDS [22, 116]. It plays a major role in the development of fibrosis during the late phase of ARDS [22, 129]. However, BALF collected from ARDS patients within 48 hours after intubation already contained elevated levels of active TGF-β_1 compared to controls [116, 130].

Destruction of epithelial barrier integrity is central to the early stage of ARDS causing alveolar edema [22]. It has been demonstrated that TGF-β_1 disrupts epithelial integrity, thus allowing fluid to flood the alveolus, which in turn leads to hypoxemia [22]. However, not only epithelial integrity but also fibroproliferation and increased collagen turnover occur in the early phase of ARDS and impact disease outcome [130-132]. Plasmids containing the procollagen I promoter which were transfected into normal human fibroblasts were significantly induced by BALF obtained from ARDS patients compared to controls [130]. This effect was attenuated with a specific TGF-β_1 antibody [130]. This study suggests that TGF-β_1-induced fibrotic changes already occur in early stages of this syndrome.

Asthma is a chronic disease characterized by airway inflammation and remodeling accompanied by airway hyperresponsiveness, and reduced lung function [96]. This disease is one of the most common chronic diseases affecting nearly 300 million people worldwide [96]. Together with many other cytokines, TGF-β_1 plays a central role in airway remodeling which includes microvascular changes, airway smooth muscle remodeling, and subepithelial fibrosis, key histopathological features of asthmatic patients [96, 97].

Other studies have demonstrated that eosinophilic cells isolated from BALF obtained from asthmatic patients demonstrated increased TGF-β_1 mRNA levels, which suggests that eosinophils may be important for the pathogenesis of inflammation and also capable of influencing specific structural changes such as subepithelial fibrosis [118]. Furthermore, alveolar macrophages isolated from BALF from asthmatic patients revealed an increased release of TGF-β_1 when challenged with allergens compared to controls [133]. Bottoms and co-workers revealed that a specific TGF-β_1 antibody

inhibited ovalbumin-induced subepithelial collagen deposition, airway and fibroblast decorin deposition, as well as monocyte and macrophage recruitment [97].

Chronic obstructive pulmonary disease is characterized by chronic airway inflammation accompanied by irreversible expiratory airflow limitation, which is caused by small airway disease (SAD) and emphysema [96]. Today COPD is one of the leading causes of death in the developed world and is associated with a high individual and socioeconomic burden [134]. Risk factors for COPD include tobacco smoke, genetic predisposition, occupational and environmental exposure, as well as asthma [96, 135].

Chronic inflammation and also dysregulation of TGF-β signaling are important regulators in the pathogenesis of this disease [96]. Small airway disease causes expiratory airflow limitation and is characterized by increased airway wall thickness as a result of tissue remodeling and peribronchiolar fibrosis [134, 136]. Transforming growth factor-β is known to drive fibrogenic processes [134, 137]. It has been demonstrated that TGF-β_1 mRNA expression levels were significantly upregulated in small airway epithelium of tobacco smokers and COPD patients [119, 138]. Furthermore, mRNA levels of the inhibitory Smad6 and Smad7 in bronchial biopsies were significantly decreased in COPD patients, suggesting a disturbed intracellular negative feedback mechanism of TGF-β signaling [120]. It has been revealed that cultured human fetal lung fibroblasts demonstrated increased production of TGF-β_1 mRNA when challenged with cigarette smoke [139]. Further investigation into the function of pulmonary fibroblasts in COPD *in vivo* revealed that these cells produced increased amounts of TGF-β_1 and also revealed increased responses to TGF-β [140, 141].

In the case of emphysema, decreased TGF-β signaling seems to contribute to the development of airspace enlargement [134, 142]. Smad3 knock-out mice spontaneously develop enlarged airspaces and are protected from fibrosis [21, 109].

1.2.11 Fibroblast-to-myofibroblast differentiation

Tissue injury activates a repair response in which fibroblasts play an essential role [143]. Upon injury fibroblasts are activated or differentiate to myofibroblasts in order to participate in wound repair [143]. In this activated or transdifferentiated state they represent a key source of ECM components, inflammatory and fibrogenic cytokines, and participate in wound contraction [143]. It has been demonstrated that TGF-β_1 is a strong activator of fibroblast-to-myofibroblast differentiation [144, 145]. As wound repair continues, myofibroblasts should gradually disappear [143]. However,

persisting myofibroblasts are associated with the development and progression of fibrosis seen in IPF, BPD, and ARDS [143]. Alpha-smooth muscle actin (ACTA2) and smooth muscle myosin heavy chain (MYH11) represent two markers of myofibroblast differentiation [144-146]. It has been demonstrated that α-smooth muscle actin expression is regulated by the Acvrl1/Smad1 pathway, which suggests that this pathway is a regulator of myofibroblast differentiation [147-151].

1.3 Glucocorticoids

Glucocorticoids are endogenously-produced steroid hormones [8]. Physiologically, the most important glucocorticoid is cortisol [8]. Depending on the rate of secretion and tissue concentration, cortisol influences a broad spectrum of physiological processes in the body [8].

1.3.1 Glucocorticoid effects in the human body

At physiological concentrations cortisol causes catabolic effects which include degradation of proteins, stimulation of gluconeogensis and the production of glycogen in the liver, and also enhances lipolytic effects of catecholamines [8]. Furthermore, cortisol increases sodium retention as well as potassium and calcium secretion in the kidney [8]. During periods of physical stress cortisol secretion is increased, and at higher concentrations cortisol has an anti-proliferative effect on fibroblasts and blocks the synthesis of collagen [8]. Cortisol also has pronounced anti-inflammatory properties, blocking unspecific and specific defense mechanisms and preventing T-lymphocyte proliferation [8]. Increased cortisol concentrations can also cause increased excitability of the brain and euphoric or depressive effects [8].

1.3.2 Glucocorticoid cell signaling

Glucocorticoids are lipophilic molecules and, therefore, bind to an intracellularly-located glucocorticoid receptor (GR) [8].

1.3.3 The intracellular glucocorticoid receptor

Glucocorticoid receptors are located in the cytoplasm of the cell and are ubiquitously expressed [6]. Heat-shock proteins are responsible for the correct folding of the GR [6]. The whole receptor is made up of three domains [6] (Fig. 1.6).

Fig. 1.6 Representation of the intracytoplasmic-located glucocorticoid receptor. This image was taken from Mutschler *et al*. (2001) [6] and modified.

1.3.4 Signal transduction

Cortisol is able to pass the lipophilic cell membrane and can then bind the ligand-binding domain at the C-terminus of the GR to form the ligand-receptor complex [6] (Fig. 1.7). Upon ligand binding, heat-shock proteins dissociate from the receptor [6]. After activation, the ligand-receptor complex passes to the nucleus, where the activated ligand-receptor complex then has two possibilities. Firstly, the DNA-binding domain can bind to specific glucocorticoid responsive elements (GRE) located on the DNA [6]. The transactivating domain is then able to activate or deactivate gene transcription [6]. Secondly, the ligand-receptor complex can bind directly to other transcription factors in the nucleus [6].

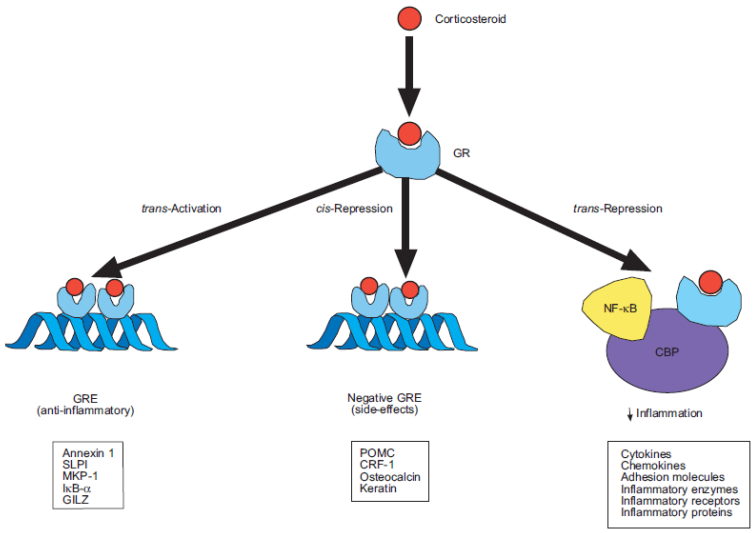

Fig. 1.7 Schematic representation of downstream glucocorticoid signaling. After entering the nucleus the activated glucocorticoid receptor (GR) is able to influence gene expression in several ways [7]. Glucocorticoid receptors bind to glucocorticoid responsive elements (GREs) in promoter or suppressor regions of steroid-sensitive genes [7]. They may promote expression of anti-inflammatory genes such as annexin 1, SLPI (secretory leukoprotease inhibitor), MKP (mitogen-activated protein kinase phosphatase)-1, IκB-α (nuclear factor of kappa light polypeptide gene enhancer in B-cells inhibitor, alpha) or GILZ (glucocorticoid-induced leucine zipper protein) [7]. On the other hand, they may repress expression of genes commonly related to side-effects of corticosteroids such as POMC (pro-opiomelanocorticotropin), CRF (corticotropin releasing factor), osteocalcin, and keratin [7]. Furthermore, they are able to interact with other transcription factors such as CBP (cAMP-response-element-binding-protein), which is activated by the pro-inflammatory transcription factor NF-κB [7]. This image was taken from Barnes (2006) [7]**.**

1.3.5 Regulation of glucocorticoid concentrations in the body

Cortisol concentrations in the body are strictly regulated by the hypothalamus and the pituitary gland [8] (Fig. 1.8). When cortisol levels in the body drop, corticotropin-releasing hormone (CRH) is secreted from the hypothalamus, which then stimulates the secretion of adrenocorticotropic hormone (ACTH) in the pituitary gland [8]. Adrenocorticotropic hormone then stimulates cortisol production in the adrenal cortex [8].

Cortisol production and secretion is regulated by a negative feedback loop mechanism in which cortisol inhibits the secretion of CRH from the hypothalamus and the secretion of ACTH from the pituitary gland [8]. Cortisol levels in the body vary greatly during the day [8]. Between 9 a.m. and midday plasma levels reach the highest concentration, while the lowest levels are reached at around midnight [8]. Stressful situations of a physical or psychological nature greatly stimulate cortisol production and secretion from the adrenal cortex [8].

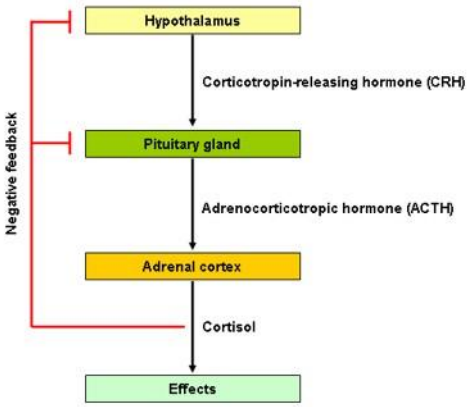

Fig. 1.8 Schematic representation of glucocorticoid regulation in the body. This image was taken from Mutschler *et al*. (2001) [8] and modified.

1.3.6 Cortisol synthesis

Anatomically, the adrenal gland is situated above the kidney. Histologically, the gland consists of the cortex and the medulla [152]. Furthermore, the adrenal cortex is divided into three different zones: the *zona glomerulosa*, *zona fasciculate*, and the *zona reticularis* [152]. Cortisol is produced in cells that are situated in the *zona fasciculate* and *zona reticularis* [152]. Cholesterol forms the basis of cortisol synthesis [9] (Fig. 1.9).

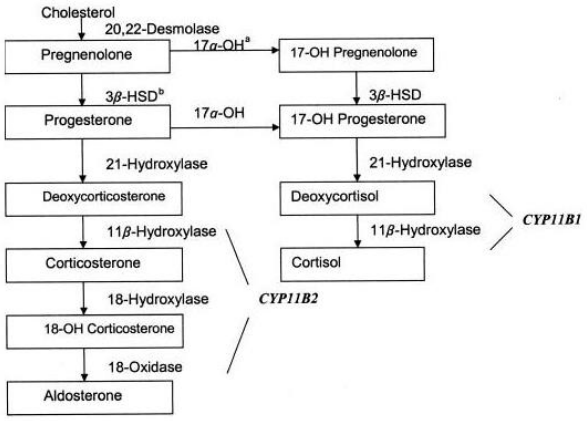

Fig. 1.9 Schematic representation of the cortisol synthesis pathway. This image was taken from Freel *et al*. (2004) [9]. 17α-OH (17-alpha hydroxylase); 3β-HSD (3-beta hydroxysteroid dehydrogenase); CYP (cytochrome p).

1.3.7 Cortisol derivatives

On the basis of the pronounced anti-inflammatory, anti-allergic, and immunosuppressive properties, glucocorticoids have found widespread clinical application [8]. Over the years a wide range of cortisol derivatives has been developed that differ structurally from one another [8].

1.3.8 General clinical use of glucocorticoids

On the basis of the previously described physiological and pharmacological properties (see chapter **1.2.1**), glucocorticoid derivatives are frequently used in patients suffering from adrenal insufficiency or from diseases in which inflammation is a key component for disease development, progression, or worsening [8]. The anti-inflammatory and immunosuppressive effects of glucocorticoids benefit patients suffering from autoimmune diseases such as rheumatoid arthritis or organ transplant patients by suppressing immunologic rejection [8]. Furthermore, corticosteroids find clinical application in patients suffering from certain allergic conditions, such as allergic rhinitis and conjunctivitis, certain dermatologic diseases such as urticaria, or oncologic diseases such as acute lymphoblastic leukemia (ALL) [8].

1.3.9 Adverse effects of glucocorticoids

Adverse impacts of glucocorticoids are determined by their physiological effects in the body [8]. Side effects increase with duration of treatment as well as dosage [8]. These effects include an increased risk of infection, delayed wound healing, muscle and skin atrophy, growth inhibition in children, and an increased risk of developing osteoporosis and diabetes. Further adverse effects include an increase in retention of sodium and water, an increased excretion of potassium, impacted central nervous

functions, the risk of developing glaucoma, Cushing's syndrome, and an increased risk of thrombosis [8].

1.3.10 Glucocorticoids in TGF-β-related lung pathologies and lung development

The following section will give a short summary of glucocorticoid effects on TGF-β-related lung pathologies and lung development.

Lung development and BPD: Animal studies have demonstrated that glucocorticoids impact the speed of lung maturation and the critical stage of alveolarization [153-155]. Preterm Rhesus monkeys that were antenatally treated with betamethasone demonstrated accelerated lung maturation but an overall decreased amount of alveoli compared to controls [153, 154]. Similar results were found in a further study investigating the effect of dex on postnatal lung development in newborn rats, which revealed that steroid therapy resulted in an "emphysematous" lung with larger and fewer airspaces [153, 155].

One fundamental problem of respiratory adaptation in premature newborns (born before 37 weeks of gestation) is the inability to synthesize sufficient amounts of surfactant, which prevents the alveoli from collapsing, and, therefore, ensures blood oxygenation [156]. Antenatal administration of glucocorticoids increases mRNA levels of surfactant protein A and B in rat and human lungs [153, 157, 158]. However, another study found that when infants at risk of developing CLD were treated with corticosteroids at 14 days of age, they did not demonstrate any improvement in surfactant function, suggesting that the time point of drug administration is critical [153, 159].

The question of whether or not to treat newborns at risk of, or suffering from, BPD remains a difficult one to answer [17]. One small clinical study has demonstrated that short-term treatment with dex improved pulmonary function, suppressed pulmonary inflammation, and decreased respiratory support in premature infants suffering from BPD [160]. A review from 2010 states that using high daily doses of dex (approximately 0.5 mg/kg/d) reduces the incidence of BPD, but is also associated with numerous short- and long-term adverse outcomes including neurodevelopmental impairment [17]. Furthermore, there is insufficient evidence that low-dose (<0.2 mg/kg/d) dex therapy is beneficial [17]. The same applies to the use of both low and high dose hydrocortisone therapy [17]. Therefore, open-label glucocorticoid therapy cannot be recommended for infants suffering from BPD [17].

In one experiment, betamethasone even worsened chorioamnionitis-related lung development in rabbits, suggesting that glucocorticoid treatment might represent

an additional risk factor for lung development in the case of preterm infection, which is also a risk factor for developing BPD [161, 162].

In **IPF** to date, no randomized controlled studies have been conducted with corticosteroid monotherapy [13, 163, 164]. Retrospective uncontrolled studies have reported no survival benefit, although a minority of patients demonstrated improved pulmonary function [13, 14, 165]. However, long-term corticosteroid therapy resulted in substantial morbidity [13, 165]. Based on these clinical facts, the current recommendation states that IPF patients should not receive corticosteroid monotherapy [13].

As IPF patients respond poorly to anti-inflammatory therapy, it has been suggested that inflammation may not play a key role in the pathogenesis of disease progression [14, 18, 20, 126]. Another possible explanation why glucocorticoids do not improve the status of fibrosis patients is that they are unable to inhibit interleukin (IL)-13-mediated differentiation of fibroblasts into myofibroblasts [166, 167].

Acute respiratory distress syndrome today remains a devastating syndrome and despite therapeutic advances, mortality rates still vary between 25-40% [15]. Currently, no drug therapy can be recommended for patients suffering from this devastating disease [15]. A clinical study exploring the effects of systemically-applied met to ARDS patients published in The New England Journal of Medicine in 2006 came to the conclusion that met should not be routinely used in patients suffering from persistent ARDS [16]. Furthermore, the study concluded that systemic met therapy administered more than two weeks after onset of ARDS might even increase the risk of mortality [16]. Fluid management, low tidal ventilation in sedation, the abdominal position, and extracorporeal membrane oxygenation (ECMO) remain the main strategies to improve outcome for ARDS patients [15].

Asthma: Currently, a wide range of drugs is available to asthmatic patients, whereas therapeutic options depend on age, progression, and severity of the disease [11]. Drug therapy consists of two components: quick relief medication including short-acting β_2-agonists and long-term control medication including inhaled corticosteroids (ICS) [11]. These types of drugs include bud and flu and are the most effective long-term control medication in asthmatic children and adults [11]. Inhaled corticosteroids reduce airway hyperresponsiveness, inhibit inflammatory cell migration and activation, block late-phase reaction to allergens, and reduce the risk of

exacerbation [11]. However, these drugs have failed to alter the progression or underlying severity of the disease in children [11].

Chronic obstructive pulmonary disease is, by its very nature, a chronic progressive disease that cannot be treated curatively [12]. The goal of COPD treatment is thus the reduction of long-term function decline, preventing and treating exacerbations, reducing the number of hospitalizations and mortalities, relieving disabling dyspnea, and improving exercise tolerance as well as the health-related quality of life [12]. As in the treatment of asthma, drug treatment depends on disease severity and stability [12]. Inhaled corticosteroids are regularly used in combination with inhaled β_2-agonists or inhaled anticholinergics but can also be employed in monotherapy [12]. It has been proven that flu reduced exacerbations in COPD patients [12, 168]. Furthermore, it has been demonstrated that there were significantly fewer cases of dyspnea in patients receiving ICS therapy compared to placebo [12, 169]. However, this same clinical study also concluded that patients receiving ICS therapy did not benefit in terms of frequency of hospitalizations [12, 169].

2. Aim of the study

Dysregulation of TGF-β signaling has been implicated in many devastating lung diseases in which fibrosis and inflammation are central features of pathogenesis [19, 22, 113-120]. Glucocorticoids have proven to be partially successful in treating patients suffering from these diseases, notably asthma and COPD [11, 12, 168, 169]. However, patients suffering from IPF, ARDS, and BPD do not overall benefit from corticosteroid therapy, despite the fact that these pathologies are characterized by inflammatory processes which glucocorticoids should blunt [13, 15-17]. Given that TGF-β plays a key pathogenic role in all of these diseases and that corticosteroid use has failed to improve the outcome for affected patients, it follows that the interaction of TGF-β and glucocorticoid signaling should be investigated.

In this study we hypothesized that the TGF-β and glucocorticoid signaling pathways interact *in vitro* and *in vivo*, and that glucocorticoids may impact TGF-β signaling, which may then in turn influence TGF-β-regulated gene expression, thus either worsening or improving lung diseases in which TGF-β signaling plays a pathogenic role. In order to address this *in vitro*, we used primary adult fibroblasts, primary mouse fibroblasts, primary human pulmonary artery endothelial cells, primary human pulmonary arterial vascular smooth muscle cells, H441 human epithelial cells, as well as NIH/3T3 mouse fibroblast-like cells. Our aim was to investigate the impact of glucocorticoids on:

1) The **proximal** part of the TGF-β signaling axis by assessing phosphorylation levels of Smad1, Smad2, and Smad3 by immunoblot analysis.

2) The **distal** part of the TGF-β signaling axis by assessing activity of the TGF-β-responsive $(CAGA)_9$ element of the $p(CAGA)_9$-luc, and activity of the BMP-responsive element of the pBRE-luc construct by dual luciferase assay as well as protein levels of ACTA2 and MYH11.

3) The mRNA and protein expression levels of betaglycan by real-time PCR and immunoblot analysis.

4) ***In vivo*** TGF-β signaling in the mouse lung, heart, kidney, and liver by assessing mRNA expression levels of *acvrl1*, *tgfbr3* and *smad1* by real-time PCR analysis, and protein expression levels of Tgfbr3, phosphorylated Smad1, total Smad1, phosphorylated Smad2 and total Smad2 by immunoblot analysis.

3. Materials and methods

3.1 Materials

3.1.1 Equipment

Adobe Photoshop CS3 Software	Adobe Systems (Inc.), USA
Buffer dam	BIO-RAD, USA
Blotting membrane: Trans-Blot Transfer Medium	BIO-RAD, USA
Camera: LAS-4000 cooled CCD	FujiFilm, Japan
Cell culture hood; SAFE 2020	Thermo Scientific, USA
Cell culture incubator; HERACELL 150i	Thermo Scientific, USA
Cell culture flask: 250 ml	Greiner Bio-One, Germany
Cell culture plates: 6 and 48 well plates	Greiner Bio-One, Germany
Cellscraper	Sarstedt, Germany
Centrifuge: Biofuge fresco	Heraeus, Germany
Centrifuge: Minispin plus	Eppendorf, Germany
Centro LB 960 microplate luminometer	BERTHOLD TECHNOLOGIES GmbH & Co. KG, Germany
Chromatography paper	Whatman™, part of GE Health Care Limited, USA
ELISA reader: Versa max, microplate reader	Molecular Devices, Germany
Electric transformer: Power Pac ™ Basic	BIO-RAD, USA
Falcon: 15, 50 ml	Greiner Bio-One, Germany
Fridge +4 °C	Bosch, Germany
Fridge -20 °C	Bosch, Germany
Fridge -40 °C	Kryotec, Germany
Fridge -80 °C	Heraeus, Germany
Glass beakers: 100, 250, 500, 1000 ml	Simax, Czech Republic
Glass bottles: 500, 1000, 2000 ml	Thermo Fisher Scientific, USA
Glass plates	BIO-RAD, USA
Heatblock	VWR, Germany
Multi Gauge MFC Software	Fujifilm Holding Corporation, Japan
Nanodrop® spectrophotometer	Peqlab, Germany
PCR-thermocycler	MJ Research, USA
Pipettes: 10, 20, 50, 100, 200, 1000 µl	Gilson, France
Pipetteboy	Eppendorf, Germany
Pipette tips: 10, 20, 100 µl	Gilson, USA

Pipette tips: 200, 1000 µl	Sarstedt, Germany
Real-time PCR machine: StepOne Plus	Applied Biosystems, USA
Running chamber: Mini Protean® Tetra Cell	BIO-RAD, USA
Serological pipettes: 5, 10, 25, 50 ml	Falcon, USA
Spacer plates: 1.5 mm	BIO-RAD, USA
Syringe: 0.5, 30 ml	B. Braun, Germany
Syringe needles: Size 14	B. Braun, Germany
Timer: Oregon scientific	Roth, Germany
Transfer chamber: Mini Protean® 3 cell	BIO-RAD, USA
Tubes: 150 µl, 0.5, 1.5, 2 ml	Sarstedt, Germany
Vortex machine	Merck Eurolab, Germany
Water bath: E100	Lauda, Germany
Well combs: 10, 15	BIO-RAD, USA

3.1.2 Reagents

Acrylamide solution, Rotiphorese Gel 30	Roth, Germany
Activin receptor-like kinase (ALK)5 inhibitor: SB431542	Sigma-Aldrich, Germany
Albumine, bovine serum	Sigma-Aldrich, Germany
Ammonium persulfate (APS)	Promega, USA
Antibiotic/antimycotic mix solution (100×)	Sigma-Aldrich, Germany
Antibodies (primary, secondary)	Listed in Section 11
Bradford substrate	BIO-RAD, USA
Budesonide powder	Sigma-Aldrich, Germany
Collagenase	Sigma-Aldrich, Germany
Complete™ protease inhibitor	Roche, Germany
Dexamethasone powder	Sigma-Aldrich, Germany
Dimethyl sulfoxide (DMSO)	Sigma-Aldrich, Germany
Dithiothreitol (DTT)	Promega, USA
D-MEM + GlutaMAX™-I (1×) medium	Life Technologies™, USA
Dulbecco's phosphate buffered saline (PBS) 1×	Invitrogen, UK
Dulbecco's phosphate buffered saline (PBS) 10×	Invitrogen, UK
Ethanol (70%)	VWR, Germany
Ethanol (100%)	VWR, Germany
Ethylendinitrilo-N, N, *N*, *N*′-tetra-acetic-acid (EDTA)	Promega, USA

Ethylene glycol-bis (2-amino-ethylether)-N, N, *N′*, *N′*-tetraacetic-acid (EGTA)	Promega, USA
Fetal calf serum (FCS)	PAA Laboratories, Austria
Glycine	Roth, Germany
Hi-Glucose D-MEM	Life Technologies™, USA
2-(4-2-hydroxyethyl)-piperazinyl-1-ethansulfonate (HEPES)	Sigma-Aldrich, Germany
Immunoblot detection kit: SuperSignal® West Femto Maximum Sensitivity Substrate	Thermo Scientific, USA
Immunoblot marker: Precision Plus Protein™ Dual Color Standards	BIO-RAD, USA
Isopropanol	Merck, Germany
Fluticasone proprionate	Sigma-Aldrich, Germany
Lipofectamine® 2000	Invitrogen, UK
Luciferase assay reagent 10-pack	Promega, USA
Luciferase cell culture lysis 5× reagent	Promega, USA
Magnesium chloride ($MgCl_2$) solution	Applied Biosystems, USA
β-mercaptoethanol	Sigma-Aldrich, Germany
6α-Methylprednisolone	Sigma-Aldrich, Germany
Methanol	Sigma-Aldrich, Germany
MnLV reverse transcriptase	Applied Biosystems, USA
N, N, *N′*, *N′*-tetra-methyl-ethylendiamine (TEMED)	Biorad, USA
Non-fat dry milk powder	Roth, Germany
NP-40	Fluka Biochemika, UK
Opti-MEM medium	Gibco BRL, Germany
PCR buffer II	Applied Biosystems, USA
PCR nucleotide mix	Promega, USA
Penicillin	Sigma-Aldrich, Germany
PeqGOLD Total RNA Kit	Peqlab, Germany
Peqlab/Ceramic Kit 1.4 mm 91-PCS-CK14	Peqlab, Germany
Platinum® SYBR® Green qPCR SuperMix -UDG-KIT	Invitrogen, UK
Random hexamers	Applied Biosystems, USA
RNase inhibitor	Applied Biosystems, USA
RNase-free water	Ambion, Germany
RPMI-1640 medium	Gibco BRL, Germany

Silencer® negative siRNA control	Ambion, Germany
Sodium dodecyl sulfate (SDS)	Promega, USA
Sodium chloride	Roth, Germany
Sodium *ortho* vanadate	Sigma-Aldrich, Germany
Streptomycin	Sigma-Aldrich, Germany
Transforming growth factor (TGF)-β_1	R&D Systems, USA
1.0 M Tris pH 6.8	Roth, Germany
1.5 M Tris pH 8.8	Roth, Germany
Trypsin-EDTA	Sigma-Aldrich, Germany
Tween 20	Sigma-Aldrich, Germany

3.2 Methods

3.2.1 Cell culture

3.2.1.1 NIH/3T3 mouse fibroblast-like cells

The NIH/3T3 mouse fibroblast-like cell line (CRL-1658™, American Type Culture Collection) was cultivated in 250 ml tissue culture flasks in 10 ml of D-MEM media supplemented with 10% fetal calf serum (FCS) and 10 ml 2-(4-2-hydroxyethyl)-piperazinyl-1-ethansulfonate (HEPES) and then incubated at 37 °C, 5% CO_2, and 95-100% humidity. After having reached 80-90% confluence, cells were passaged.

Firstly, media was removed. Cells were then washed with 1× PBS and incubated in 3 ml of trypsin/EDTA solution at 37 °C for 3 min. Then, 7 ml of supplemented D-MEM media (see above) were added. Before being transferred to a new tissue culture flask, cells were diluted in supplemented D-MEM media to a concentration of 1:10. For cell culture experiments cells were seeded into 6- or 48-well plates in supplemented D-MEM media.

3.2.1.2 Isolation of primary mouse lung fibroblasts

In order to isolate primary adult mouse lung fibroblasts for one experiment fibroblasts were isolated from two C57BL/6J mice.

Mice were sacrificed by an overdose of isoflurane. Before opening the body cavities the skin of the mice was soaked in 70% ethanol. After de-gloving the skin above the chest the anterior abdomen was cut open using sterile scissors. The diaphragm was then carefully punctured from the abdominal side. To avoid blood contamination the aorta was cut in the abdominal section.

In order to wash out blood from the pulmonary vascular system the right ventricle was cannulated and 10 ml of 1× PBS were administered. Both lung lobes and the heart were then cut free from the mediastinum and placed in 15 ml cold 1× PBS in a 10-cm dish. These steps were then repeated for a second mouse. Lung lobes and hearts from both animals were combined into the 10-cm dish.

In order to dissociate lung tissue, the dish containing lung lobes and hearts was transferred to a sterile laminar flow hood. The heart was then detached using new sterile scissors. Any visible bronchi and mediastinal tissue were then carefully removed from both lung lobes.

Lung lobes were then placed in a dry 50-ml Falcon tube and minced finely with scissors for several minutes. The minced tissue was then left to incubate in 25 ml of collagenase (2 ng/ml) preheated to 37 °C on a shaker at 125 revolutions per minute (rpm) for 45 min at 37 °C. After titrating the suspension up to 12 times through a cannula firmly attached to a 30-ml syringe, tissue chunks were left to settle. The suspension was then pipetted through two strainers (70 µm diameter followed by 40 µm diameter) into a 50-ml Falcon tube and then spun down at 400 g for 8 min at 4 °C.

The cell suspension was then re-suspended in 15 ml of growth media (see section **3.2.1.3**), seeded in a T-75 flask and left to incubate for 24 h. Cells which did not attach in that time were then removed.

Isolation medium

Hi Glucose D-MEM media

20% FCS

1% Penicillin/Streptomycin

3.2.1.3 Cultivating primary mouse lung fibroblasts

Primary mouse lung fibroblasts were cultivated like NIH/3T3 mouse fibroblast-like cells (see section **3.2.1.1**) only using a special growth media consisting of Hi Glucose D-MEM containing 10% FCS and 1% Penicillin/Streptomycin.

Growth medium

Hi Glucose D-MEM media

10% FCS

1% Penicillin/Streptomycin

3.2.1.4 Primary human lung fibroblasts

Primary human lung fibroblasts (CC-2512, Lonza) were cultured following the manufacturer's instructions.

3.2.1.5 Primary human pulmonary artery endothelial cells

Primary human pulmonary artery endothelial cells (C0085C, Life Technologies™) were cultured following the manufacturer's instructions.

3.2.1.6 Primary human pulmonary artery smooth muscle cells

Primary human pulmonary artery smooth muscle cells (C0095C, Life Technologies™) were cultured following the manufacturer's instructions.

3.2.1.7 H441 human Clara cell-like airway epithelial cells

H441 human Clara cell-like airway epithelial cells (HTB-174^{TM}, American Type Culture Collection) were cultured following the manufacturer's instructions.

3.2.1.8 Experimental cell culture setup

Cells were stimulated with corresponding glucocorticoids (dex, 20 nM; met, 20 nM; bud, 2 nM; flu, 2 nM) for 18 h, where indicated. These concentrations represent the mean, circulating, clinically relevant doses when these drugs are employed therapeutically [170, 171].

In order to determine Smad protein phosphorylation levels, cells were additionally stimulated with TGF-β_1 (2 ng/ml) for 30 min and the corresponding glucocorticoid (total, 18.5 h). When cells were intended for gene expression analysis by real-time (RT) polymerase chain reaction (PCR) or for protein expression analysis by immunoblot after TGF-β_1 stimulation, cells were stimulated in 6-well plates with TGF-β_1 (2 ng/ml) for 12 h and the appropriate glucocorticoid after 18 h of pre-treatment with the corresponding glucocorticoid (total, 30 h).

Assessment of the BMP-responsive element pBRE-luc construct and the TGF-β-responsive p(CAGA)$_9$-luc construct induction by dual luciferase assay will be discussed separately in section **3.2.13.2**.

Cell experiments, in which small interfering RNA (siRNA) or overexpressing plasmid constructs were employed, will also be discussed separately in sections **3.2.11** and **3.2.12**.

3.2.2 mRNA isolation

In order to isolate mRNA from according cell experiments and mouse organ tissues, two different techniques were chosen.

3.2.2.1 mRNA isolation from cells

The PeqGOLD Total RNA Kit was used to isolate mRNA from cultured NIH/3T3 mouse fibroblast-like cells following the manufacturer's instructions.

3.2.2.2 mRNA isolation from mouse lung, heart, liver, and kidney

The Peqlab/Ceramic Kit 1.4 mm 91-PCS-CK14 was used to isolate mRNA from whole organ homogenates following the manufacturer's instructions.

3.2.3 Determining mRNA concentrations

According to the Peqlab protocol, 1.5 µl of sample solution was administered to Peqlab's Nanodrop® spectrophotometer to determine the concentration of isolated mRNA.

3.2.4 Reverse transcription reaction

The reverse transcription reaction is an enzymatic reaction in which the reverse transcriptase enzyme synthesizes complementary DNA (cDNA) from template mRNA. In order to perform this technique, RNase-free water was added to 1000 ng of the according mRNA sample to form a total volume of 20 µl. For denaturation this reaction mixture was heated at 70 °C for 10 min before adding 20 µl of mastermix (Table 3.2) and performing the reverse transcription reaction (Table 3.1).

Table 3.1 Reverse transcription reaction

Cycle	Temperature [°C]	Duration [min]	Effect
1	21	10	Attachment of random hexamers
2	43	75	Reverse transcription
3	99	5	Reverse transcription inactivation
4	4	Not specific	Cooling down

Table 3.2 Mastermix composition for the reverse transcription reaction

Mastermix [amount/sample]	
Reagent	**Volume [µl]**
10× PCR-buffer	4
$MgCl_2$ solution	8
PCR nucleotide mix	2
Random hexamers	2
RNase inhibitor	1
MnLV reverse transcriptase	2
RNase-free water	1

After amplification, 60 µl of RNase free water were added to each sample to form a total volume of 100 µl. Samples were then directly used RT PCR experiments or frozen at -20 °C.

3.2.5 Real-time polymerase chain reaction

Real-time PCR is a DNA polymerase-driven reaction, in which specific cDNA sequences can be amplified with according primers (listed in section **11.3**) and quantified at the same time. In general, the amplification process consists of three steps which form one cycle.

Denaturation: separation of double-stranded DNA into two single strands
Annealing: primer binding to the according sequence of single DNA strands
Elongation: synthesis of double-stranded DNA from single-stranded DNA by DNA polymerase

In order to quantify relative mRNA levels of a certain gene, a fluorescent dye (SYBR® Green I) is added to the RT PCR reaction mix (Table 3.3). SYBR® Green I binds directly to double-stranded DNA and its fluorescence intensity can be detected specifically after each PCR cycle using the StepOne Plus RT PCR Detection System. This fluorescence intensity is proportionate to the amount of amplified DNA of a certain gene. The RT PCR reaction program is described in Table 3.4.

Table 3.3 Composition of the reaction mix for real-time PCR analysis

Real-time PCR reaction mix [amount/well]	
Reagent	**Volume [µl]**
Platinum® SYBR® Green qPCR SuperMix-UDG	13
50 mM $MgCl_2$	1
10 µM forward primer	0.5
10 µM reverse primer	0.5
H_2O (autoclaved)	8
cDNA template	2

Table 3.4 Real-time PCR reaction program

Real-time PCR reaction program			
Step	**Temperature [°C]**	**Duration**	**Cycles**
Initialization/polymerase activation	95	10 min	
Denaturation	95	10 sec	40
Annealing of primers	59	10 sec	40
Elongation	72	10 sec	40
Denaturation	95	1 min	40
Melting curve	55 - 95	Variable	40
Cooling down	25	Not specific	

3.2.6 Determining relative mRNA expression by StepOne Software

The StepOne Software was used to determine relative mRNA levels of the according gene by following the developer's instructions. All results were normalized to relative mRNA expression levels of the constitutively expressed glyceraldehyde 3-phosphate dehydrogenase gene (*gapdh*), which served as an internal control. Relative mRNA levels of the according gene were calculated as ΔCt values ($\Delta Ct=Ct_{internal\ control}-Ct_{target}$). ΔΔCt values were calculated ($\Delta\Delta Ct=\Delta Ct_{treated}-\Delta Ct_{control}$). All ΔΔCt values correspond approximately to the binary logarithm of the fold change. Finally, changes in mRNA expression were shown as fold-change using the following formula: fold-change=$2^{\Delta\Delta Ct}$ values.

3.2.7 Protein isolation

In order to isolate proteins from cell culture experiments and mouse lung tissue, two different techniques were chosen.

3.2.7.1 Protein isolation from cells

Lysis buffer (Table 3.5) was prepared before isolating proteins from cultured cells. Then, 40 µl of sodium *ortho* vanadate and 160 µl of Complete™ protease inhibitor were then added to 4 ml of lysis buffer and vortexed. After pipetting 150 µl of this mixture into each well on a 6-well plate containing cultured cells from experiments, cells were detached by using a cellscraper and transferred to a 1.5 ml tube. The cell suspension was then incubated on ice for 30 min, during which it was vortexed every 5 min. After centrifuging, the suspension for 15 min at 13000 rpm and 4 °C, the resulting supernatant was used as cell extract, transferred to a 0.5 ml tube and frozen at -40 °C.

Table 3.5 Composition of the protein lysis buffer

Protein lysis buffer	
Reagent	**Concentration**
Tris, pH 7.5	20 mM
NaCl	150 mM
Ethylene dinitrilo-N, N, *N*, *N*′-tetra-acetic-acid (EDTA)	1 mM
Ethylene glycol-bis (2-amino-ethylether)-N, N, *N*′, *N*′-tetraacetic-acid (EGTA)	1 mM
NP-40	0.5%

3.2.7.2 Protein isolation from mouse lungs

The Peqlab/Ceramic Kit 1.4 mm 91-PCS-CK14 was used to isolate proteins from whole organ homogenates following the manufacturer's instructions. For cell lysis buffer composition see section **3.2.7.1**.

3.2.8 Determining protein concentrations

Protein concentrations from cell and tissue extracts were spectro-photometrically assessed by using Bradford reagent and an ELISA plate reader. Bradford reagent is able to bind to basic and aromatic amino acid residues, which results in a change of color. Color intensity depends on the sample protein concentration and can be quantified by using a spectrophotometer. Defined

concentrations of bovine serum albumin (0.05-0.5 µg/µl) were used to create a standard protein curve. The sample protein concentration was determined by comparing the sample's absorbance with the absorbance of the known protein concentrations on the standard protein curve.

3.2.9 SDS polyacrylamide gel electrophoresis

Protein samples were separated by use of SDS polyacrylamide gel electrophoresis. Resolving (Table 3.6) and stacking gels (Table 3.7) were prepared in advance. The resolving gel was poured between two glass plates with a spacer in between and was left to polymerize for approximately 30 min with isopropanol on top. After polymerization, isopropanol was removed. The stacking gel was poured on top of the resolving gel and left to polymerize for approximately 30 min, after adding a comb to form wells in each gel. Each protein sample contained 25 µl of protein. Then, 10% of 10× SDS loading buffer was added to each 25 µl protein sample before denaturation at 95 °C for 10 min. After denaturation, protein samples were pipetted into the according wells and electrophoresis was carried out in 1× running buffer (Table 3.8) by applying 110 V for 90 min. The first well in a gel always contained 10 µl of standard protein marker, which served as a protein molecular mass kDa reference.

Table 3.6 Composition of a 10% resolving gel for immunoblot analysis

10% resolving gel [amount/gel]	
Reagent	**Volume**
H_2O	3.2 ml
30% acrylamide	2.67 ml
1.5 M Tris, pH 8.8	2 ml
10% SDS	80 µl
10% APS	80 µl
TEMED	8 µl

Table 3.7 Composition of a 10% stacking gel for immunoblot analysis

10% stacking gel [amount/gel]	
Reagent	**Volume**
H_2O	3.4 ml
30% acrylamide	0.8 ml
1.0 M Tris, pH 6.8	0.6 ml
10% SDS	50 µl
10% APS	50 µl
TEMED	5 µl

Table 3.8 Composition of a 10× SDS running buffer for immunoblot analysis

10× SDS running buffer for 1L stock solution	
Reagent	**Amount [g]**
Tris	30
Glycine	144
SDS	10

Bring up the volume to 1 L with distilled water. For 1× running buffer mix 100 ml of 10× SDS running buffer with 900 ml of distilled water.

3.2.10 Immunoblot analysis

Immunoblot analysis is performed in order to detect and visualize certain proteins which have been separated by SDS polyacrylamide gel electrophoresis (see section **3.2.9**).

3.2.10.1 Immunoblotting

Immunoblotting was performed after protein separation by SDS polyacrylamide gel electrophoresis. Proteins were transferred from a polyacrylamide gel to a 0.2 µm thick pure nitrocellulose membrane in 1× transfer buffer (Table 3.9) by applying 110 V for 60 min. After transfer, nitrocellulose membranes were blocked in 5% milk-blocking buffer (Table 3.10) for 60 min at room temperature.

Table 3.9 Composition of a 10× transfer buffer for immunoblot analysis

10× transfer buffer for 1L stock solution	
Reagent	**Amount [g]**
Tris	24.5
Glycine	122

Bring up the volume to 1 L with distilled water. For a 1× transfer buffer, mix 100 ml of 10× transfer buffer with 700 ml of distilled water and 200 ml of methanol.

Table 3.10 Composition of a 5% milk-blocking buffer for immunoblot analysis

5% milk-blocking buffer	
Reagent	**Amount**
Dry milk powder	5 g
1× PBS washing buffer	100 ml

Table 3.11 Composition of a 1× PBS washing buffer for immunoblot analysis

1× PBS washing buffer	
Reagent	**Volume [ml]**
10× PBS	99
Tween 20	1
Distilled water	900

3.2.10.2 Protein visualization

After blocking, membranes were incubated with the appropriate primary antibody diluted in 5% milk-blocking buffer (Table 3.10) overnight at 4 °C. All primary antibodies were used at appropriate concentrations (Table 11.1). Membranes were then washed in 1× PBS-washing buffer (Table 3.11) for 30 min, during which the washing buffer was changed every 10 min. Next, membranes were incubated with the according horseradish peroxidase (HRP)-coupled secondary antibody diluted in 5% milk-blocking buffer for 60 min at room temperature. All secondary antibodies were used at according concentrations (Table 11.2). After incubation with the second antibody, membranes were again washed in 1× PBS washing buffer for 60 min, during

which the washing buffer was changed every 10 min. Finally, protein bands were visualized using the SuperSignal® West Femto Maximum Sensitivity Substrate chemiluminescence detection kit following the manufacturer's instructions. Membranes were then exposed to a digital imaging system (LAS-4000 cooled CCD camera, FujiFilm, Japan) for quantitative imaging. Pictures were saved as ".tif" files and subsequently processed with the Adobe Photoshop CS3 Software.

3.2.10.3 Membrane stripping

In order to reprobe certain membranes with different primary and appropriate secondary antibodies, membranes were stripped in 50 ml of stripping buffer (Table 3.12) and 347 µl of β-mercaptoethanol at 52 °C for 5 min. Protein visualization with the according primary and secondary antibodies was then performed as described in section **3.2.10.2**.

Table 3.12 Composition of a stripping buffer for immunoblot analysis

Stripping buffer	
Reagent	**Volume [ml]**
1.0 M Tris, pH 6.8	31
10% SDS	10
1× PBS washing buffer	459

3.2.10.4 Determining protein density by Multi Gauge MFC Software

The Multi Gauge MFC Software was used to quantify protein density by following the developer's instructions. Statistical analysis of the data was performed as described in section **3.2.15**.

3.2.11 Transfection of cells with small interfering RNA

Specific small interfering RNA oligonucleotides directed against mouse *tgfbr3* and *smad1* mRNA (Table 11.4) were employed for transfection of NIH/3T3 mouse fibroblast-like cells. Cells were transfected with 200 nM of the according siRNA using Lipofectamin™ 2000 and OptiMEM. In order to control these experiments, control cells were also treated with a non-specific siRNA (Table 11.4) which served as a negative control for siRNA-mediated ablation of the according gene mRNA expression. OptiMEM was first added to the according amount of siRNA and left to incubate for 15 min at room temperature. OptiMEM was also added to the according amount of Lipofectamin™ 2000 and also left to incubate for 15 min at room temperature. These

two mixtures were then added together and left to incubate for another 15 min at room temperature. After this last incubation period, a certain amount of this mixture was then added directly to supplemented D-MEM media (see section **3.2.1.1**) and the according cells. Before specific treatment with dex, cells were left to incubate with the according siRNA for 6 h. Depending on whether cells were intended for Smad protein phosphorylation analysis by immunoblot (see section **3.2.11.1**) or for induction analysis of the appropriate promoter by dual luciferase assay analysis (see section **3.2.13.3**), different protocols were applied.

3.2.11.1 Experimental cell culture setup for knock-down experiments

After a 6-h incubation period with specific siRNA alone, cells remained untreated or stimulated with dex (20 nM) for 18 h, during which time siRNA was not removed (total mRNA ablation time, 24 h). After this 24-h mRNA ablation period, media was changed and cells intended for Smad protein phosphorylation analysis by immunoblot or induction analysis of the according promoter cells by dual luciferase assay analysis were stimulated as described in section **3.2.1.1**.

3.2.12 Transfection of cells with *TGFBR3*-expressing plasmid constructs

The human *TGFBR3* gene, which was amplified from human lung cDNA, was cloned into the pIRES hrGFPII plasmid vector (supplied by Gero Niess). Cells were transfected with these plasmids using Lipofectamin^{TM} 2000 and OptiMEM. In order to control these experiments, cells were also treated with empty pIRES hrGFPII plasmids to serve as a negative control. Firstly, OptiMEM was added to plasmids and left to incubate for 15 min at room temperature. OptiMEM was also added to the appropriate amount of Lipofectamin^{TM} 2000 and also left to incubate for 15 min at room temperature. These two mixtures were then added together and left to incubate for another 15 min at room temperature. After this last incubation period, a certain amount of this mixture was then directly added to supplemented D-MEM media (see section **3.2.1.1**) and according cells. Before specific treatment with TGF-β_1 (2 ng/ml), cells were left to incubate with appropriate plasmids for 6 h. Depending on whether cells were intended for Smad protein phosphorylation analysis by immunoblot (see section **3.2.12.1**) or for induction analysis of the appropriate promoter by dual luciferase assay analysis (see section **3.2.13.4**), different protocols were applied.

3.2.12.1 Experimental cell culture setup for overexpression experiments

For Smad1 protein phosphorylation analysis, transfected cells were then stimulated with TGF-β_1 (2 ng/ml) for 30 min. Cells which were intended for induction

analysis of the appropriate promoter by dual luciferase assay analysis, were treated as described in section **3.2.1.1**.

3.2.13 Dual luciferase ratio assay analysis

The dual luciferase ratio (DLR) assay analysis is a technique to assess promoter induction of a certain gene which is incorporated into an according plasmid. Therefore, this technique is able to detect the activity of according signaling pathways. In principle, the according gene promoter is cloned into a special plasmid construct upstream of the firefly luciferase gene, which encodes for the luciferase enzyme. This special plasmid is then transfected into cells. The luciferase enzyme activity can be measured by employing a special fluorescence luciferase assay reagent substrate (Promega, USA). Fluorescence, which is emitted during the luciferase enzyme-driven reaction can be detected with a microplate luminometer. Fluorescence intensity is proportional to promoter induction of the firefly luciferase gene and, therefore, to the signaling pathway activity of interest. In order to control this experiment, the constitutively-active *Renillla* luciferase simian virus 40 (SV40)-based plasmid construct is simultaneously transfected into cells containing the firefly luciferase reporter to serve as a reference. This *Renilla* luciferase gene encodes for the luciferase enzyme and is constitutively active. This enzyme activity can also be measured by employing a special fluorescence luciferase substrate (Promega, USA). The fluorescence which is emitted during this enzymatic reaction can also be detected with a microplate luminometer. After transfecting cells with according plasmids (see section **3.2.13.1**), cells were stimulated according to protocol (see sections, **3.2.13.2**, **3.2.13.3** and **3.2.13.4**). For normalization, all raw firefly values were then divided by the corresponding *Renilla* values from the same cell lysate.

3.2.13.1 Transfection of cells with corresponding plasmids

After passaging, the cells intended for dual luciferase assay experiments were pipetted into the wells of a 48-well cell culture plate and left to become confluent for 24 h. OptiMEM was first added to a suspension containing the firefly luciferase plasmid construct ($p(CAGA)_9$-luc construct or pBRE-luc construct containing the gene promoter of interest and the *Renilla* luciferase reporter plasmid construct to form a total volume of 50 µl. This suspension was mixed carefully and left to incubate for 15 min. Then, 49.25 µl of OptiMEM were also added to 0.75 µl of Lipofectamin^{TM} 2000 and also left to incubate for 15 min at room temperature. These two mixtures were then added together to form a total volume of 100 µl, mixed carefully and left to incubate for another 20 min at room temperature. Media was then removed from each well and

cells were washed with ice cold 1× PBS solution. After removing 1× PBS solution from each well, 100 µl of transfection mixture was pipetted into each well and left to incubate for 6 h at 37 °C, 5% CO_2, and 95-100% humidity. After a 6-h incubation period, the transfection mixture was removed from each well and cells were stimulated according to protocol (see sections **3.2.13.2**, **3.2.13.3** and **3.2.13.4**). In order to control this experiment, cells on one 48-well cell culture plate were also transfected with a constitutively-active firefly luciferase plasmid construct and the constitutively-active *Renilla* luciferase plasmid construct as positive control. Furthermore, cells were transfected with a constitutively inactive-firefly luciferase plasmid construct and the constitutively-active *Renilla* luciferase plasmid construct serving as a negative control. Another group of cells was transfected with the constitutively-active *Renilla* luciferase plasmid construct only, another group with OptiMEM and Lipofectamin™ 2000 only, and the last group did not receive any transfection reagents.

3.2.13.2 Experimental cell culture setup for dual luciferase assay

After a 6-h incubation period, transfection reagents containing corresponding plasmid constructs were removed from all wells. Cells then remained untreated or were stimulated with the corresponding glucocorticoid (concentration as indicated) for 18 h. After this 18-h pre-treatment with the appropriate glucocorticoid, untreated cells were either stimulated with TGF-β_1 (2 ng/ml) for 12 h (total, 30 h) or remained unstimulated at 37 °C, 5% CO_2, and 95-100% humidity. Pre-treated cells were either stimulated with the corresponding glucocorticoid or with TGF-β_1 and the same glucocorticoid for 12 h (total, 30 h) at 37 °C, 5% CO_2, and 95-100% humidity. After drug and hormone treatment, cells were washed with ice cold 1× PBS solution and either directly used for dual luciferase experiments or frozen at -80 °C.

3.2.13.3 Experimental cell culture setup with small interfering RNA

A different protocol was applied for cells intended for analysis of promoter induction by dual luciferase assay and also employing siRNA for mRNA ablation. After a 6-h incubation period, transfection reagents containing according plasmid constructs were removed from all wells. Next, the corresponding siRNA was prepared as described as in section **3.2.11**, diluted in supplemented D-MEM media (see section **3.2.1.1**) to the indicated concentrations, added to the according cells and left to incubate for 6 h at 37 °C, 5% CO_2, and 95-100% humidity. Drug and hormone treatment was then performed as explained in section **3.2.13.2**.

3.2.13.4 Experimental cell culture setup with *TGFBR3*-expressing plasmids

A different protocol was applied for cells intended for analysis of promoter induction analysis by dual luciferase assay and also employing TGFBR3 overexpressing plasmids. After a 6-h incubation period, transfection reagents containing according plasmid constructs were removed from all wells. The TGFBR3 overexpressing constructs were then prepared as described as in section **3.2.12**, diluted in supplemented D-MEM media (see section **3.2.1.1**) to the indicated concentrations, added to the according cells, and left to incubate for 6 h at 37 °C, 5% CO_2, and 95-100% humidity. Drug and hormone treatment was then performed as explained in section **3.2.13.2**.

3.2.13.5 Cell lysis

For cell lysis 5 ml of the 5× Luciferase Lysis reagent (Promega, USA) were diluted in 20 ml of RNase-free water. Next, 100 µl of this lysis solution were then pipetted into each well containing transfected cells intended for analysis of luciferase activity and left to incubate for 20 min on a shaker at room temperature.

3.2.13.6 Determining luciferase activity

Lysed cells were then analyzed for luciferase activity by using the Luciferase assay reagent pack (Promega, USA) and the Centro LB 960 microplate luminometer (BERTHOLD TECHNOLOGIES GmbH & Co. KG, Germany) following the manufacturer's instructions. Raw values were treated as described in section **3.2.13**. Statistical data analysis was performed as described in section **3.2.15**.

3.2.14 Animal studies

All animal experiments were approved by institutional and national authorities under approval number B2/331 from the *Regierungspräsidium Darmstadt* [housing the Institutional Animal Care and Use Committee].

3.2.14.1 Pulmonary effects of dexamethasone in mice

In order to assess the impact of glucocorticoid administration on TGF-β signaling *in vivo* in the mouse lung, 50 mg of dex powder were dissolved in 10 ml of DMSO and 10 ml of 1× PBS (vehicle) to a concentration of 2.5 mg/ml. Twelve wild-type female C57BL/J6 mice were used for this animal experiment. Each mouse was 11 weeks old and weighed approximately 20 g. Then, six mice received a 0.2 ml intraperitoneal injection of dex and vehicle at 10 mg/kg bodyweight, while six control mice received a 0.2 ml intraperitoneal injection of vehicle only. Next, 24 h after drug

administration mice were sacrificed using an overdose of isoflurane, and lung lobes, the liver, the heart, and kidneys were explanted for mRNA and protein isolation.

3.2.14.2 Organ storage

After explantation, organs were immediately shock-frozen in liquid nitrogen and stored at -80 °C.

3.2.15 Statistical analysis

Data are indicated as mean ± standard deviation (S.D.). Statistical comparisons were made with an unpaired Student's *t*-test and by one-way ANOVA, followed by a Bonferroni *post-hoc* test, to evaluate whether differences between means were significant.

4. Results

4.1 Glucocorticoids inhibit classical Tgfbr1/Smad2/3 signaling in NIH/3T3 mouse fibroblast-like cells

4.1.1 p(CAGA)$_9$ induction analysis by dual luciferase assay

The interaction of glucocorticoid and TGF-β signaling was first analyzed by induction analysis of the (CAGA)$_9$ Smad3-binding element which is common in genes regulated by the TGF-β/Tgfbr1/Smad2/3 pathway. In order to analyze induction the luminescence-based dual luciferase assay was employed (Fig. 4.1).

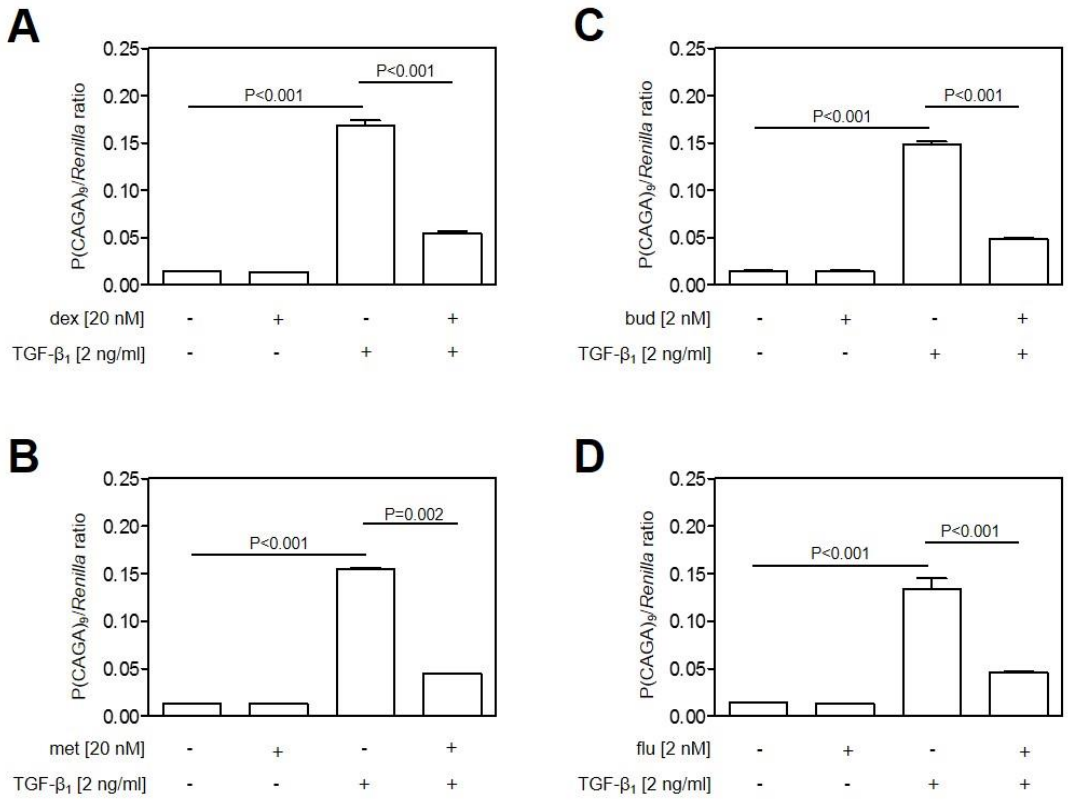

Fig. 4.1. Glucocorticoids inhibit transforming growth factor-β$_1$-induced activation of the p(CAGA)$_9$-luc promoter construct. The TGF-β$_1$-responsive p(CAGA)$_9$-luc promoter construct was transfected into NIH/3T3 cells for a duration of 6 h. Then transfected cells were stimulated with dexamethasone [dex] at a concentration of 20 nM (*A*), methylprednisolone [met] at a concentration of 20 nM (*B*), budesonide [bud] at a concentration of 2 nM (*C*), and fluticasone [flu] at a concentration of 2 nM (*D*) for a period of 18 h. Then one group of cells was stimulated with TGF-β$_1$ only at a concentration of 2 ng/ml for a duration of 12 h. Glucocorticoid-treated cells were either treated with the same glucocorticoid or the same glucocorticoid and TGF-β$_1$ at a concentration of 2 ng/ml for 12 h. Media was then removed, cells were washed in ice cold 1× PBS, and finally incubated in lysis buffer. A dual luciferase assay was employed to assess activity of the p(CAGA)$_9$-luc construct. Data are presented as mean ± S.D. Experiments were repeated six times. One-way ANOVA and Bonferroni *post-hoc* analyses were used to analyze whether differences between groups were significant. *P*-values <0.05 were considered significant.

Stimulation with TGF-β_1 stimulation for 12 h resulted in strong activation of the $(CAGA)_9$ element of the p$(CAGA)_9$-luc construct (Fig. 4.1*A*, *B*, *C*, *D*) when comparing the first and third bar. Glucocorticoid treatment with indicated concentrations did not affect activation of the p$(CAGA)_9$ element (Fig. 4.1*A*, *B*, *C*, *D*) when comparing the first and second bar. Interestingly, when comparing the third and fourth bar, treatment with dex in the presence of TGF-β_1 inhibited the activation of the p$(CAGA)_9$ element (Fig*A*. 4.1). Methylprednisolone, bud, and flu all had a similar effect on TGF-β_1-induced Tgfbr1/Smad2/3 pathway activation. Overall, this indicates that corticosteroids are able to effectively inhibit activation of the p$(CAGA)_9$ element via Tgfbr1/Smad2/3 signaling.

4.1.2 Immunoblot analysis of phospho-Smad2 and phospho-Smad3

After examining distal effects along the Tgfbr1/Smad2/3 axis, the impact of corticosteroids on proximal Smad2 and Smad3 activation was assessed by immunoblot analysis (Fig. 4.2).

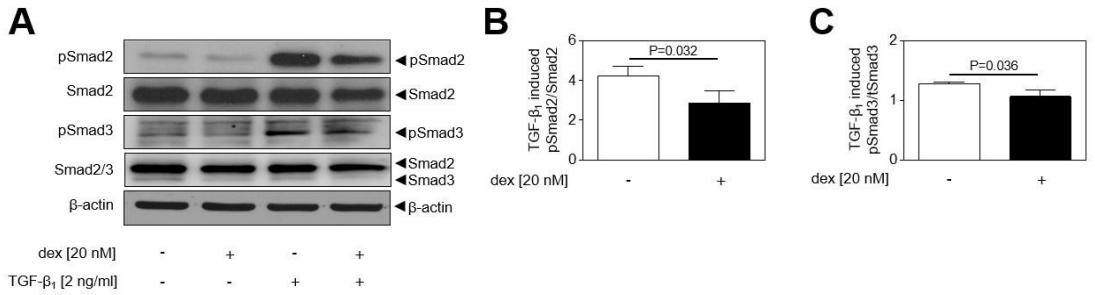

Fig. 4.2 Corticosteroids inhibit transforming growth factor-β_1-induced phosphorylation of Smad2 and Smad3. Cells were stimulated with dexamethasone [dex] at a concentration of 20 nM for 18 h. Then one group of cells was stimulated with TGF-β_1 only at a concentration of 2 ng/ml for 30 min. Dexamethasone-treated cells were either then again treated with dexamethasone or dexamethasone in combination with TGF-β_1 at a concentration of 2 ng/ml for a duration of 30 min. Media was then removed, cells were washed in ice cold 1× PBS, and finally incubated in lysis buffer. Proteins were then isolated in order to assess Smad2 and Smad3 phosphorylation by immunoblot analysis (*A*). Densitometric analysis was used to quantify Smad2 and Smad3 phosphorylation (*B*,*C*). Data in *B* and *C* are presented as mean ± S.D. Experiments were repeated three times. An unpaired Student's *t*-test was used to analyze whether differences between groups were significant. *P*-values <0.05 were considered significant.

After activation by TGF-β_1, Tgfbr1 phosphorylates the intracellular signaling messengers Smad2 and Smad3. Stimulation of NIH/3T3 cells with TGF-β_1 for 30 min resulted in strong phosphorylation of Smad2 and Smad3. This was evident when comparing the first and third lane in Fig. 4.2*A*. Dexamethasone treatment of NIH/3T3 alone already resulted in less phosphorylation of Smad2 and Smad3 which was visible when comparing the first and second lane in Fig. 4.2*A*. After pre-treatment with dex, when comparing lane three and lane four in Fig. 4.2*A*, TGF-β_1-induced activation of Smad2 and Smad3 was significantly less pronounced. Smad2 (Fig. 4.2*B*) and Smad3

(Fig. 4.2*C*) phosphorylation were quantified by densitometric analysis. Overall, these immunoblot data taken together with the dual luciferase analysis (Fig. 4.1) suggest that glucocorticoids inhibit the proximal and distal part of the Tgfbr1/Smad2/3 signaling pathway in NIH/3T3 cells.

4.2 Dexamethasone increases relative *tgfbr3* mRNA expression levels in NIH/3T3 mouse fibroblast-like cells

Dexamethasone, met, bud, and flu were all able to block activation of the Tgfbr1/Smad2/3 signaling pathway. In order to explain this observation the impact of dexamethasone and TGF-β_1 on different TGF-β receptor mRNA expression levels was assessed by RT PCR (Fig. 4.3).

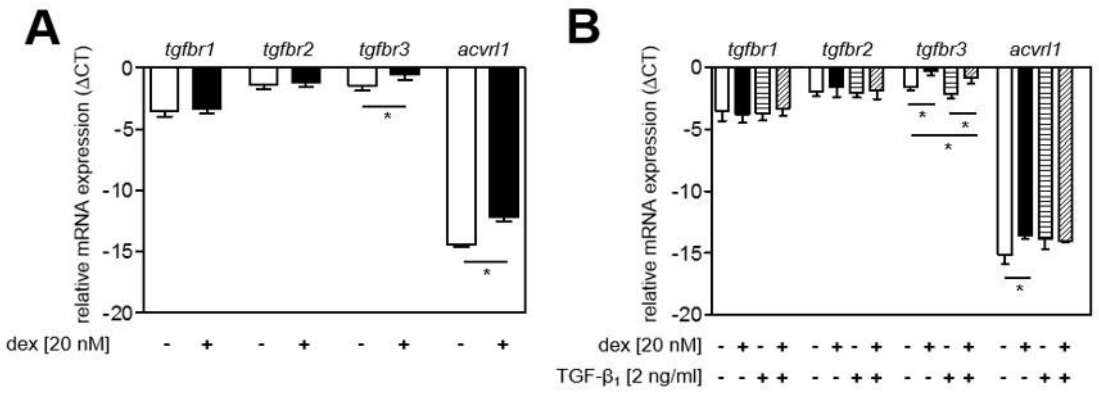

Fig. 4.3 Glucocorticoids induce relative *tgfbr3* mRNA expression levels in NIH/3T3 mouse fibroblast-like cells. In the first experiment cells were treated with dexamethasone [dex] only for 18 h at a concentration of 20 nM (*A*). Experiments were repeated 4 times. In a second experiment cells were treated with dexamethasone at a concentration of 20 nM for a duration of 18 h (*B*). Then one group of cells was stimulated with TGF-β_1 only at a concentration of 2 ng/ml for a duration of 12 h. Dexamethasone-treated cells were either then again treated with dexamethasone or dexamethasone in combination with TGF-β_1 at a concentration of 2 ng/ml for a period of 12 h (*B*). Media was then removed, cells were washed in ice cold 1× PBS, and finally incubated in lysis buffer. Relative mRNA expression was assessed by RT PCR in order to assess levels of *tgfbr1*, *tgfbr2*, *tgfbr3*, and *acvrl1*. These experiments were repeated four times. Data are presented as mean ± S.D. An unpaired Student's *t*-test was used to analyze whether differences between groups were significant. *P*-values <0.05 were considered significant. * indicates a *P*-value <0.05.

Cells treated with dex for a duration of 18 h demonstrated increased relative *tgfbr3* mRNA expression levels (Fig. 4.3*A*). In a second experiment dex in the presence of TGF-β_1 was still able to increase *tgfbr3* mRNA expression levels (Fig. 4.3*B*). Also, cells receiving dex treatment only demonstrated increased relative *acvrl1* expression levels after 18 h (Fig. 4.3*A*) and 30 h (Fig. 4.3*B*). This significant increase was lost in the presence of TGF-β_1 (Fig. 4.3*B*). Relative *tgfbr1* and *tgfbr2* mRNA expression levels remained unaffected by dex and TGF-β_1 treatment (Fig. 4.3*A*,*B*). Taken together, dex, even in the presence of TGF-β_1 (2 ng/ml), increased *tgfbr3* mRNA levels in NIH/3T3 mouse fibroblast-like cells.

4.3 Glucocorticoids recruit Tgfbr3 to shift TGF-β signaling from the Tgfbr1/Smad2/3 axis to the Acvrl1/Smad1 axis

4.3.1 p(CAGA)$_9$ induction analysis by dual luciferase assay after *tgfbr3* knock-down

Dexamethasone upregulated *tgfbr3* mRNA expression in NIH/3T3 cells after 18 and 30 h (Fig. 4.3*A*,*B*). This was paralleled by increased Tgfbr3 protein expression in the same cell type after dex treatment when comparing lane one and lane three in Fig. 4.5*A*. In order to assess the functional relevance of Tgfbr3 on dex effects on Tgfbr1/Smad2/3 pathway activity a *tgfbr3* knock-down experiment was performed employing siRNA directed against *tgfbr3* mRNA (Fig. 4.4*A*).

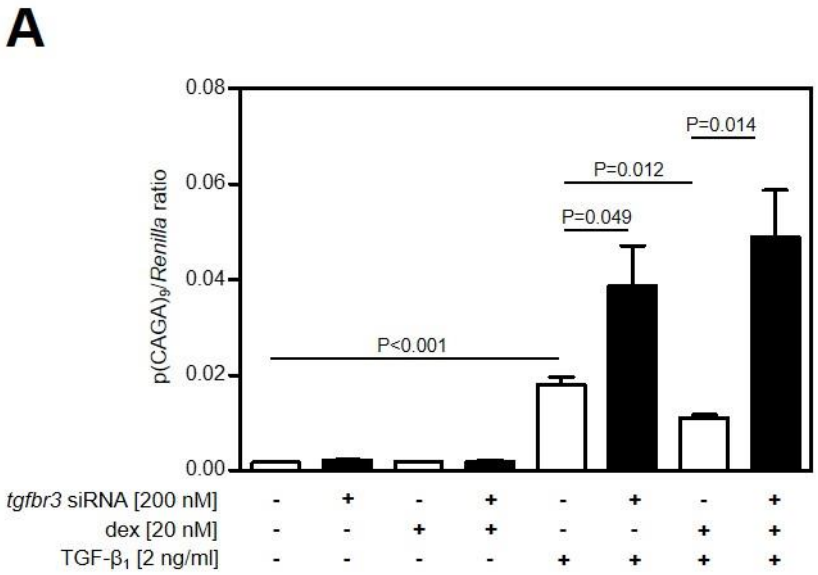

Fig. 4.4 p(CAGA)$_9$ induction analysis by dual luciferase assay after *tgfbr3* knock-down. The TGF-β_1-responsive p(CAGA)$_9$-luc promoter construct was transfected into NIH/3T3 cells for a duration of 6 h. Next, *tgfbr3* siRNA at a concentration of 200 nM and indicated by black bars (*A*) and scrambled siRNA at a concentration of 200 nM and indicated by white bars (*A*) were transfected into these cells for another 6-h period. Transfected cells were stimulated with dexamethasone [dex] at a concentration of 20 nM (*A*) for a period of 18 h. Then one group of cells was stimulated with TGF-β_1 only at a concentration of 2 ng/ml for a duration of 12 h. Dexamethasone-treated cells were either then treated with dexamethasone again or dexamethasone in combination with TGF-β_1 at a concentration of 2 ng/ml for another 12 h. Media was then removed, cells were washed in ice cold 1× PBS, and finally incubated in lysis buffer. A dual luciferase assay was used to assess activity of the p(CAGA)$_9$-luc promoter construct. Data are presented as mean ± S.D. Experiments were repeated six times. One-way ANOVA and Bonferroni *post-hoc* analyses were used to analyze whether differences between groups were significant. *P*-values <0.05 were considered significant.

Transforming growth factor-β_1 strongly induced p(CAGA)$_9$ element activity (Fig. 4.4*A*) which is visible when analyzing the first and third bar. When Tgfbr3 expression was knocked down, the effect of TGF-β_1 on p(CAGA)$_9$ element activity was

even stronger (Fig. 4.4*A*). This is visible when comparing the fifth and sixth bar. This indicates that Tgfbr3 may act inhibitory on Tgfbr1/Smad2/3 signaling in this cell type. As demonstrated in the first experiment (Fig. 4.1*A*), dex significantly reduced TGF-β_1-induced p$(CAGA)_9$ element activity (Fig. 4.4*A*). However, this blocking effect of dex was lost in cells lacking Tgfbr3 indicating that this accessory receptor may mediate the effects of dex on Tgfbr1/Smad2/3 pathway activity when comparing bar seven and bar eight in Fig. 4.4*A*.

4.3.2 Immunoblot analysis of phospho-Smad1/5/8, phospho-Smad2, and phospho-Smad3 after *tgfbr3* knock-down

Next, the proximal aspects of Tgfbr1/Smad2/3 and Acvrl1/Smad1 signaling were investigated in the context of a *tgfbr3* knock-down (Fig. 4.5).

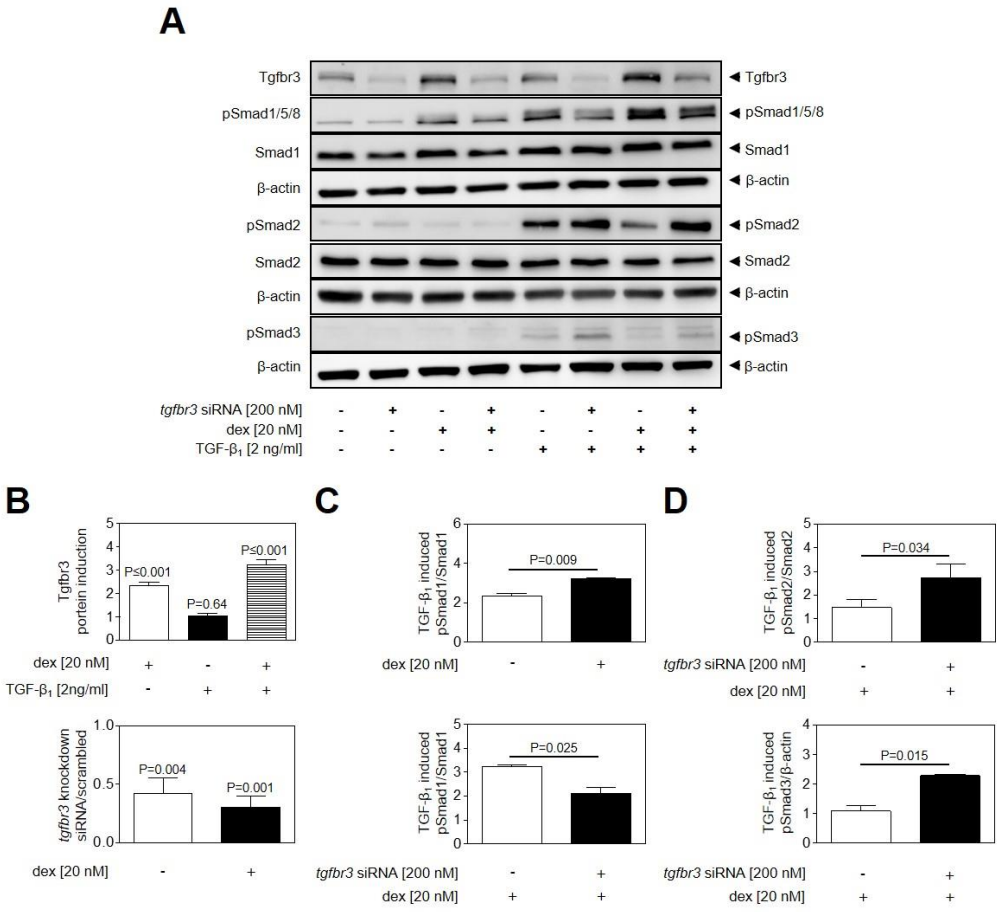

Fig. 4.5 Immunoblot analysis of phospho-Smad1/5/8, phospho-Smad2, and phospho-Smad3 after *tgfbr3* knock-down. Knock-down *tgfbr3* siRNA at a concentration of 200 nM and indicated by black bars (*A*) and scrambled siRNA at a concentration of 200 nM and indicated by white bars (*A*) were transfected into NIH/3T3 cells for a duration of 6 h. Transfected cells were stimulated with dexamethasone [dex] at a concentration of 20 nM (*A*) for a period of 18 h. Then one group of cells was stimulated with TGF-β_1 only at a concentration of 2 ng/ml for a duration 30 min. Dexamethasone-treated cells were either then treated with dexamethasone again or dexamethasone in combination with TGF-β_1 at a concentration of 2 ng/ml for another 30 min. Media was then removed, cells were washed in ice cold 1× PBS, and finally incubated in lysis buffer. Proteins were then isolated in order to assess Smad1, Smad2, and Smad3 phosphorylation as well as total Smad1, Smad2, Smad3, and Tgfbr3 protein levels by immunoblot analysis (*A*). Densitometric analysis was used to quantify immunoblot bands (*B*,*C*,*D*). Data in *B*, *C*, and *D* are presented as mean ± S.D. Experiments were repeated three times. An unpaired Student's *t*-test was used to analyze whether differences between groups were significant. *P*-values <0.05 were considered significant. Significances in *B* were calculated with an unpaired Student's *t*-test comparing dexamethasone and TGF-β_1-induced protein induction with non-treated cells.

Phosphorylation of Smad1, Smad2, and Smad3 were analyzed by immunoblot (Fig. 4.5*A*) and quantified in three individual experiments. Knock-down efficiency was assessed by analyzing Tgfbr3 protein expression in cells transfected with siRNA

directed against *tgfbr3* mRNA and quantified. Transforming growth factor-β_1 strongly phosphorylated Smad2 and Smad3 after 30 min (Fig. 4.5*A*). This effect was visible when comparing the first and fifth lane. In lane six cells lacking Tgfbr3 demonstrated pronounced activation of Smad2 and Smad3 (Fig. 4.5*A*). This indicates that Tgfbr3 acts antagonistically to Tgfbr1/Smad2/3 in NIH/3T3 cells. Furthermore, the inhibitory effect of dex on aTGF-β_1-induced phosphorylation of Smad2 and Smad3 was lost in the absence of Tgfbr3 (Fig. 4.5*A*). This became clear when comparing lane seven and lane eight. This indicates that dex requires the accessory Tgfbr3 to inhibit the Tgfbr1/Smad2/3 signaling pathway.

Interestingly, in lane three dex induced Smad1 phosphorylation (Fig. 4.5*A*). Smad1 is activated by Acvrl1 and, therefore, represents an alternative TGF-β signaling route. Transforming growth factor-β_1 alone also stimulated Smad1 phosphorylation (Fig. 4.5*A*). This was visible when comparing lane five with lane one. This effect was potentiated in the presence of dex (Fig. 4.5*A*) which was visible when comparing lane seven with the first, third, and fifth lane. In cells lacking Tgfbr3, less Smad1 phosphorylation was observed in all cases (Fig. 4.5*A*). This indicates that dex uses Tgfbr3 to redirect TGF-β signaling from the Tgfbr1/Smad2/3 pathway to the Acvrl1/Smad1 pathway.

4.4 Overexpression of TGFBR3 activates the Acvrl1/Smad1 axis

4.4.1 Immunoblot analysis of phospho-Smad1/5/8 after TGFBR3 overexpression

In order to test whether Tgfbr3 alone was able to activate the Acvrl1/Smad1 signaling axis, a plasmid construct expressing *TGFBR3* was transfected into NIH/3T3 cells (Fig. 4.6*A*). Overexpression of TGFBR3 in this cell type dose-dependently resulted in increased Smad1 phosphorylation. This was visible when analyzing lanes seven, nine, and eleven and lanes one, three, and five (Fig. 4.6*A*). In combination with TGF-β_1 this effect could even be potentiated (Fig. 4.6*A*). This became evident by comparing lane eight with lane seven, lanes ten with lane nine, and lane twelve with lane eleven. Furthermore, TGFBR3 overexpression resulted in a similar protein increase as seen after stimulation with dex (Fig. 4.5*A*). This proves that this increase in Tgfbr3 protein levels is enough to activate the Acvrl1/Smad1 signaling pathway.

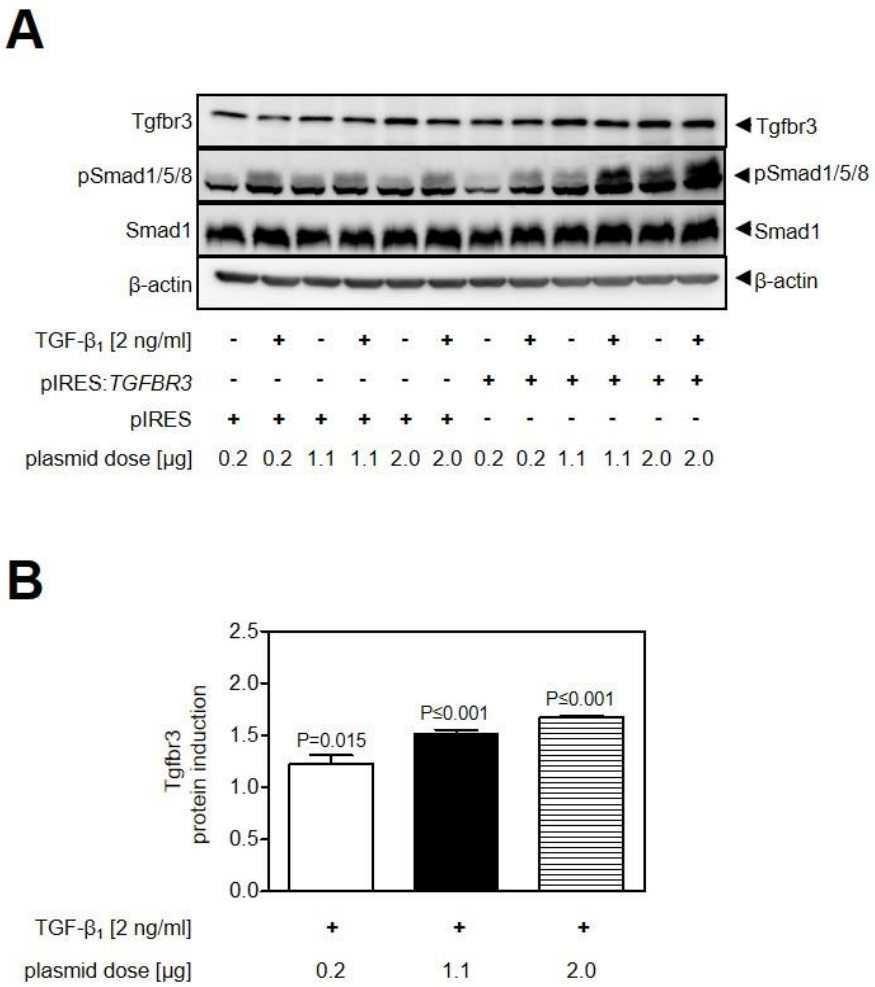

Fig. 4.6 Immunoblot analysis of phospho-Smad1/5/8 after TGFBR3 overexpression. NIH/3T3 mouse fibroblast-like cells were transfected with a plasmid construct overexpressing TGFBR3 (pIRES::*TGFBR3*) and an empty vector construct (pIRES) serving as control (*A*). For this experiment 3 different doses were used. Cells were then partly stimulated with TGF-β_1 [2 ng/ml] for 30 min. Media was then removed, cells were washed in ice cold 1× PBS, and finally incubated in lysis buffer. Proteins were then isolated in order to assess Smad1/5/8 phosphorylation by immunoblot analysis. Immunoblot bands were then quantified by densitometric analysis in *B*. Data in *B* are presented as mean ± S.D. Experiments were repeated three times. An unpaired Student's *t*-test was used to analyze whether differences between groups were significant. *P*-values <0.05 were considered significant. In this case *P*-values in *B* compare mean values of cells transfected with the *TGFBR3*-expressing construct and cells transfected with the empty vector.

4.4.2 pBRE induction analysis by dual luciferase assay after TGFBR3 overexpression

Overexpression of TGFBR3 alone and in combination with TGF-β_1 resulted in increased proximal activation of the Acvrl1/Smad1 axis which was reflected by increased Smad1 phosphorylation. The next experiment was aimed at assessing distal activation of the Acvrl1/Smad1 pathway (Fig. 4.7*A*). For this, a plasmid containing the Smad1-responsive pBRE was transfected into NIH/3T3 cells after these cells were transfected with the *TGFBR3*-expressing construct (pIRES::*TGFBR3*; 2 µg) or the

pIRES empty vector construct serving as control. Overexpression of TGFBR3 resulted in increased pBRE-luc construct activity indicating increased downstream activity of the Acvrl1/Smad1 pathway. Overall, overexpression of TGFBR3 in NIH/3T3 cells resulted in increased proximal and distal activation of the Acvrl1/Smad1 pathway suggesting that this type III TGF-β co-receptor favors this TGF-β pathway in this cell type.

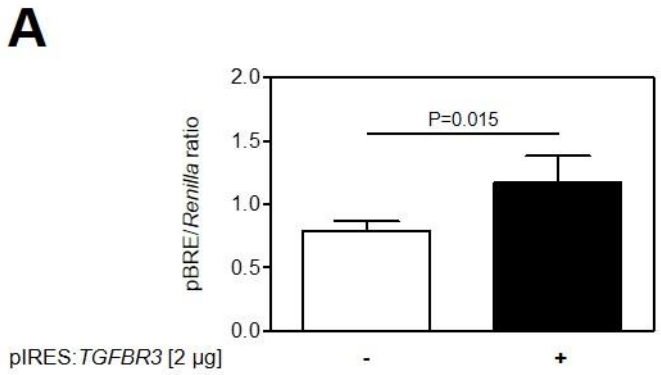

Fig. 4.7 p(BRE) induction analysis by dual luciferase assay after TGFBR3 overexpression. NIH/3T3 mouse fibroblast-like cells were transfected with the pBRE-luc promoter construct for 6 h. Next, *TGFBR3*-expressing plasmids (pIRES::*TGFBR3*) and empty vector constructs (pIRES) were transfected into these cells. Media was then removed, cells were washed in ice cold 1× PBS, and finally incubated in lysis buffer. A dual luciferase assay was used to assess the activation of the pBRE-luc plasmid construct. Data are presented as mean ± S.D. This experiment was repeated six times. An unpaired Student's *t*-test was used to analyze whether differences between groups were significant. *P*-values <0.05 were considered significant.

4.5 Glucocorticoids also require Smad1 to effectively inhibit Tgfbr1/Smad2/3 signaling

4.5.1 p(CAGA)$_9$ induction analysis by dual luciferase assay after *smad1* knock-down

Dexamethasone and TGF-β_1 treatment as well as overexpression of TGFBR3 all resulted in increased Smad1 phosphorylation (Fig. 4.5*A* and Fig. 4.6*A*). This suggested that this intracellular messenger might also be involved in the ability of glucocorticoids to redirect TGF-β signaling to the Acvrl1/Smad1 axis. Therefore, the next experiment was aimed at examining the effects of dex and TGF-β_1 on downstream activity of the Tgfbr1/Smad2 pathway in the absence of Smad1 by employing siRNA directed against *smad1* mRNA (Fig. 4.8*A*). As previously demonstrated, TGF-β_1 increased p(CAGA)$_9$ activity when comparing bar five and bar one in Fig. 4.8*A*. Similar to the results obtained from the *tgfbr3* knock-down experiment (Fig. 4.5*A*) the effect of TGF-β_1 stimulation on p(CAGA)$_9$ activity in the absence of *smad1* was stronger indicating a negative regulatory effect of Smad1 on Tgfbr1/Smad2/3 signaling. This

was evident when comparing bar five with bar six in Fig. 4.8*A*. As expected dex decreased TGF-β_1-induced p(CAGA)$_9$ activity when comparing bar five with bar seven in Fig. 4.8*A*. This inhibitory effect was lost in *smad1*-deficient cells indicating that dex also requires Smad1 in order to inhibit Tgrbr1/Smad2/3 downstream activity.

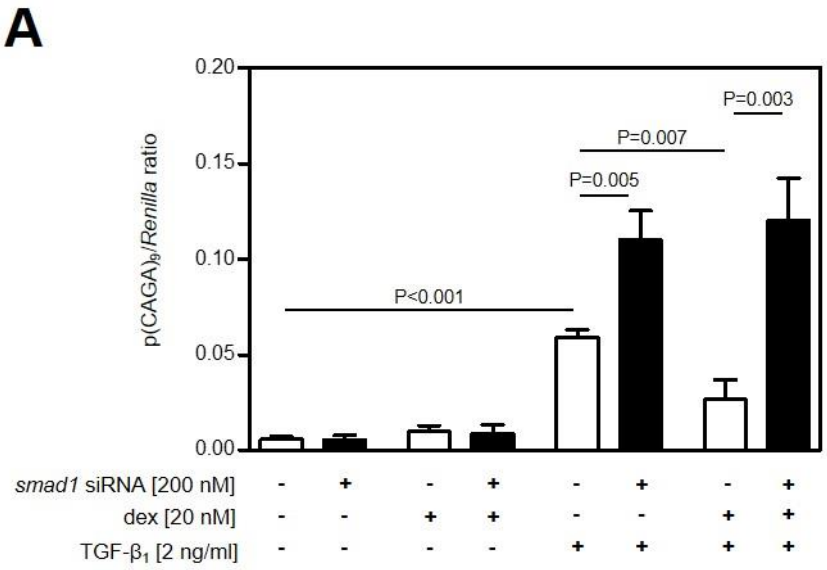

Fig. 4.8 p(CAGA)$_9$ induction analysis by dual luciferase assay after *smad1* knock-down. Knock-down *smad1* siRNA at a concentration of 200 nM and indicated by black bars (*A*) and scrambled siRNA at a concentration of 200 nM and indicated by white bars (*A*) were transfected into NIH/3T3 cells for a duration of 6 h. Transfected cells were stimulated with dexamethasone [dex] at a concentration of 20 nM (*A*) for a period of 18 h. Then one group of cells was stimulated with TGF-β_1 only at a concentration of 2 ng/ml for a duration of 12 h. Dexamethasone-treated cells were either then treated with dexamethasone again or dexamethasone in combination with TGF-β_1 at a concentration of 2 ng/ml for another 12 h. Media was then removed, cells were washed in ice cold 1× PBS, and finally incubated in lysis buffer. A dual luciferase assay was used to assess activity of the p(CAGA)$_9$-luc promoter construct. Data are presented as mean ± S.D. Experiments were repeated six times. One-way ANOVA and Bonferroni *post-hoc* analyses were used to analyze whether differences between groups were significant. *P*-values <0.05 were considered significant.

4.5.2 Immunoblot analysis of phospho-Smad2 after *smad1* knock-down

In the previous experiment *smad1*-deficient cells demonstrated increased Tgfbr1/Smad2/3 signaling after TGF-β_1 stimulation. Furthermore, this phenomenon could not be inhibited by dex treatment in cells lacking *smad1*. The next experiment was aimed at analyzing proximal signaling activity in the context of a *smad1* knock-down (Fig. 4.9). As expected TGF-β_1 stimulation for 30 min resulted in increased phosphorylation of Smad2. This was evident when comparing lane five with lane one in Fig. 4.9*A*. This effect, similar to the results obtained from the *tgfbr3* knock-down experiment, was more pronounced in *smad1*-deficient cells indicating antagonistic effects of Smad1 on Smad2 phosphorylation when comparing lane five with lane six in Fig. 4.9*A*. Dexamethasone inhibited TGF-β_1-induced phosphorylation of Smad2 which is visible when comparing lane seven and lane nine (Fig. 4.9*A*). However, this blocking

effect of dex was lost in smad1-deficient cells (Fig. 4.9*A*). This becomes visible when comparing lane eight and lane seven (Fig. 4.9*A*). In conclusion, these data suggest that Smad1 antagonizes the Tgfbr1/Smad2/3 pathway. Furthermore, dex recruits Smad1 to block Tgfbr1/Smad2/3 activity.

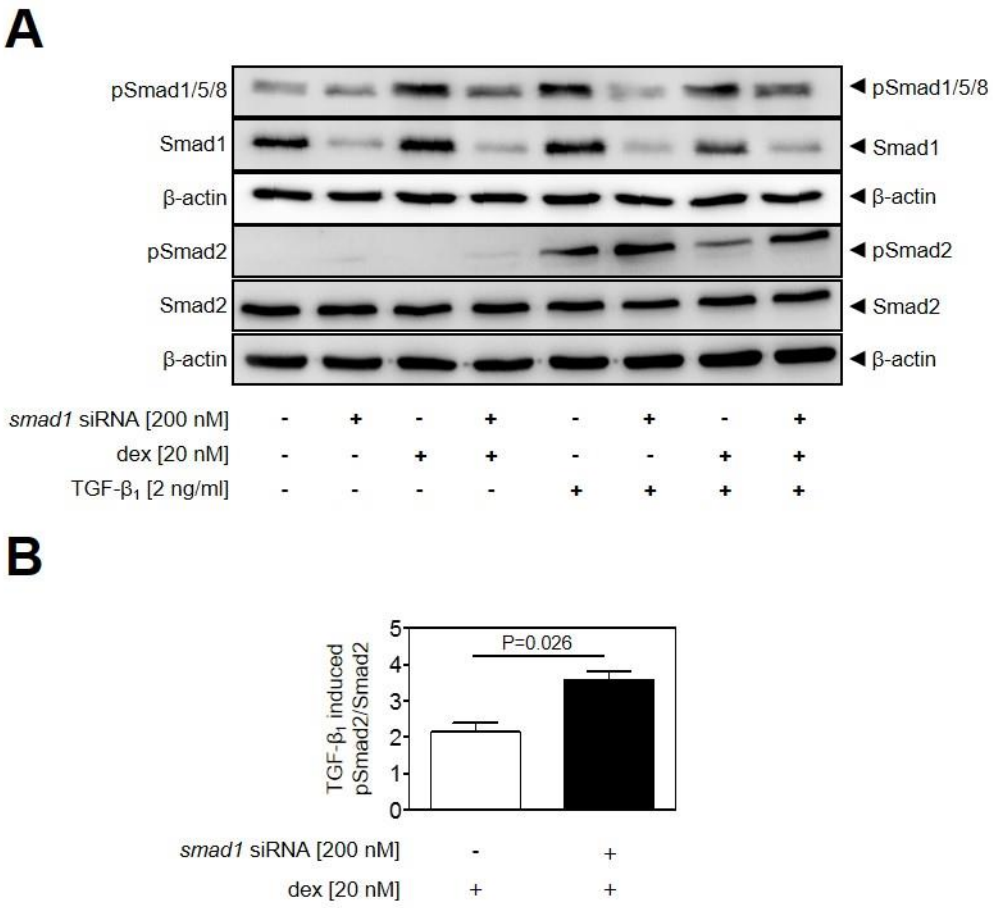

Fig. 4.9 Immunoblot analysis of phospho-Smad2 after *smad1* knock-down. Knock-down *smad1* siRNA at a concentration of 200 nM and indicated by black bars (*A*) and scrambled siRNA at a concentration of 200 nM and indicated by white bars (*A*) were transfected into NIH/3T3 cells for a duration of 6 h. Transfected cells were stimulated with dexamethasone [dex] at a concentration of 20 nM (*A*) for a period of 18 h. Then one group of cells was stimulated with TGF-β_1 only at a concentration of 2 ng/ml for a duration of 30 min. Dexamethasone-treated cells were either then treated with dexamethasone again or dexamethasone in combination with TGF-β_1 at a concentration of 2 ng/ml for another 30 min. Media was then removed, cells were washed in ice cold 1× PBS, and finally incubated in lysis buffer. Proteins were then isolated in order to assess Smad1 and Smad2 phosphorylation as well as total Smad1 and total Smad2 protein levels by immunoblot analysis (*A*). Densitometric analysis was used to quantify immunoblot bands (*B*). Data in *B* are presented as mean ± S.D. Experiments were repeated three times. An unpaired Student's *t*-test was used to analyze whether differences between the two groups were significant. *P*-values <0.05 were considered significant.

4.6 Effect of dexamethasone on primary lung fibroblasts

In NIH/3T3 mouse fibroblast-like cells dex inhibited proximal and distal Tgfbr1/Smad2/3 pathway activity and redirected TGF-β signaling to the Acvrl1/Smad1 axis. However, this cell type is often only used as a cell model for fibroblasts. In order to translate these observations into primary cells, fibroblasts were isolated from mouse lungs and subjected to the same stimulation protocol used for NIH/3T3 cells (Fig. 4.10*A*,*B*). As expected TGF-β_1 stimulation increased p(CAGA)$_9$ element activity (Fig. 4.10*A*). This was visible by comparing the first and third bar. Comparing the fourth with the third bar dex significantly inhibited TGF-β_1-stimulated p(CAGA)$_9$ element activity (Fig. 4.10*A*). This observation is in line with the data obtained from the same experiment in NIH/3T3 cells. Like in NIH/3T3 cells stimulation with TGF-β_1 for 30 min resulted in increased Smad2 and Smad3 phosphorylation (Fig. 4.10*B*). This effect was visible when comparing lane three and lane one. As seen in 3T3 cells dex significantly inhibited TGF-β_1-induced Smad3 phosphorylation whereas TGF-β_1-induced Smad1 phosphorylation was potentiated. This effect was visible when comparing lane four with lane three. Smad2 phosphorylation in contrast to 3T3 cells remained unaffected (Fig. 4.10*B*).

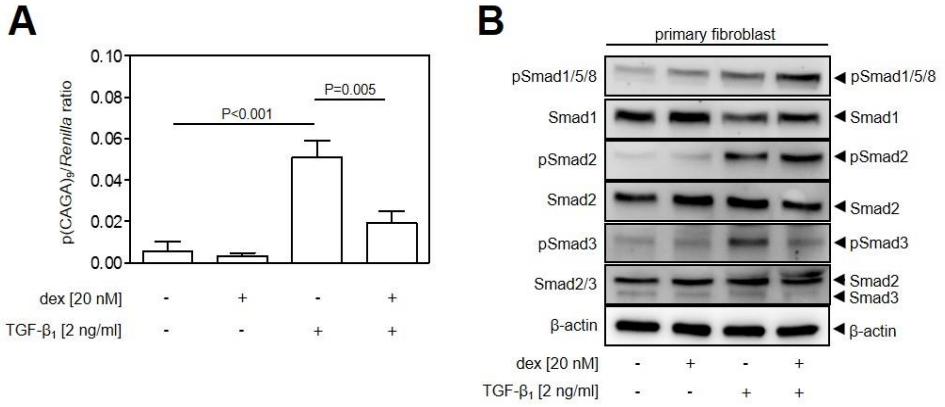

Fig. 4.10 Dexamethasone modulates Tgfbr1/Smad2/3 and Acvrl1/Smad1 signaling in primary mouse lung fibroblasts. Primary mouse lung fibroblasts were isolated from mouse lungs as described in section **3.2.1.2**. *A*, The TGF-β_1-responsive p(CAGA)$_9$-luc promoter construct was transfected into these isolated cells for a duration of 6 h. Then transfected cells were stimulated with dexamethasone [dex] at a concentration of 20 nM (*A*) for a period of 18 h. Then one group of cells was stimulated with TGF-β_1 only at a concentration of 2 ng/ml for a duration of 12 h. Dexamethasone-treated cells were either treated with dexamethasone or dexamethasone and TGF-β_1 at a concentration of 2 ng/ml for 12 h. A dual luciferase assay was employed to assess activity of the p(CAGA)$_9$-luc promoter construct. Data are presented as mean ± S.D. Experiments were repeated three times. One-way ANOVA and Bonferroni *post-hoc* analyses were used to analyze whether differences between groups were significant. *P*-values <0.05 were considered significant. *B*, Cells were stimulated with dexamethasone [dex] at a concentration of 20 nM for 18 h. Then one group of cells was stimulated with TGF-β_1 only at a concentration of 2 ng/ml for 30 min. Dexamethasone-treated cells were either then again treated with dexamethasone or dexamethasone in combination with TGF-β_1 at a concentration of 2 ng/ml for a duration of 30 min. Media was then removed, cells were washed in ice cold 1× PBS, and finally incubated in lysis buffer. Proteins were then isolated in order to assess Smad2 and Smad3 phosphorylation by immunoblot analysis.

4.7 Effects of dexamethasone on other constituent cell types of the lung

Next, the effect of dex and TGF-β_1 on Tgfbr1/Smad2/3 and Avcrl1/Smad1 signaling was analyzed in primary human pulmonary artery endothelial cells (HPAEC), primary human pulmonary artery smooth muscle cells (HPASMC), and H441 human Clara-like airway epithelial cells (Fig. 4.11). Dexamethasone treatment alone induced SMAD1 phosphorylation in HPASMC and H441 cells. This was evident when comparing the first and second lane in Fig. 4.11*B*,*C*. In HPAEC this was not the case, however, when comparing lane four and lane three in Fig. 4.11*A*, in the presence of TGF-β_1, SMAD1 phosphorylation was potentiated by dex. The ability of dex to activate SMAD1 was demonstrated in all cell types. This observation is interesting as corticosteroids, therefore, may be able to activate the Acvrl1/Smad1 pathway in many pulmonary cell types. In all cell types TGF-β_1 stimulation resulted in SMAD2 and SMAD3 phosphorylation (Fig. 4.11*A*,*B*,*C*) which was evident when analyzing lane one and lane three. Similar to the observations made in fibroblasts dex strongly inhibited TGF-β_1-induced SMAD3 activation in HPAEC and HPASMC (Fig. 4.11*A*,*C*). Interestingly, SMAD2 activation in these cell types behaved in an opposite way (Fig. 4.11*A*,*C*). When comparing lane four with lane three in Fig. 4.11*B*, TGF-β_1-induced SMAD2 and SMAD3 activation remained resistant to dex treatment in H441 cells.

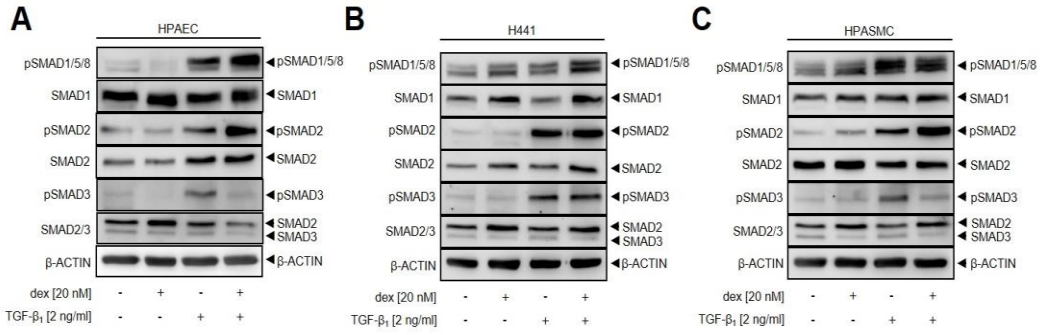

Fig. 4.11 Dexamethasone modulates Tgfbr1/Smad2/3 and Acvrl1/Smad1 signaling in other pulmonary cell types. Primary human pulmonary artery endothelial cells (HPAEC) (*A*), H441 human Clara cell-like airway epithelial cells (*B*), and primary human pulmonary artery smooth muscle cells (HPASMC) (*C*) were stimulated with dexamethasone [dex] at a concentration of 20 nM for 18 h. Then one group of cells was stimulated with TGF-β_1 only at a concentration of 2 ng/ml for 30 min. Dexamethasone-treated cells were either then again treated with dexamethasone or dexamethasone in combination with TGF-β_1 at a concentration of 2 ng/ml for a duration of 30 min. Media was then removed, cells were washed in ice cold 1× PBS, and finally incubated in lysis buffer. Proteins were then isolated in order to assess SMAD1, SMAD2, and SMAD3 phosphorylation by immunoblot analysis.

4.8 Dexamethasone functionally impacts TGF-β-regulated physiological processes

Fibroblast-to-myofibroblast differentiation plays a crucial pathogenic role in inflammatory and fibrotic pulmonary diseases and is characterized by accumulation of MYH11 and ACTA2 which has been demonstrated to be an Acvrl1/Smad1-mediated process [144, 146-150]. Therefore, the next experiment was aimed at studying the effects of dex and TGF-β_1 on this process in primary human adult fibroblasts (Fig. 4.12). Neither dex, when comparing lane one with lane two in Fig. 4.12*A*, nor TGF-β_1, when comparing lane three with lane one in Fig. 4.12*A*, alone affected MYH11 protein levels. However, in combination MYH11 protein levels increased indicating a potentiating effect on myofibroblast differentiation. This was evident when comparing lane three with lane four in Fig. 4.12*A*. In contrast, when comparing lane one with lane two in Fig. 4.12*A* dex and TGF-β_1 stimulation alone increased ACTA2 protein levels in human fibroblasts. In combination, this effect was even more pronounced. This effect was evident by comparing lane four with lane three and two in Fig. 4.12*A*. Immunoblot data were quantified by densitometric analysis and are presented in Fig. 4.12*B* and *C*. Overall, these results indicate that myofibroblast differentiation is strongly induced in human fibroblasts when stimulated with dex and TGF-β_1. This observation is in line with previous results demonstrating increased pathway activity of the Acvrl1/Smad1 axis in fibroblasts stimulated with dex and TGF-β_1. This fact may be relevant in respect to patients suffering from inflammatory or fibrotic pulmonary diseases and receiving glucocorticoid treatment.

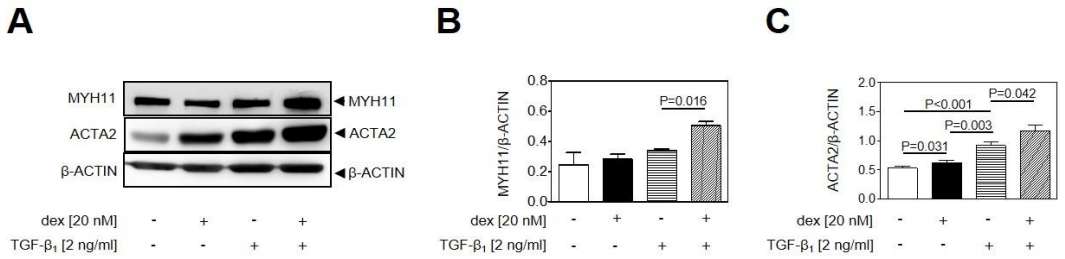

Fig. 4.12 Dexamethasone potentiates transforming growth factor-β_1-driven fibroblast-to-myofibroblast differentiation. *A*, Primary human adult fibroblasts were treated with dexamethasone [dex; 20 nM], TGF-β_1 [2 ng/ml], and TGF-β_1 [2 ng/ml] for 12 h, after 18 h pre-treatment with dexamethasone. Smooth muscle myosin (MYH11) and α-smooth muscle actin (ACTA2) served as markers of myofibroblast differentiation and were assessed by immunoblot. In order to quantify protein levels of MYH11 (*B*) and ACTA2 (*C*) densitometric analysis was performed. Results are presented as mean ± S.D. Experiments were repeated three times. One-way ANOVA and Bonferroni *post-hoc* analyses were used to analyze whether differences between groups were significant. *P*-values <0.05 were considered significant.

4.9 Glucocorticoids modulate TGF-β signaling *in vivo*

4.9.1 Glucocorticoids modulate relative *tgfbr3*, *acvrl1*, and *smad1* mRNA expression levels in whole mouse lung homogenates

In vitro experiments throughout the whole study demonstrated that glucocorticoids were able to redirect TGF-β signaling from the Tgfbr1/Smad2/3 to the Acvrl1/Smad1 signaling axis. This effect in fibroblasts resulted in increased myofibroblast differentiation which may be of pathophysiological relevance in patients suffering from the mentioned pulmonary diseases and receiving glucocorticoid treatment. In order to assess the impact of glucocorticoids on *in vivo* pulmonary Tgfbr1/Smad2/3 and Acvrl1/Smad1 signaling, dex (10 mg/kg body weight) was intraperitoneally applied to six live adult female C57BL/6J mice (Fig. 4.13).

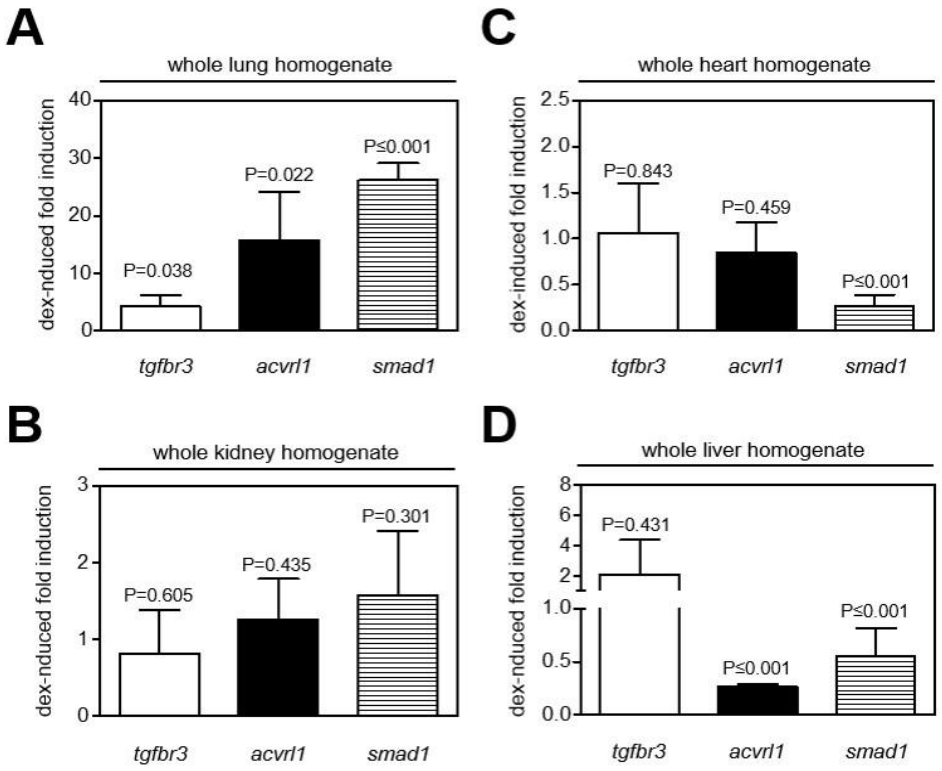

Fig. 4.13 Dexamethasone drives *tgfbr3*, *acvrl1*, and *smad1* mRNA expression in whole mouse lung homogenates. Dexamethasone [dex] at a concentration of 10 mg/kg body weight was injected intraperitoneally into six adult female C57BL/6J mice. Six control adult female C57BL/6J mice received an intraperitoneal injection of vehicle. This consisted of 200 µl of 1× PBS. Isoflurane was used to sacrifice all mice after 24 h. After opening the abdominal and chest cavities, the lungs, the heart, the kidneys, and the liver were explanted. Proteins and mRNA were then isolated according to protocol. Real-time PCR was used to assess relative mRNA levels of *smad1*, *tgfbr3*, and *acvrl1*. An unpaired Student's *t*-test was used to analyze whether differences between groups were significant. *P*-values <0.05 were considered significant. Fold-induction demonstrates expression changes of target genes between dex-treated and control animals.

Another six control mice were intraperitoneally-injected with 200 µl vehicle consisting of 1× PBS. All mice were sacrificed after 24 h. The lungs, the heart, the kidneys, and the liver were explanted for analysis. Relative *tgfbr3*, *acvrl1*, and *smad1* mRNA expression levels were increased in whole lung homogenates from dex-treated mice (Fig. 4.13*A*). The induction of these three target genes was only evident in the lung. There is no known explanation for this phenomenon. Relative expression of all target genes in the kidneys (Fig. 4.13*B*) remained unchanged. Down-regulation of *acvrl1* was detected in the liver (Fig. 4.12*D*). Relative *smad1* mRNA levels were decreased in the heart (Fig. 4.13*C*) and the liver (Fig. 4.13*D*). Overall, these *in vivo* observations demonstrate that intraperitoneal application of dex to live mice results in similar *in vitro* effects of dex on NIH/3T3 cells.

4.9.2 Dexamethasone impacts Acvrl1/Smad1 signaling in whole mouse lung homogenates

Dexamethasone increased relative *tgfbr3*, *acvrl1*, and *smad1* mRNA expression levels in mouse lung homogenates (Fig. 4.13*A*). In order to assess whether dex treatment also affected protein levels immunoblot analyses were performed on proteins isolated from whole mouse lung homogenates (Fig. 4.14). Dexamethasone increased Tgfbr3 (Fig. 4.14*D*) and Smad1 (Fig. 4.14*C*) protein expression in whole mouse lung homogenates. This was evident when comparing the first five with the last five bands in Fig. 4.14*A*. Furthermore, when comparing the first five with the last five lanes in Fig. 4.14*A*, total Smad1 levels were also increased in dex-treated animals. Therefore, Smad1 phosphorylation was also stronger in dex-treated mice. This was also visible when comparing the first five with the last five lanes in the same figure. This indicates that increased Smad1 activation is probably the consequence of increased total Smad1 levels in mouse lungs. Finally, when comparing the last five with the first five lanes in Fig. 4.14*A*, neither phospho-Smad2 nor total Smad2 protein levels were altered in dex-treated mice. All immunoblots are quantified in Fig. 4.14*B*. Unfortunately, phospho-Smad3 and total Smad3 protein levels were not reliably detectable. Overall, dex injection to live mice increased mRNA and protein expression of Tgfbr3 as well as increased *acvrl1* mRNA expression. Additionally, dex activated the Acvrl1/Smad1 pathway *in vivo* in mouse lungs. This is in line with the observations made in all pulmonary cell types. This demonstrates that glucocorticoid and TGF-β signaling crosstalk occurs *in vivo* in mice lungs. Whether this is also the case in human lungs will have to be assessed in future studies.

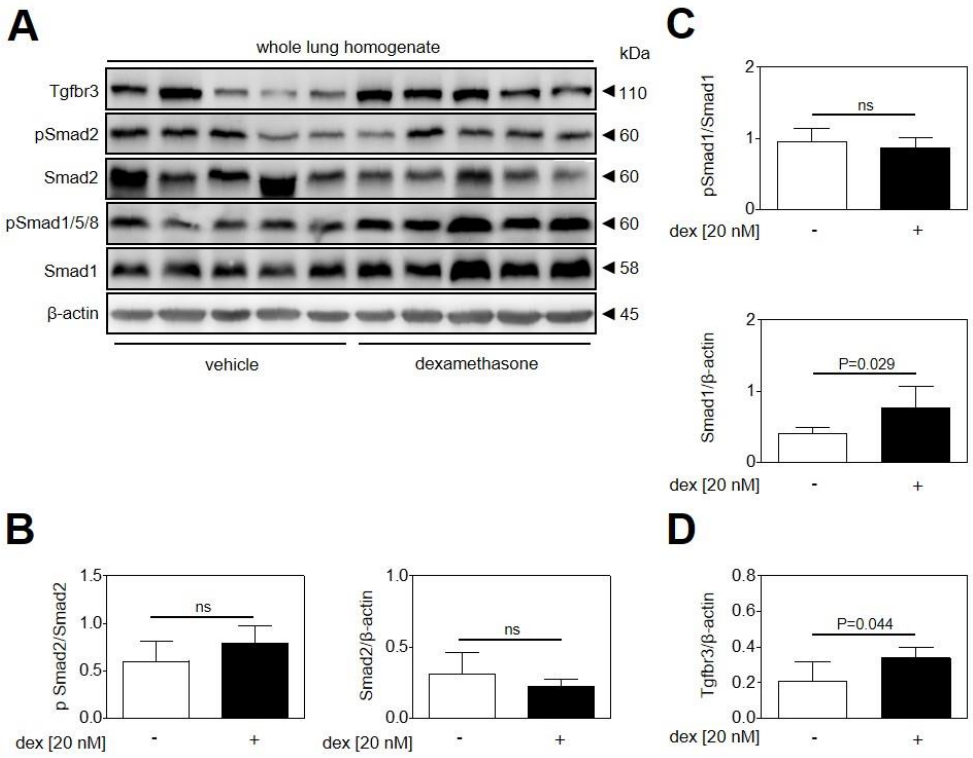

Fig. 4.14 Dexamethasone drives total Smad1 and Tgfbr3 protein expression in whole mouse lung homogenates. Dexamethasone [dex] at a concentration of 10 mg/kg body weight was injected intraperitoneally into six adult female C57BL/6J mice. Six control adult female C57BL/6J mice received an intraperitoneal injection of vehicle. This consisted of 200 µl of 1× PBS. Isoflurane was used to sacrifice all mice after 24 h. After opening the abdominal and chest cavities, the lungs, the heart, the kidneys, and the liver were explanted. Proteins and mRNA were then isolated according to protocol. Immunoblot analysis was used to assess activation of Smad1 and Smad2, as well as total Smad1, Smad2, and Tgfbr3 protein expression (*A*). Densitometry was applied to quantify immunblot bands in *B*, *C*, and *D*. Data are presented as mean ± S.D. Each group consisted of five animals. An unpaired Student's *t*-test was used to analyze whether differences between groups were significant. *P*-values <0.05 were considered significant.

5. Discussion

Corticosteroids provide outstanding management of asthma. However, this drug type has not performed well in patients suffering from ARDS, COPD, IPF, impaired lung development, and BPD in pre-term infants. The reasons why glucocorticoids fail to help patients suffering from these diseases are not clear. Transforming growth factor-β signaling is critically deregulated in all five of these diseases. Therefore, it was interesting to explore possible glucocorticoid/TGF-β signaling crosstalk as this might give new insights into why glucocorticoids do not help patients who suffer from these pulmonary diseases.

This study revealed that glucocorticoids impacted TGF-β signaling in lung fibroblasts. These observations were also made in other pulmonary cell types which were included in this study. Finally, glucocorticoid/TGF-β crosstalk was also demonstrated in lungs of living mice. Since TGF-β signaling is a disease underlying mechanism in inflammatory and fibrotic pulmonary diseases these findings are very important. Despite strong anti-inflammatory effects of glucocorticoids, application of these drugs to COPD, ARDS, BPD, and IPF patients fails to improve disease outcome. The fibroblast cell has been demonstrated to play an important role during normal lung development and physiological tissue repair. In inflammatory and fibrotic pulmonary diseases, however, this cell type is a key disease-mediating factor. Exploring possible glucocorticoid/TGF-β crosstalk in the lung may reveal why corticosteroid treatment fails in these lung pathologies.

5.1 Glucocorticoids redirect TGF-β signaling – new mechanistic insights

First experiments in this study revealed that glucocorticoids, most notably dex, were able to counter proximal Tgfbr1/Smad2/3 signaling by inhibiting phosphorylation of the intracellular messengers Smad2 and Smad3 in lung fibroblasts. As a consequence, TGF-β-induced Tgfbr1/Smad2/Smad3 downstream pathway activity was strongly reduced in the presence of glucocorticoids. Screening of TGF-β receptors and co-receptors revealed an upregulation of *tgfbr3* on gene and protein levels as a consequence of dex treatment. Therefore, it was hypothesized that this accessory receptor was somehow involved in mediating dex-induced inhibition of Smad2 and Smad3 phosphorylation. Knock-down experiments of *tgfbr3* demonstrated that the ability of dex to inhibit proximal and distal TGF-β-induced Tgrbr1 pathway activation was lost in fibroblasts lacking Tgfbr3. Analysis in this context also revealed that loss of Tgfbr3 resulted in a stronger TGF-β-induced Tgfbr1 activation in fibroblasts indicating that this co-receptor acts inhibitory on Tgfbr1/Smad2/3 signaling. This was demonstrated by increased Smad2 and Smad3 phosphorylation as well as increased

TGF-β-responsive $p(CAGA)_9$-driven luciferase production. Interestingly, Smad1 activation, which lies in the alternative Acvrl1 signaling pathway, behaved completely oppositely in fibroblasts lacking Tgfbr3. Dexamethasone treatment not only increased Tgfbr3 protein levels but also resulted in increased Smad1 phosphorylation. Furthermore, TGF-β_1 treatment also drove Smad1 phosphorylation and this effect was potentiated in the presence of dex. In the absence of Tgfbr3 activation of Smad1 was greatly decreased. Therefore, it can be stated that dex requires Tgfbr3 to redirect TGF-β signaling from the Tgfbr1/Smad2/3 pathway to the Acvrl1/Smad1 signaling axis.

In order to prove that Tgfbr3 was able to activate Smad1 in the absence of dex, the TGFBR3 was overexpressed in NIH/3T3 cells. Cells which were transefected with *TGFBR3*-expressing constructs demonstrated significantly increased Smad1 phosphorylation and this phenomenon was even more pronounced in the presence of TGF-β_1. One further experiment also revealed increased Acvrl1/Smad1 downstream activation which was detected by dual luciferase assay employing the Smad1-responsive pBRE-luc construct. Overexpression of TGFBR3 in this cell type resulted in the same increase of Tgfbr3 protein expression observed in dex-treated cells proving that this increase was sufficient to activate the Acvrl1/Smad1 pathway.

As mentioned earlier on, dex was also able to increase Smad1 phosphorylation whereas this effect can be interpreted as a Tgfbr3-mediated effect. This suggested that Smad1 might also be functionally involved in countering Tgfbr1/Smad2/3 signaling. Therefore, the next experiments were aimed at assessing Tgfbr1 pathway activation in the absence of Smad1 which was achieved in a knock-down experiment employing siRNA directed against *smad1*. Interestingly, similar observations were made as in the *tgfbr3* knock-down experiments. Transforming growth factor-β_1-induced activation of the Tgfbr1/Smad2/3 was greatly potentiated in the absence of Smad1 whereas dex lost the ability to inhibit Smad2/3 activation as well as downstream activation of TGF-β_1-driven $p(CAGA)_9$-driven luciferase production in cells lacking *smad1*.

Taken together, glucocorticoids seem to inhibit Tgfbr1/Smad2/3 signaling by two related mechanisms. Firstly, dex-induced upregulation of Tgfbr3 results in increased Acvrl1/Smad1 activation which secondly, results in decreased activation of the Tgfbr1/Smad2/3 pathway by antagonistic effects of phospho-Smad1 on Smad2 and Smad3 activation.

As NIH/3T3 mouse fibroblast-like cells serve as cell models for fibroblasts, the next experiments primary mouse lung fibroblasts were subjected to the same dex and TGF-β_1 treatment as NIH/3T3 cells. Overall, similar observations were made whereas dex potently inhibited TGF-β_1-driven Smad3 and $p(CAGA)_9$-driven luciferase production. Smad2 activation by TGF-β_1 remained unaffected by dex whereas dex

potentiated TGF-β_1-induced Smad1 activation indicating increased Acvrl1/Smad1 pathway activity.

On the basis of this present study it can only be speculated in what way betaglycan acts as a “switch” between these major TGF-β signaling axes on a functional molecular level in lung fibroblasts. One possible explanation might be that Tgfbr3 could facilitate complex formation between Tgfbr2 and Acvrl1, therefore, facilitating activation of the Acvrl1/Smad1/5/8 signaling pathway. In the past, betaglycan has been demonstrated to interact with the Tgfbr1 and Tgfbr2 in several cell types [5]. Depending on cell type and context-dependent mechanisms betaglycan can either inhibit or promote signaling properties of certain TGF-β superfamily members [5]. Whether this actually is the case on a functional molecular level will have to be the aim of future studies investigating the ability of betaglycan to modulate TGF-β signaling in lung fibroblasts.

5.2 Glucocorticoids drive fibroblast-to-myofibroblast differentiation

The first part of this study focused on exploring mechanistic insights into glucocorticoid/TGF-β signaling crosstalk. In the second part experiments were aimed at identifying a functional consequence of these observations. Fibroblast-to-myofibroblast differentiation is critical for normal physiological wound repair [143]. However, dysregulation of this physiological wound repair process has been demonstrated to play a pathological role in IPF, BPD, and ARDS [143]. In the past, TGF-β has been demonstrated to be a strong activator of this phenomenon [144, 145].

Data demonstrated that dex and TGF-β_1 synergistically drove ACTA2 and MYH11 protein expression in primary human lung fibroblasts. These findings are interesting since ACTA2 and MYH11 are both strongly expressed during fibroblast-to-myofibroblast differentiation. The expression of ACTA2 has been demonstrated to be regulated by the Acvrl1/Smad1 signaling axis [147-150]. Dysregulation of Smad1 signaling was demonstrated in a hepatic fibrosis model in rats as well as systemic sclerosis in humans, indicating that this signaling pathway may play a role in the development and progression of these partly fibrotic diseases [103, 104]. Furthermore, Smad1 signaling is activated during experimental allergic airway inflammation and suspected of driving pathology [172].

Taken together, these recent experimental findings and data from this study demonstrating synergism of glucocorticoid and TGF-β signaling in respect to activation of the Acvrl1/Smad1 axis and fibroblast-to-myofibroblast differentiation, this might provide a possible explanation as to why glucocorticoids have failed to counter progression of IPF, BPD, and ARDS. Furthermore, it should be taken into account, that

administration of glucocorticoids to critically ill patients suffering from these pulmonary diseases may even worsen disease progression due to signaling synergism in respect to Acvrl1/Smad1 signaling and activation of fibroblast-to-myofibroblast differentiation.

5.3 Pulmonary effects of dexamethasone in mice

The last part of this study was aimed at exploring whether intraperitoneal application of dex to live mice would lead to similar alterations of pulmonary *in vivo* TGF-β signaling as seen in cell models. Dexamethasone-treated mice revealed increased mRNA and protein expression of Tgfbr3 and Smad1 as well as mRNA expression of *acvrl1* in whole lung homogenates. As a consequence of increased total Smad1 levels phosphorylation of Smad1 was significantly increased. Unfortunately, it was not possible to reliably detect Smad3 or phospho-Smad3 protein levels in whole lung homogenates. Furthermore, Smad2 and phospho-Smad2 protein levels remained unaffected, which is consistent with the data obtained from primary lung fibroblasts. Interestingly, the observed effects were lung-specific. No changes in mRNA expression levels were observed in the kidneys whereas *smad1* was decreased in the heart. Furthermore, RT PCR analysis in whole liver homogenates revealed decreased expression levels of *smad1* and *acvrl1*. The reason why dex only positively impacts expression levels of target genes and proteins in the lung are not known.

Taken together, our observations suggest that glucocorticoids are able to potently activate pulmonary *in vivo* TGF-β/Acvrl1/Smad1 signaling. This is in line with our findings in lung fibroblasts. This underlies the idea that application of glucocorticoids to patients suffering from certain pulmonary diseases in which fibroblast-to-myofibroblast differentiation plays a central role could possibly even accelerate disease progression, as myofibroblast differentiation is regulated by the Acvrl1/Smad1 signaling pathway.

5.4 Glucocorticoid use in the context of lung development and BPD

Antenatal administration of glucocorticoids to pregnant mothers in danger of preterm birth have been demonstrated to be beneficial for preterm babies, as they are able to drive pulmonary surfactant production, which prevents alveoli from collapsing [153, 158]. This ultimately improves the respiratory outcome of preterm newborns. However, preterm newborns are at a high risk of developing BPD characterized by pulmonary airway and vessel simplification, which ultimately leads to an arrest of lung development [94, 121]. The number of alveoli decreases during corticosteroid treatment whereas lung maturation is stimulated [153-155]. Transforming growth factor-β signaling controls early normal and postnatal lung

development. Deregulation of TGF-β signaling plays a central role in the development and progression of BPD and CLD. Therefore, it is important to review potential glucocorticoid/TGF-β signaling crosstalk in this context [19, 105, 122]. Current recommendations state that glucocorticoid therapy is not safe in infants suffering from BPD, due to the possibility numerous short- and long-term adverse outcomes, including neurodevelopmental impairment [17].

As experiments have demonstrated, conditional overexpression of TGF-β_1 in fetal monkey lungs between postnatal days 7 and 14 resulted in a BPD-like picture [108]. As TGF-β_1 mainly signals via the Tgfbr1/Smad2/3 axis, it may be that activation of this pathway during this period of lung maturation causes inhibition of alveolarization. This study demonstrates that dex inhibits TGF-β_1-driven Smad3 phosphorylation in lung fibroblasts, human pulmonary artery endothelial cells, and human pulmonary artery smooth muscle cells. This possibly suggests that application of glucocorticoids during this period could prove beneficial for babies suffering from BPD as it might decrease pathological Smad2/3 signaling.

However, it must also be taken into account that inhibition of Smad2/3 signaling in Smad3-deficient mice between post natal days 14 and 28 caused airspace enlargement. This demonstrated that the Smad2/3 signaling had a positive effect on alveolarization during this period of lung maturation [21, 105, 109]. This study demonstrates that glucocorticoids inhibit Smad3 phosphorylation and thus activation of Tgfbr1/Smad2/3 signaling in several constituent cell types of the lung. This might explain why antenatal administration of betamethasone to preterm Rhesus monkeys resulted in a decreased number of alveoli compared to controls [153, 154]. Therefore, impairment of alveolarization is a possibility that should be taken into account when treating preterm babies with glucocorticoids.

Overall, normal lung development very much depends on TGF-β signaling being “just right” between certain time points [110]. Modulation of Tgfbr1/Smad2/3 signaling should always be considered when preterm neonates are being treated with glucocorticoids to increase pulmonary surfactant synthesis in order to prevent alveoli from collapsing. However, as experimental studies suggest, the timing of glucocorticoid administration may be critical.

Bronchopulmonary dysplasia pathogenesis is highly complex. However, ventilator-induced lung injury which may also result in local pulmonary hyperoxia represents a major risk factor for developing CLD. Unfortunately, intubation of preterm newborns may be necessary in order to provide sufficient arterial oxygenation. Experiments have revealed that the above-mentioned condition leads to increased TGF-β signaling as well as increased myofibroblast differentiation, which is associated

with arrested alveolar development [123, 124]. This study demonstrates that dex and TGF-β_1 synergistically drive myofibroblast differentiation *in vitro* via the Acvrl1/Smad1 signaling pathway, which is also activated in adult mice lungs *in vivo*. This poses the question whether administration of glucocorticoids may activate this pathological feature of BPD in preterm neonates and ultimately worsen pulmonary outcome.

5.5 Glucocorticoid use in the context of lung disease

Idiopathic pulmonary fibrosis is a devastating disease and characterized by progressive worsening of dyspnea and lung function and is associated with a poor prognosis [13]. Although inflammation seems to play a central role in disease development, it does not seem to feature prominently in the pathogenesis of disease progression as patients do not benefit from anti-inflammatory therapy [13, 14, 18, 20, 126]. Interestingly, Smad3-deficient mouse lungs demonstrated only little evidence of fibrosis and no upregulation of fibrogenesis-associated genes, suggesting a key role for Smad3 as an intracellular mediator of TGF-β signaling in the pathogenesis of progression in IPF [18, 21]. This observation raises the question why glucocorticoids do not negatively impact disease progression, as data from this study demonstrates a negative impact of dex on Smad3 phosphorylation and Tgfbr1/Smad2/3 downstream activation in lung fibroblasts.

A further study revealed that upregulation of *CCN2*, which represents a strong pro-fibrotic component, was mediated by Acvrl1/Smad1 signaling in a model of scleroderma fibrosis [173]. This is interesting, since *CCN2* is also regulated by the Tgfbr1/Smad2/3 axis [77]. Fibroblasts from systemic sclerosis patients demonstrated increased Smad1 phosphorylation levels, which strongly correlated with CTGF levels and directly increased *CCN2* promoter activity [103]. This implicates that classical Tgfbr1/Smad2/3 signaling may not be the only major TGF-β pathway dysregulated in pulmonary fibrosis. As this study suggests dex and TGF-β_1 potently and synergistically activate Acvrl1/Smad1 signaling, which could potentially worsen disease progression and might be an explanation as to why glucocorticoids do not work in patients suffering from this disease.

What is also known so far is that glucocorticoids are not able to counter IL-13-mediated differentiation of fibroblasts into myofibroblasts, which is also dysregulated in pulmonary fibrosis [166, 167]. This is in line with this study's observations, however, from the data it can be concluded that glucocorticoids alone and in combination with TGF-β_1 synergistically drive myofibroblast differentiation in lung fibroblasts which is a Smad1-regulated process. Therefore, it can be concluded that glucocorticoids redirect TGF-β signaling towards the (i) potentially pro-fibrotic

Acvrl1/Smad1 pathway and (ii) towards increased fibroblast-to-myofibroblast differentiation.

Further studies employing corticosteroids in pulmonary fibrosis animal studies should perhaps specifically target the Acvrl1/Smad1 pathway with inhibitors, and at the same time employ glucocorticoids to inhibit classical Tgfbr1/Smad2/3 signaling.

Acute respiratory distress syndrome results in bilateral diffuse pulmonary inflammation, which leads to increased pulmonary vascular permeability and ultimately to a loss of arterial blood oxygenation [128]. Dysregulation of TGF-β signaling has been associated with epithelial destruction and formation of alveolar edema during the early phase of ARDS, as well as with progressive pulmonary fibrosis, which can occur in the late phase of this disease [22, 129].

Glucocorticoids should blunt diffuse pulmonary inflammation and decrease vascular permeability but have actually failed to demonstrate benefits for patients suffering from this devastating syndrome. It was demonstrated that fibroblast proliferation and increased collagen turnover occur in the early phase of ARDS, which have both been associated with increased mortality [130-132]. It is known that glucocorticoids, when employed in high concentrations, inhibit fibroblast proliferation and collagen synthesis [8]. One study employing the dual luciferase ratio assay demonstrated that plasmids containing the procollagen I promoter transfected into human fibroblasts were induced by stimulation with BALF from ARDS patients, whereas specific TGF-β_1 antibodies attenuated this effect [130]. Unfortunately, this study did not assess proximal TGF-β signaling, as this would have given insights into whether this effect is mediated by Tgfbr1/Smad2/3 or the Acvrl1/Smad1/5/8 axis or even both. Indeed, as mentioned earlier it can be assumed that certain genes like *CCN2* can be regulated by both pathways [77, 173]. Therefore, also concluding from the data presented in the present study dex strongly reduces TGF-β_1-driven Smad3 activation while Acvrl1/Smad1 signaling in lung fibroblasts is increased, which may be bad.

Similar as observed in IPF and BPD, it can be assumed that dysregulation of fibroblast-to-myofibroblast differentiation plays a major role in the pathogenesis of ARDS [143]. In this context, it is again possible that, in combination with endogenous TGF-β signaling, glucocorticoids could potentially worsen this phenomenon in patients suffering from this disease. Therefore, future studies of corticosteroid effects in ARDS animal models should assess activation of pulmonary Acvrl1/Smad1 signaling and downstream targets of this pathway.

Asthma is a chronic disease characterized by inflammation and remodeling of the airways, with airway hyper-responsiveness and reduced lung function [96]. Transforming growth factor-β_1 plays a central role in airway remodeling, which includes microvascular changes, airway smooth muscle remodeling and subepithelial fibrosis: key histopathological features of asthmatic patients [96, 97]. Together with β_2-agonists inhaled corticosteroid treatment has been very effective in children and adults suffering from asthma [11]. They reduce airway hyperresponsiveness, inhibit inflammatory cell migration as well as activation, block late-phase reaction to allergens, and reduce the risk of exacerbation [11]. However, in children it is reported that they do not alter progression or underlying severity of the disease [11].

One experimental study focussing on airway inflammation found that Smad1 phosphorylation was greatly increased in bronchial epithelial cells in experimental allergic airway inflammation [172]. It is suspected that this could possibly drive pathology. This study demonstrates that dex drives phosphorylation of SMAD1 in human H441 cells which serve as a cell model for bronchial epithelial cells. Interestingly, dex did not counter TGF-β_1-driven SMAD2 and SMAD3 phosphorylation in this cell type. This demonstrates two important facts: namely that (i) dex may possibly drive SMAD1 signaling, which is a potential disease-underlying pathway in asthmatic patients and (ii) dex does not counter classical TGFBR1/SMAD2/3 signaling in this cell type, which is also dysregulated in asthma.

Chronic obstructive pulmonary disease is characterized by chronic airway inflammation accompanied by irreversible expiratory airflow limitation, which is caused by SAD and emphysema [96]. Chronic inflammation and dysregulation of TGF-β signaling are central mediators in disease pathology [96]. Interestingly, TGF-β signaling seems to behave in contradictory ways in SAD and emphysema. While TGF-β signaling seems to be increased in small airway epithelium, decreased TGF-β signaling seems to contribute to airway enlargement and emphysema [119, 134, 138, 142]. Inhaled corticosteroids have been demonstrated to reduce symptoms of dyspnea and the number of exacerbations, but have failed to reduce the frequency of hospitalizations [12, 168, 169]. Overall, corticosteroid treatment cannot counter progression of this disease. The reason for this is not apparent. If the data from this study are interpreted in the context of COPD, two important facts come to mind. First of all, as mentioned in the context of asthma, human epithelial cells are resistant to dex-mediated inhibition of TGFBR1/SMAD2/3 signaling. This might also be the case in COPD patients. Secondly, dex, the inhaled corticosteroids flu and bud, decrease Tgfbr1/Smad2/3 in lung fibroblasts, suggesting that this may potentially have an

adverse effect on the development of emphysema, as decreased Smad3 signaling seems to contribute to the development of airspace enlargement.

6. References

1. Unsöld, C., *et al.*, *Latent TGF-beta binding protein LTBP-1 contains three potential extracellular matrix interacting domains.* Journal of Cell Science, 2001. **114**(Pt 1): p. 187-197.
2. Koli, K., *et al.*, *Latency, activation, and binding proteins of TGF-beta.* Microscopy Research and Technique, 2001. **52**(4): p. 354-362.
3. Bobik, A., *Transforming growth factor-betas and vascular disorders.* Arteriosclerosis, Thrombosis, and Vascular Biology, 2006. **26**(8): p. 1712-20.
4. Attisano, L. and Wrana, J.L., *Mads and Smads in TGF beta signalling.* Current Opinion in Cell Biology, 1998. **10**(2): p. 188-94.
5. Bilandzic, M. and Stenvers, K.L., *Reprint of: Betaglycan: a multifunctional accessory.* Molecular and Cellular Endocrinology, 2012. **359**(1-2): p. 13-22.
6. Mutschler, E., Geisslinger, G., Kroemer, H. K., Schäfer-Korting, M., *Mutschler Arzneimittelwirkung*. 8th ed. 2001, Stuttgart, G: Wissenschaftliche Verlagsgesellschaft mit beschränkter Haftung Stuttgart 2001: p. 63.
7. Barnes, P.J., *Corticosteroid effects on cell signalling.* European Respiratory Journal, 2006. **27**(2): p. 413-26.
8. Mutschler, E., Geisslinger, G., Kroemer, H. K., Schäfer-Korting, M., *Mutschler Arzneimittelwirkung*. 8th ed. 2001, Stuttgart, G: Wissenschaftliche Verlagsgesellschaft mit beschränkter Haftung Stuttgart 2001: p. 423-428.
9. Freel, E.M. and Connell, J.M., *Mechanisms of hypertension: the expanding role of aldosterone.* Journal of the American Society of Nephrology, 2004. **15**(8): p. 1993-2001.
10. Rhen, T. and Cidlowski, J.A., *Antiinflammatory action of glucocorticoids-new mechanisms for old drugs.* New England Journal of Medicine, 2005. **353**(16): p. 1711-23.
11. *Expert Panel Report 3 (EPR-3): Guidelines for the Diagnosis and Management of Asthma-Summary Report 2007.* Journal of Allergy and Clinical Immunology, 2007. **120**(5 Suppl): p. S94-138.
12. Qaseem, A., *et al*., *Diagnosis and management of stable chronic obstructive pulmonary disease: a clinical practice guideline update from the American College of Physicians, American College of Chest Physicians, American Thoracic Society, and European Respiratory Society.* Annals of Internal Medicine, 2011. **155**(3): p. 179-91.
13. Raghu, G., *et al.*, *An official ATS/ERS/JRS/ALAT statement: idiopathic pulmonary fibrosis: evidence-based guidelines for diagnosis and management.* American Journal of Respiratory and Critical Care Medicine **183**(6): p. 788-824.

14. Flaherty, K.R., *et al.*, *Steroids in idiopathic pulmonary fibrosis: a prospective assessment of adverse reactions, response to therapy, and survival.* American Journal of Medicine, 2001. **110**(4): p. 278-82.
15. Kluge, S., Muller, T., and Pfeifer, M., *[Current approaches to the treatment of severe hypoxic respiratory insufficiency (acute lung injury; acute respiratory distress syndrome)].* Deutsche Medizinische Wochenschrift, 2011. **136**(5): p. 186-9.
16. Steinberg, K.P., *et al.*, *Efficacy and safety of corticosteroids for persistent acute respiratory distress syndrome.* New England Journal of Medicine, 2006. **354**(16): p. 1671-84.
17. Jarreau, P.H., *et al.*, *The use of postnatal corticosteroid therapy in premature infants to prevent or treat bronchopulmonary dysplasia: current situation and recommendations.* Archives of Pediatrics, 2010. **17**(10): p. 1480-7.
18. Gauldie, J., *et al.*, *TGF-beta, Smad3 and the process of progressive fibrosis.* Biochemical Society Transactions, 2007. **35**(Pt 4): p. 661-4.
19. Gauldie, J., *et al.*, *Transfer of the active form of transforming growth factor-beta 1 gene to newborn rat lung induces changes consistent with bronchopulmonary dysplasia.* The American Journal of Pathology, 2003. **163**(6): p. 2575-2584.
20. Gauldie, J., Kolb, M., and Sime, P.J., *A new direction in the pathogenesis of idiopathic pulmonary fibrosis?* Respiratory Research, 2002. **3**: p. 1.
21. Bonniaud, P., *et al.*, *Smad3 null mice develop airspace enlargement and are resistant to TGF-beta-mediated pulmonary fibrosis.* Journal of Immunology, 2004. **173**(3): p. 2099-108.
22. Pittet, J.F., *et al.*, *TGF-beta is a critical mediator of acute lung injury.* Journal of Clinical Investigation, 2001. **107**(12): p. 1537-44.
23. Horbelt, D., Denkis, A., and Knaus, P., *A portrait of Transforming Growth Factor β superfamily signalling: Background matters.* The International Journal of Biochemistry and Cell Biology, 2012. **44**(3): p. 469-474.
24. Yang, T., *et al.*, *MiR-29 mediates TGFβ1-induced extracellular matrix synthesis through activation of PI3K-AKT pathway in human lung fibroblasts.* Journal of Cellular Biochemistry, 2013. **114**(6): p. 1336–1342.
25. Li, F., *et al.*, *Effect of celecoxib on proliferation, collagen expression, ERK1/2 and SMAD2/3 phosphorylation in NIH/3T3 fibroblasts.* European Journal of Pharmacology, 2012. **678**(1-3): p. 1-5.

26. Kottler, U.B., *et al.*, *Comparative effects of TGF-beta 1 and TGF-beta 2 on extracellular matrix production, proliferation, migration, and collagen contraction of human Tenon's capsule fibroblasts in pseudoexfoliation and primary open-angle glaucoma.* Experimental Eye Research, 2005. **80**(1): p. 121-134.
27. Baarsma, H.A., *et al*., *Glycogen synthase kinase-3 (GSK-3) regulates TGF-β_1-induced differentiation of pulmonary fibroblasts.* British Journal of Pharmacology, 2013. **169**(3): p. 590-603.
28. Meyer, C., *et al.*, *Caveolin-1 abrogates TGF-β mediated hepatocyte apoptosis.* Cell Death & Disease, 2013. **4**: p. e466.
29. Li, M.O., Wan, Y.Y., and Flavell, R.A., *T cell-produced transforming growth factor-beta1 controls T cell tolerance and regulates Th1- and Th17-cell differentiation.* Immunity, 2007. **26**(5): p. 579-591.
30. Li, M.O., Sanjabi, S., and Flavell, R.A., *Transforming growth factor-beta controls development, homeostasis, and tolerance of T cells by regulatory T cell-dependent and -independent mechanisms.* Immunity, 2006. **25**(3): p. 455-471.
31. Fujii, D., *et al.*, *Transforming growth factor beta gene maps to human chromosome 19 long arm and to mouse chromosome 7.* Somatic Cell and Molecular Genetics, 1986. **12**(3): p. 281-288.
32. Barton, D.E., *et al.*, *Chromosomal mapping of genes for transforming growth factors beta 2 and beta 3 in man and mouse: dispersion of TGF-beta gene family.* Oncogene Research, 1988. **3**(4): p. 323-331.
33. Dijke, P., *et al.*, *Molecular characterization of transforming growth factor type beta 3.* Annals of the New York Academy of Sciences, 1990. **593**: p. 26-42.
34. Lawrence, D.A., *et al.*, *Normal embryo fibroblasts release transforming growth factors in a latent form.* Journal of Cellular Physiology, 1984. **121**(1): p. 184-188.
35. Gentry, L.E., *et al.*, *Molecular events in the processing of recombinant type 1 pre-pro-transforming growth factor beta to the mature polypeptide.* Molecular and Cellular Biology, 1988. **8**(10): p. 4162-4168.
36. Gray, A.M. and A.J. Mason, *Requirement for activin A and transforming growth factor--beta 1 pro-regions in homodimer assembly.* Science, 1990. **247**(4948): p. 1328-1330.
37. Dubois, C.M., *et al.*, *Processing of transforming growth factor beta 1 precursor by human furin convertase.* The Journal of Biological Chemistry, 1995. **270**(18): p. 10618-10624.

38. Taipale, J., Koli, K., and Keski-Oja, J., *Release of transforming growth factor-beta 1 from the pericellular matrix of cultured fibroblasts and fibrosarcoma cells by plasmin and thrombin.* The Journal of Biological Chemistry, 1992. **267**(35): p. 25378-25384.
39. Jullien, P., Berg, T.M., and Lawrence, D.A., *Acidic cellular environments: activation of latent TGF-beta and sensitization of cellular responses to TGF-beta and EGF.* International Journal of Cancer, 1989. **43**(5): p. 886-891.
40. Barcellos-Hoff, M.H. and Dix, T.A., *Redox-mediated activation of latent transforming growth factor-beta 1.* Molecular Endocrinology, 1996. **10**(9): p. 1077-1083.
41. Yu, Q. and Stamenkovic, I., *Cell surface-localized matrix metalloproteinase-9 proteolytically activates TGF-beta and promotes tumor invasion and angiogenesis.* Genes & Development, 2000. **14**(2): p. 163-176.
42. Munger, J.S., *et al.*, *The integrin alpha v beta 6 binds and activates latent TGF beta 1: a mechanism for regulating pulmonary inflammation and fibrosis.* Cell, 1999. **96**(3): p. 319-328.
43. Glick, A.B., *et al.*, *Retinoic acid induces transforming growth factor-beta 2 in cultured keratinocytes and mouse epidermis.* Cell Regulation, 1989. **1**(1): p. 87-97.
44. Oursler, M.J., Riggs, B.L., and Spelsberg, T.C., *Glucocorticoid-induced activation of latent transforming growth factor-beta by normal human osteoblast-like cells.* Endocrinology, 1993. **133**(5): p. 2187-2196.
45. Shi, Y. and Massagué, J., *Mechanisms of TGF-beta signaling from cell membrane to the nucleus.* Cell, 2003. **113**(6): p. 685-700.
46. Manning, G., *et al.*, *The protein kinase complement of the human genome.* Science, 2002. **298**(5600): p. 1912-34.
47. Massagué, J., *TGF-beta signal transduction.* Annual Review of Biochemistry, 1998. **67**: p. 753-791.
48. Laiho, M., Weis, M.B., and Massagué, J., *Concomitant loss of transforming growth factor (TGF)-beta receptor types I and II in TGF-beta-resistant cell mutants implicates both receptor types in signal transduction.* The Journal of Biological Chemistry, 1990. **265**(30): p. 18518-18524.
49. Mathews, L.S. and Vale, W.W., *Expression cloning of an activin receptor, a predicted transmembrane serine kinase.* Cell, 1991. **65**(6): p. 973-82.
50. ten Dijke, P., *et al.*, *Activin receptor-like kinases: a novel subclass of cell-surface receptors with predicted serine/threonine kinase activity.* Oncogene, 1993. **8**(10): p. 2879-87.

51. Attisano, L., *et al.*, *Novel activin receptors: distinct genes and alternative mRNA splicing generate a repertoire of serine/threonine kinase receptors.* Cell, 1992. **68**(1): p. 97-108.
52. Ebner, R., *et al.*, *Cloning of a type I TGF-beta receptor and its effect on TGF-beta binding to the type II receptor.* Science, 1993. **260**(5112): p. 1344-8.
53. Franzen, P., *et al.*, *Cloning of a TGF beta type I receptor that forms a heteromeric complex with the TGF beta type II receptor.* Cell, 1993. **75**(4): p. 681-92.
54. Carcamo, J., *et al.*, *Type I receptors specify growth-inhibitory and transcriptional responses to transforming growth factor beta and activin.* Molecular and Cellular Biology, 1994. **14**(6): p. 3810-21.
55. Yamashita, H., *et al.*, *Formation of hetero-oligomeric complexes of type I and type II receptors for transforming growth factor-beta.* The Journal of Biological Chemistry, 1994. **269**(31): p. 20172-8.
56. Chen, R.H. and Derynck, R., *Homomeric interactions between type II transforming growth factor-beta receptors.* The Journal of Biological Chemistry, 1994. **269**(36): p. 22868-74.
57. Wrana, J.L., *et al.*, *TGF beta signals through a heteromeric protein kinase receptor complex.* Cell, 1992. **71**(6): p. 1003-14.
58. Moustakas, A., *et al.*, *The transforming growth factor beta receptors types I, II, and III form hetero-oligomeric complexes in the presence of ligand.* The Journal of Biological Chemistry, 1993. **268**(30): p. 22215-8.
59. Inagaki, M., *et al.*, *Growth inhibition by transforming growth factor beta (TGF-beta) type I is restored in TGF-beta-resistant hepatoma cells after expression of TGF-beta receptor type II cDNA.* Proceedings of the National Academy of Sciences USA, 1993. **90**(11): p. 5359-63.
60. Hinck, A.P., *Structural studies of the TGF-betas and their receptors - insights into evolution of the TGF-beta superfamily.* Federation of European Biochemical Society Letters, 2012. **586**(14): p. 1860-70.
61. Finnson, K.W., *et al.*, *ALK1 opposes ALK5/Smad3 signaling and expression of extracellular matrix components in human chondrocytes.* Journal of Bone and Mineral Research, 2008. **23**(6): p. 896-906.
62. Zhang, Y., *et al.*, *Receptor-associated Mad homologues synergize as effectors of the TGF-beta response.* Nature, 1996. **383**(6596): p. 168-72.
63. Chen, Y., Bhushan, A., and Vale, W., *Smad8 mediates the signaling of the ALK-2 [corrected] receptor serine kinase.* Proceedings of the National Academy of Sciences USA, 1997. **94**(24): p. 12938-43.

64. Graff, J.M., Bansal, A., and Melton, D.A., *Xenopus Mad proteins transduce distinct subsets of signals for the TGF beta superfamily.* Cell, 1996. **85**(4): p. 479-87.
65. Suzuki, A., *et al.*, *Smad5 induces ventral fates in Xenopus embryo.* Developmental Biology, 1997. **184**(2): p. 402-5.
66. Thomsen, G.H., *Xenopus mothers against decapentaplegic is an embryonic ventralizing agent that acts downstream of the BMP-2/4 receptor.* Development, 1996. **122**(8): p. 2359-66.
67. Macias-Silva, M., *et al.*, *MADR2 is a substrate of the TGFbeta receptor and its phosphorylation is required for nuclear accumulation and signaling.* Cell, 1996. **87**(7): p. 1215-24.
68. Nakao, A., *et al.*, *TGF-beta receptor-mediated signalling through Smad2, Smad3 and Smad4.* European Molecular Biology Organization Journal, 1997. **16**(17): p. 5353-62.
69. Wu, R.Y., *et al.*, *Heteromeric and homomeric interactions correlate with signaling activity and functional cooperativity of Smad3 and Smad4/DPC4.* Molecular and Cellular Biology, 1997. **17**(5): p. 2521-8.
70. Lagna, G., *et al.*, *Partnership between DPC4 and SMAD proteins in TGF-beta signalling pathways.* Nature, 1996. **383**(6603): p. 832-6.
71. Hayashi, H., *et al.*, *The MAD-related protein Smad7 associates with the TGFbeta receptor and functions as an antagonist of TGFbeta signaling.* Cell, 1997. **89**(7): p. 1165-73.
72. Imamura, T., *et al.*, *Smad6 inhibits signalling by the TGF-beta superfamily.* Nature, 1997. **389**(6651): p. 622-6.
73. Nakao, A., *et al.*, *Identification of Smad7, a TGFbeta-inducible antagonist of TGF-beta signalling.* Nature, 1997. **389**(6651): p. 631-5.
74. Denissova, N.G., *et al.*, *Transforming growth factor beta-inducible independent binding of SMAD to the Smad7 promoter.* Proceedings of the National Academy of Sciences USA, 2000. **97**(12): p. 6397-402.
75. Stopa, M., *et al.*, *Participation of Smad2, Smad3, and Smad4 in transforming growth factor beta (TGF-beta)-induced activation of Smad7. The TGF-beta response element of the promoter requires functional Smad binding element and E-box sequences for transcriptional regulation.* The Journal of Biological Chemistry, 2000. **275**(38): p. 29308-17.

76. Dennler, S., *et al.*, *Direct binding of Smad3 and Smad4 to critical TGF beta-inducible elements in the promoter of human plasminogen activator inhibitor-type 1 gene.* European Molecular Biology Organization Journal, 1998. **17**(11): p. 3091-100.
77. Wickert, L., *et al.*, *Glucocorticoids activate TGF-beta induced PAI-1 and CTGF expression in rat hepatocytes.* Comparative Hepatology, 2007. **6**: p. 5.
78. Katagiri, T., *et al.*, *Identification of a BMP-responsive element in Id1, the gene for inhibition of myogenesis.* Genes to Cells, 2002. **7**(9): p. 949-60.
79. Wang, S., *et al.*, *Up-regulation of BMP-2 antagonizes TGF-beta1/ROCK-enhanced cardiac fibrotic signalling through activation of Smurf1/Smad6 complex.* Journal of Cellular and Molecular Medicine, 2012. **16**(10): p. 2301-10.
80. Lee, N.Y., *et al.*, *The transforming growth factor-beta type III receptor mediates distinct subcellular trafficking and downstream signaling of activin-like kinase (ALK)3 and ALK6 receptors.* Molecular Biology of the Cell, 2009. **20**(20): p. 4362-70.
81. Lopez-Casillas, F., *et al.*, *Structure and expression of the membrane proteoglycan betaglycan, a component of the TGF-beta receptor system.* Cell, 1991. **67**(4): p. 785-95.
82. Gougos, A. and Letarte, M., *Primary structure of endoglin, an RGD-containing glycoprotein of human endothelial cells.* The Journal of Biological Chemistry, 1990. **265**(15): p. 8361-4.
83. Lopez-Casillas, F., Wrana, J.L., J. Massague, J., *Betaglycan presents ligand to the TGF beta signaling receptor.* Cell, 1993. **73**(7): p. 1435-44.
84. Yamashita, H., *et al.*, *Endoglin forms a heteromeric complex with the signaling receptors for transforming growth factor-beta.* The Journal of Biological Chemistry, 1994. **269**(3): p. 1995-2001.
85. Cheifetz, S., *et al.*, *Endoglin is a component of the transforming growth factor-beta receptor system in human endothelial cells.* The Journal of Biological Chemistry, 1992. **267**(27): p. 19027-30.
86. Cheifetz, S., Andres, J.L., and Massague, J., *The transforming growth factor-beta receptor type III is a membrane proteoglycan. Domain structure of the receptor.* The Journal of Biological Chemistry, 1988. **263**(32): p. 16984-91.
87. Wang, X.F., *et al.*, *Expression cloning and characterization of the TGF-beta type III receptor.* Cell, 1991. **67**(4): p. 797-805.
88. Segarini, P.R., Rosen, D.M., and Seyedin, S.M., *Binding of transforming growth factor-beta to cell surface proteins varies with cell type.* Molecular Endocrinology, 1989. **3**(2): p. 261-72.

89. Cheifetz, S. and Massague, J., *Isoform-specific transforming growth factor-beta binding proteins with membrane attachments sensitive to phosphatidylinositol-specific phospholipase C.* The Journal of Biological Chemistry, 1991. **266**(31): p. 20767-72.
90. Kirkbride, K.C., *et al.*, *Bone morphogenetic proteins signal through the transforming growth factor-beta type III receptor.* The Journal of Biological Chemistry, 2008. **283**(12): p. 7628-37.
91. Stenvers, K.L., *et al.*, *Heart and liver defects and reduced transforming growth factor beta2 sensitivity in transforming growth factor beta type III receptor-deficient embryos.* Molecular and Cellular Biology, 2003. **23**(12): p. 4371-85.
92. Goumans, M.J., *et al.*, *Activin receptor-like kinase (ALK)1 is an antagonistic mediator of lateral TGFbeta/ALK5 signaling.* Molecular Cell, 2003. **12**(4): p. 817-28.
93. Murakami, M., *et al.*, *Receptor expression modulates the specificity of transforming growth factor-beta signaling pathways.* Genes to Cells, 2009. **14**(4): p. 469-82.
94. Kinsella, J.P., Greenough, A., and Abman, S.H., *Bronchopulmonary dysplasia.* The Lancet, 2006. **367**(9520): p. 1421-1431.
95. Dhainaut, J.F., J. Charpentier, and J.D. Chiche, *Transforming growth factor-beta: a mediator of cell regulation in acute respiratory distress syndrome.* Critical Care Medicine, 2003. **31**(4 Suppl): p. S258-64.
96. Yang, Y.C., *et al.*, *Transforming growth factor-beta1 in inflammatory airway disease: a key for understanding inflammation and remodeling.* Allergy, 2012. **67**(10): p. 1193-202.
97. Bottoms, S.E., *et al.*, *Tgf-Beta isoform specific regulation of airway inflammation and remodelling in a murine model of asthma*. PLoS One, 2010. **5**(3): p. e9674.
98. Roelen, B.A., van Rooijen, M.A., and Mummery, C.L., *Expression of ALK-1, a type 1 serine/threonine kinase receptor, coincides with sites of vasculogenesis and angiogenesis in early mouse development.* Developmental Dynamics, 1997. **209**(4): p. 418-30.
99. Goumans, M.J. and Mummery, C., *Functional analysis of the TGFbeta receptor/Smad pathway through gene ablation in mice.* The International Journal of Developmental Biology, 2000. **44**(3): p. 253-65.
100. Cao, Y., *et al.*, *Neuropilin-1 mediates divergent R-Smad signaling and the myofibroblast phenotype.* The Journal of Biological Chemistry, 2010. **285**(41): p. 31840-8.

101. Daly, A.C., Randall, R.A., and Hill, C.S., *Transforming growth factor beta-induced Smad1/5 phosphorylation in epithelial cells is mediated by novel receptor complexes and is essential for anchorage-independent growth.* Molecular and Cellular Biology, 2008. **28**(22): p. 6889-902.

102. Liu, I.M., *et al.*, *TGFbeta-stimulated Smad1/5 phosphorylation requires the ALK5 L45 loop and mediates the pro-migratory TGFbeta switch.* European Molecular Biochemistry Organization Journal, 2009. **28**(2): p. 88-98.

103. Pannu, J., *et al.*, *Smad1 pathway is activated in systemic sclerosis fibroblasts and is targeted by imatinib mesylate.* Arthritis & Rheumatology, 2008. **58**(8): p. 2528-37.

104. Wiercinska, E., *et al.*, *Id1 is a critical mediator in TGF-beta-induced transdifferentiation of rat hepatic stellate cells.* Hepatology, 2006. **43**(5): p. 1032-41.

105. Morty, R.E., Koenigshoff, M., and Eickelberg, O., *Transforming growth factor-beta signaling across ages: from distorted lung development to chronic obstructive pulmonary disease.* Proceedings of the American Thoracic Society, 2009. **6**(7): p. 607-13.

106. Roth-Kleiner, M. and Post, M., *Genetic control of lung development.* Biology of the Neonate, 2003. **84**(1): p. 83-8.

107. Cardoso, W.V., *Molecular regulation of lung development.* Annual Review of Physiology, 2001. **63**: p. 471-94.

108. Vicencio, A.G., *et al.*, *Conditional overexpression of bioactive transforming growth factor-beta1 in neonatal mouse lung: a new model for bronchopulmonary dysplasia?* American Journal of Respiratory Cell and Molecular Biology, 2004. **31**(6): p. 650-6.

109. Chen, H., *et al.*, *Abnormal mouse lung alveolarization caused by Smad3 deficiency is a developmental antecedent of centrilobular emphysema.* American Journal of Physiology - Lung Cellular and Molecular Physiology, 2005. **288**(4): p. L683-91.

110. Warburton, D., *Developmental responses to lung injury: repair or fibrosis.* Fibrogenesis & Tissue Repair, 2012. **5 Suppl 1**: p. S2.

111. Alejandre-Alcazar, M.A., *et al.*, *TGF-beta signaling is dynamically regulated during the alveolarization of rodent and human lungs.* Developmental Dynamics, 2008. **237**(1): p. 259-69.

112. Lamouille, S., *et al.*, *Activin receptor-like kinase 1 is implicated in the maturation phase of angiogenesis.* Blood, 2002. **100**(13): p. 4495-501.

113. Kotecha, S., *et al.*, *Increase in the concentration of transforming growth factor beta-1 in bronchoalveolar lavage fluid before development of chronic lung disease of prematurity.* The Journal of Pediatrics, 1996. **128**(4): p. 464-469.
114. Khalil, N., *et al.*, *Increased production and immunohistochemical localization of transforming growth factor-beta in idiopathic pulmonary fibrosis.* American Journal of Respiratory Cellular and Molecular Biology, 1991. **5**(2): p. 155-62.
115. Khalil, N., *et al.*, *Regulation of the effects of TGF-beta 1 by activation of latent TGF-beta 1 and differential expression of TGF-beta receptors (T beta R-I and T beta R-II) in idiopathic pulmonary fibrosis.* Thorax, 2001. **56**(12): p. 907-15.
116. Fahy, R.J., *et al.*, *The acute respiratory distress syndrome: a role for transforming growth factor-beta 1.* American Journal of Respiratory Cellular and Molecular Biology, 2003. **28**(4): p. 499-503.
117. Halwani, R., *et al.*, *Role of transforming growth factor-beta in airway remodeling in asthma.* American Journal of Respiratory Cellular and Molecular Biology, 2011. **44**(2): p. 127-33.
118. Ohno, I., *et al.*, *Transforming growth factor beta 1 (TGF beta 1) gene expression by eosinophils in asthmatic airway inflammation.* American Journal of Respiratory Cellular and Molecular Biology, 1996. **15**(3): p. 404-9.
119. Takizawa, H., *et al.*, *Increased expression of transforming growth factor-beta1 in small airway epithelium from tobacco smokers and patients with chronic obstructive pulmonary disease (COPD).* American Journal of Respiratory and Critical Care Medicine, 2001. **163**(6): p. 1476-83.
120. Springer, J., *et al.*, *SMAD-signaling in chronic obstructive pulmonary disease: transcriptional down-regulation of inhibitory SMAD 6 and 7 by cigarette smoke.* Biological Chemistry, 2004. **385**(7): p. 649-53.
121. Vosdoganes, P., *et al.*, *Cell Therapy: A Novel Treatment Approach for Bronchopulmonary Dysplasia.* Pediatrics, 2012. **130**(4): p. 727-737.
122. Kunzmann, S., *et al.*, *Antenatal inflammation induced TGF-beta1 but suppressed CTGF in preterm lungs.* American Journal of Physiology - Lung Cellular and Molecular Physiology, 2006. **292**(1): p. L223-L231.
123. Wu, S., *et al.*, *High tidal volume ventilation activates Smad2 and upregulates expression of connective tissue growth factor in newborn rat lung.* Pediatric Research, 2008. **63**(3): p. 245-250.
124. Dasgupta, C., *et al.*, *Hyperoxia-induced neonatal rat lung injury involves activation of TGF-{beta} and Wnt signaling and is protected by rosiglitazone.* American Journal of Physiology - Lung Cellular and Molecular Physiology, 2009. **296**(6): p. L1031-41.

125. Crystal, R.G., *et al.*, *Interstitial lung diseases of unknown cause. Disorders characterized by chronic inflammation of the lower respiratory tract.* New England Journal of Medicine, 1984. **310**(4): p. 235-44.

126. King, T.E., Jr., *et al.*, *Idiopathic pulmonary fibrosis: relationship between histopathologic features and mortality.* American Journal of Respiratory and Critical Care Medicine, 2001. **164**(6): p. 1025-32.

127. Khalil, N., *et al.*, *TGF-beta 1, but not TGF-beta 2 or TGF-beta 3, is differentially present in epithelial cells of advanced pulmonary fibrosis: an immunohistochemical study.* American Journal of Respiratory Cellular and Molecular Biology, 1996. **14**(2): p. 131-8.

128. Ranieri, V.M., *et al.*, *Acute respiratory distress syndrome: the Berlin Definition.* Journal of the American Medical Association. **307**(23): p. 2526-33.

129. Giri, S.N., Hyde, D.M., and Hollinger, M.A., *Effect of antibody to transforming growth factor beta on bleomycin induced accumulation of lung collagen in mice.* Thorax, 1993. **48**(10): p. 959-66.

130. Budinger, G.R., *et al.*, *Active transforming growth factor-beta1 activates the procollagen I promoter in patients with acute lung injury.* Intensive Care Medicine, 2005. **31**(1): p. 121-8.

131. Marshall, R.P., *et al.*, *Fibroproliferation occurs early in the acute respiratory distress syndrome and impacts on outcome.* American Journal of Respiratory and Critical Care Medicine, 2000. **162**(5): p. 1783-8.

132. Clark, J.G., *et al.*, *Type III procollagen peptide in the adult respiratory distress syndrome. Association of increased peptide levels in bronchoalveolar lavage fluid with increased risk for death.* Annals of Internal Medicine, 1995. **122**(1): p. 17-23.

133. Vignola, A.M., *et al.*, *Release of transforming growth factor-beta (TGF-beta) and fibronectin by alveolar macrophages in airway diseases.* Clinical & Experimental Immunology, 1996. **106**(1): p. 114-9.

134. Koenigshoff, M., Kneidinger, N., and Eickelberg, O., *TGF-beta signaling in COPD: deciphering genetic and cellular susceptibilities for future therapeutic regimen.* Swiss Medical Weekly, 2009. **139**(39-40): p. 554-63.

135. Yao, H., de Boer, W.I., and Rahman, I., *Targeting lung inflammation: novel therapies for the treatment of COPD.* Current Respiratory Medicine Reviews, 2008. **4**(1): p. 57-68.

136. Hogg, J.C., *Pathophysiology of airflow limitation in chronic obstructive pulmonary disease.* The Lancet, 2004. **364**(9435): p. 709-21.

137. Gharaee-Kermani, M., *et al.*, *Recent advances in molecular targets and treatment of idiopathic pulmonary fibrosis: focus on TGFbeta signaling and the myofibroblast.* Current Medical Chemistry, 2009. **16**(11): p. 1400-17.
138. Aubert, J.D., *et al.*, *Transforming growth factor beta 1 gene expression in human airways.* Thorax, 1994. **49**(3): p. 225-32.
139. Wang, H., *et al.*, *Effect of cigarette smoke on fibroblast-mediated gel contraction is dependent on cell density.* American Journal of Physiology - Lung Cellular and Molecular Physiology, 2003. **284**(1): p. L205-13.
140. Baarsma, H.A., *et al*., *Activation of WNT/beta-catenin signaling in pulmonary fibroblasts by TGF-beta(1) is increased in chronic obstructive pulmonary disease*. PLoS One, 2011. **6**(9): p. e25450.
141. Togo, S., *et al.*, *Lung fibroblast repair functions in patients with chronic obstructive pulmonary disease are altered by multiple mechanisms.* American Journal of Respiratory and Critical Care Medicine, 2008. **178**(3): p. 248-60.
142. Morris, D.G., *et al.*, *Loss of integrin alpha(v)beta6-mediated TGF-beta activation causes Mmp12-dependent emphysema.* Nature, 2003. **422**(6928): p. 169-73.
143. Phan, S.H., *Genesis of the myofibroblast in lung injury and fibrosis.* Proceedings of the American Thoracic Society, 2012. **9**(3): p. 148-52.
144. Popova, A.P., *et al.*, *Autocrine production of TGF-beta1 promotes myofibroblastic differentiation of neonatal lung mesenchymal stem cells.* American Journal of Physiology - Lung Cellular and Molecular Physiology, 2010. **298**(6): p. L735-43.
145. Gu, L., *et al.*, *Effect of IFN-gamma and dexamethasone on TGF-beta1-induced human fetal lung fibroblast-myofibroblast differentiation.* Acta Pharmacologia Sinica, 2004. **25**(11): p. 1479-88.
146. Rice, N.A. and Leinwand, L.A., *Skeletal myosin heavy chain function in cultured lung myofibroblasts.* The Journal of Cellular Biology, 2003. **163**(1): p. 119-29.
147. Araoka, T., *et al.*, *Transcription factor 7-like 2 (TCF7L2) regulates activin receptor-like kinase 1 (ALK1)/Smad1 pathway for development of diabetic nephropathy.* Molecules and Cells, 2010. **30**(3): p. 209-18.
148. Abe, H., *et al.*, *Scleraxis modulates bone morphogenetic protein 4 (BMP4)-Smad1 protein-smooth muscle alpha-actin (SMA) signal transduction in diabetic nephropathy.* The Journal of Biological Chemistry, 2012. **287**(24): p. 20430-42.
149. Mima, A., *et al.*, *Activation of Src mediates PDGF-induced Smad1 phosphorylation and contributes to the progression of glomerulosclerosis in glomerulonephritis.* PLoS One, 2011. **6**(3): p. e17929.

150. Jeffery, T.K., *et al.*, *BMP4 inhibits proliferation and promotes myocyte differentiation of lung fibroblasts via Smad1 and JNK pathways.* American Journal of Physiology - Lung Cellular and Molecular Physiology, 2005. **288**(2): p. L370-8.

151. Matsubara, T., *et al.*, *Expression of Smad1 is directly associated with mesangial matrix expansion in rat diabetic nephropathy.* Laboratory Investigation, 2006. **86**(4): p. 357-68.

152. Kumar, V. and Robbins, S.L., *Robbins basic pathology*. 8th ed. 2007, Philadelphia, PA: Saunders/Elsevier. xiv, 946 p.

153. Vyas, J. and Kotecha, S., *Effects of antenatal and postnatal corticosteroids on the preterm lung.* Archives of Disease in Childhood. Fetal and Neonatal Edition, 1997. **77**(2): p. F147-50.

154. Beck, J.C., *et al.*, *Betamethasone and the rhesus fetus: effect on lung morphometry and connective tissue.* Pediatric Research, 1981. **15**(3): p. 235-40.

155. Tschanz, S.A., Damke, B.M., and Burri, P.H., *Influence of postnatally administered glucocorticoids on rat lung growth.* Biology of the Neonate, 1995. **68**(4): p. 229-45.

156. Kumar, V. and Robbins, S.L., *Robbins basic pathology*. 8th ed. 2007, Philadelphia, PA: Saunders/Elsevier. xiv, 946 p.

157. Schellhase, D.E. and Shannon, J.M., *Effects of maternal dexamethasone on expression of SP-A, SP-B, and SP-C in the fetal rat lung.* American Journal of Respiratory Cellular and Molecular Biology, 1991. **4**(4): p. 304-12.

158. Liley, H.G., *et al.*, *Regulation of messenger RNAs for the hydrophobic surfactant proteins in human lung.* Journal of Clinical Investigation, 1989. **83**(4): p. 1191-7.

159. Ashton, M.R., *et al.*, *Surfactant phosphatidylcholine composition during dexamethasone treatment in chronic lung disease.* Archives of Disease in Childhood, 1994. **71**(2): p. F114-7.

160. Yoder, M.C., Jr., Chua, R. and Tepper, R., *Effect of dexamethasone on pulmonary inflammation and pulmonary function of ventilator-dependent infants with bronchopulmonary dysplasia.* American Review of Respiratory Diseases, 1991. **143**(5 Pt 1): p. 1044-8.

161. Joram, N., *et al.*, *Betamethasone worsens chorioamnionitis-related lung development impairment in rabbits.* American Journal of Perinatology, 2011. **28**(8): p. 605-12.

162. Yoon, B.H., *et al.*, *Amniotic fluid cytokines (interleukin-6, tumor necrosis factor-alpha, interleukin-1 beta, and interleukin-8) and the risk for the development of bronchopulmonary dysplasia.* American Journal of Obstetrics & Gynecology, 1997. **177**(4): p. 825-30.

163. Davies, H.R., Richeldi, L., and Walters, E.H., *Immunomodulatory agents for idiopathic pulmonary fibrosis.* Cochrane Database of Systematic Reviews, 2003(3): p. CD003134.

164. Richeldi, L., *et al.*, *Corticosteroids for idiopathic pulmonary fibrosis.* Cochrane Database of Systematic Reviews, 2003 (3): p. CD002880.

165. Gay, S.E., *et al.*, *Idiopathic pulmonary fibrosis: predicting response to therapy and survival.* American Journal of Respiratory and Critical Care Medicine, 1998. **157**(4 Pt 1): p. 1063-72.

166. Wilson, M.S. and Wynn, T.A., *Pulmonary fibrosis: pathogenesis, etiology and regulation.* Mucosal Immunology, 2009. **2**(2): p. 103-21.

167. Ingram, J.L., *et al.*, *IL-13 and IL-1beta promote lung fibroblast growth through coordinated up-regulation of PDGF-AA and PDGF-Ralpha.* Federation of American Societies for Experimental Biology Journal, 2004. **18**(10): p. 1132-4.

168. Calverley, P.M., *et al.*, *Salmeterol and fluticasone propionate and survival in chronic obstructive pulmonary disease.* New England Journal of Medicine, 2007. **356**(8): p. 775-89.

169. Lung Health Study Research Group, *Effect of inhaled triamcinolone on the decline in pulmonary function in chronic obstructive pulmonary disease.* New England Journal of Medicine, 2000. **343**(26): p. 1902-9.

170. Czock, D., *et al.*, *Pharmacokinetics and pharmacodynamics of systemically administered glucocorticoids.* Clinical Pharmacokinetics, 2005. **44**(1): p. 61-98.

171. Hubner, M., Hochhaus, G., and Derendorf, H., *Comparative pharmacology, bioavailability, pharmacokinetics, and pharmacodynamics of inhaled glucocorticosteroids.* Immunology and Allergy Clinics in North America, 2005. **25**(3): p. 469-88.

172. Rosendahl, A., *et al.*, *Activation of bone morphogenetic protein/Smad signaling in bronchial epithelial cells during airway inflammation.* American Journal of Respiratory Cellular and Molecular Biology, 2002. **27**(2): p. 160-9.

173. Pannu, J., *et al.*, *Transforming growth factor-beta receptor type I-dependent fibrogenic gene program is mediated via activation of Smad1 and ERK1/2 pathways.* The Journal of Biological Chemistry, 2007. **282**(14): p. 10405-13.

7. Declaration

Erklärung zur Dissertation

„Hiermit erkläre ich, dass ich die vorliegende Arbeit selbständig und ohne unzulässige Hilfe oder Benutzung anderer als der angegebenen Hilfsmittel angefertigt habe. Alle Textstellen, die wörtlich oder sinngemäß aus veröffentlichten oder nichtveröffentlichten Schriften entnommen sind, und alle Angaben, die auf mündlichen Auskünften beruhen, sind als solche kenntlich gemacht. Bei den von mir durchgeführten und in der Dissertation erwähnten Untersuchungen habe ich die Grundsätze guter wissenschaftlicher Praxis, wie sie in der „Satzung der Justus-Liebig-Universität Gießen zur Sicherung guter wissenschaftlicher Praxis“ niedergelegt sind, eingehalten sowie ethische, datenschutzrechtliche und tierschutzrechtliche Grundsätze befolgt. Ich versichere, dass Dritte von mir weder unmittelbar noch mittelbar geldwerte Leistungen für Arbeiten erhalten haben, die im Zusammenhang mit dem Inhalt der vorgelegten Dissertation stehen, oder habe diese nachstehend spezifiziert. Die vorgelegte Arbeit wurde weder im Inland noch im Ausland in gleicher oder ähnlicher Form einer anderen Prüfungsbehörde zum Zweck einer Promotion oder eines anderen Prüfungsverfahrens vorgelegt. Alles aus anderen Quellen und von anderen Personen übernommene Material, das in der Arbeit verwendet wurde oder auf das direkt Bezug genommen wird, wurde als solches kenntlich gemacht. Insbesondere wurden alle Personen genannt, die direkt und indirekt an der Entstehung der vorliegenden Arbeit beteiligt waren. Mit der Überprüfung meiner Arbeit durch eine Plagiatserkennungssoftware bzw. ein internetbasiertes Softwareprogramm erkläre ich mich einverstanden.“

_____ _____

Ort, Datum Unterschrift

8. Publication

THE JOURNAL OF BIOLOGICAL CHEMISTRY VOL. 289, NO. 6, pp. 3262–3275, February 7, 2014

Glucocorticoids Recruit Tgfbr3 and Smad1 to Shift Transforming Growth Factor-β Signaling from the Tgfbr1/Smad2/3 Axis to the Acvrl1/Smad1 Axis in Lung Fibroblasts*

Received for publication, December 6, 2013 Published, JBC Papers in Press, December 17, 2013, DOI 10.1074/jbc.M113.541052

Julian T. Schwartze[‡§1], Simone Becker[‡§], Elpidoforos Sakkas[‡§], Łukasz A. Wujak[‡§], Gero Niess[‡§], Jakob Usemann[‡§2], Frank Reichenberger[§¶], Susanne Herold[§], István Vadász[§], Konstantin Mayer[§], Werner Seeger[‡§], and Rory E. Morty[‡§3]

From the [‡]Department of Lung Development and Remodelling, Max Planck Institute for Heart and Lung Research, D-61231 Bad Nauheim, Germany, the [§]Department of Internal Medicine (Pulmonology), University of Giessen and Marburg Lung Center, German Center for Lung Research, D-35392 Giessen, Germany, and the [¶]Division of Pulmonology, Asklepios Lung Center Munich-Gauting, D-82131 Gauting, Germany

Background: TGF-β is a mediator of lung diseases treated with glucocorticoids, but TGF-β/glucocorticoid interactions in the lung have not been studied.
Results: Glucocorticoids drive Smad1 and inhibit Smad3 TGF-β signaling in lung cells.
Conclusion: Glucocorticoids modulate pulmonary TGF-β signaling *in vitro* and *in vivo*.
Significance: Glucocorticoid effects on TGF-β signaling are relevant drug/cell interactions and may be relevant drug/disease interactions.

Glucocorticoids represent the mainstay therapy for many lung diseases, providing outstanding management of asthma but performing surprisingly poorly in patients with acute respiratory distress syndrome, chronic obstructive pulmonary disease, lung fibrosis, and blunted lung development associated with bronchopulmonary dysplasia in preterm infants. TGF-β is a pathogenic mediator of all four of these diseases, prompting us to explore glucocorticoid/TGF-β signaling cross-talk. Glucocorticoids, including dexamethasone, methylprednisolone, budesonide, and fluticasone, potentiated TGF-β signaling by the Acvrl1/Smad1/5/8 signaling axis and blunted signaling by the Tgfbr1/Smad2/3 axis in NIH/3T3 cells, as well as primary lung fibroblasts, smooth muscle cells, and endothelial cells. Dexamethasone drove expression of the accessory type III TGF-β receptor Tgfbr3, also called betaglycan. Tgfbr3 was demonstrated to be a "switch" that blunted Tgfbr1/Smad2/3 and potentiated Acvrl1/Smad1 signaling in lung fibroblasts. The Acvrl1/Smad1 axis, which was stimulated by dexamethasone, was active in lung fibroblasts and antagonized Tgfbr1/Smad2/3 signaling. Dexamethasone acted synergistically with TGF-β to drive differentiation of primary lung fibroblasts to myofibroblasts, revealed by acquisition of smooth muscle actin and smooth muscle myosin, which are exclusively Smad1-dependent processes in fibroblasts. Administration of dexamethasone to live mice recapitulated these observations and revealed a lung-specific impact of dexamethasone on lung Tgfbr3 expression and phospho-Smad1 levels *in vivo*. These data point to an interesting and hitherto unknown impact of glucocorticoids on TGF-β signaling in lung fibroblasts and other constituent cell types of the lung that may be relevant to lung physiology, as well as lung pathophysiology, in terms of drug/disease interactions.

Glucocorticoids are endogenously produced steroid hormones such as cortisol that bind to the ubiquitously expressed glucocorticoid receptor and thereby regulate the expression of glucocorticoid-responsive genes. In this way, glucocorticoids influence a broad spectrum of physiological processes, including fat, protein and carbohydrate metabolism, and inflammation (1, 2). Synthetic glucocorticoids, including the earlier generation drugs dexamethasone and methylprednisolone and later generation budesonide and fluticasone, by virtue of their anti-inflammatory and other properties, have found widespread clinical application (1).

Although widely and successfully used in respiratory medicine, for example in the management of obstructive airway diseases such as asthma (3, 4) and antenatal use in pregnant women at risk for preterm birth (5), glucocorticoids have performed surprisingly poorly in the management of other respiratory diseases, including stable chronic obstructive pulmonary disease (6, 7), the acute respiratory distress syndrome (8, 9), and lung fibrosis (10), as well as in the postnatal management of bronchopulmonary dysplasia (11–14), where the use of glucocorticoid therapy cannot be currently recommended and may even be deleterious and dangerous. The failure of glucocorticoids in the context of stable chronic obstructive pulmonary disease, lung fibrosis, acute respiratory distress syndrome, and

* This work was supported by the Max Planck Society; the German Research Foundation through Individual Grant Mo1789/1-1 (to R. E. M.) and Excellence Cluster 147 "Cardio-Pulmonary System" (to K. M., S. H., I. V., W. S., and R. E. M.); the Federal Ministry of Higher Education, Research and the Arts of the State of Hessen LOEWE-Programme (to K. M., S. H., I. V., W. S., and R. E. M.); and the German Center for Lung Research (Deutsches Zentrum für Lungenforschung).
[1] Present address: Div. of Endocrinology, Dept. of Paediatrics, University Children's Hospital Leipzig, D-04103 Leipzig, Germany.
[2] Present address: Div. of Pneumology and Immunology, Dept. of Paediatrics, Charité University Hospital, Campus Virchow, D-10117 Berlin, Germany.
[3] To whom correspondence should be addressed: Dept. of Lung Development and Remodelling, Max Planck Inst. for Heart and Lung Research, Parkstr. 1, D-61231 Bad Nauheim, Germany. Tel.: 49-6032-705-271; Fax: 49-6032-705-360; E-mail: rory.morty@mpi-bn.mpg.de.

bronchopulmonary dysplasia therapy may well reflect (i) our somewhat limited understanding of the disease mechanisms at play, (ii) our limited understanding of alternative as yet undiscovered activities of these powerful steroids, and (iii) a lack of consideration of the interaction between glucocorticoids and disease mechanisms.

Although the anti-inflammatory properties of glucocorticoids have been well characterized, less attention has been paid to the impact of glucocorticoids on other pathological signaling pathways (2). Among these pathways, signaling by the TGF-β family of polypeptide growth factors has been ascribed a key role, not only in the regulation of inflammation (15), but also in the pathophysiological mechanisms at play in several lung diseases. In lung fibrosis, the pro-fibrotic activities of TGF-β drive the production of the fibrotic mediator connective tissue growth factor and plasminogen activator inhibitor-1 (encoded by the *SERPINE1* gene in humans) by lung fibroblasts and promote fibroblast to pathological myofibroblast differentiation (16). TGF-β also drives aberrant production of extracellular matrix molecules such pro-collagen, which limit alveolar repair and proper alveolar development in diseases such as chronic obstructive pulmonary disease (17–19), lung fibrosis (17, 20), acute respiratory distress syndrome (21), and bronchopulmonary dysplasia (22, 23). In general, matrix production relies on TGF-β signaling by the type I TGF-β receptor Tgfbr1 (also called Alk-5), in complex with the type II receptor (Tgfbr2), which together recruit the downstream signaling molecules Smad2 and Smad3 to transduce signals to the nucleus, regulating the expression of TGF-β-responsive genes in the so-called "Tgfbr1/Smad2/3 axis" (24–26).

In the pulmonary vasculature and systemic circulation, an alternative type 1 TGF-β receptor Acvrl1 (also called Alk-1) similarly recruits Smad1 (and perhaps Smad5 and Smad8) to drive expression of a different subset of TGF-β-responsive genes via the "Acvrl1/Smad1 axis" (27–29). This Acvrl1/Smad1 axis is thought to play a role in pulmonary vascular diseases such as such as pulmonary hypertension and the hereditary hemorrhagic telangiectasias (27). The Acvrl1/Smad1 axis, which can promote the acquisition of smooth muscle actin and smooth muscle myosin in several cell types, including lung fibroblasts, is emerging as a regulator of fibroblast to myofibroblast differentiation (30–36). Several accessory molecules, including the inhibitory Smad proteins Smad6 and Smad7, as well as the accessory type III TGF-β receptors endoglin (also called CD105) and Tgfbr3 (also called betaglycan) (37), play poorly defined regulatory roles, although Tgfbr3 has emerged as a mediator of cancer progression (38) and epithelial to mesenchymal differentiation (39). Although both the glucocorticoid and TGF-β signaling pathways have been well characterized individually, few studies to date have addressed the intersection of the TGF-β and glucocorticoid signaling pathways in pulmonary physiology. Such information may prove useful, both to further our understanding of how the TGF-β system may be regulated by endogenous glucocorticoids such as cortisol, as well as possible (deleterious or desired) drug-disease interactions, given the widespread use of glucocorticoids in the management of lung and other diseases.

In this study, it was hypothesized that the TGF-β signaling pathway, which plays a key pathological role in a broad spectrum of restrictive and obstructive lung diseases, is impacted by glucocorticoids, which are a class of drugs that are widely but generally unsuccessfully (with the exception of asthma) used to treat these same diseases. To address this idea, the influence of glucocorticoids on TGF-β signaling was assessed *in vitro* in a mouse fibroblast cell line and primary lung fibroblasts and *in vivo* in C57BL/6J mice. These investigations revealed that four widely used synthetic glucocorticoids dramatically impact TGF-β signaling in lung fibroblasts, shifting the balance of TGF-β signaling from the Tgfbr1/Smad2/3 axis to the Acvrl1/Smad1 axis. Mechanistically, glucocorticoids impacted the expression of components of the TGF-β signaling machinery. In particular, glucocorticoids recruited Tgfbr3, which acted as a switch between the two TGF-β signaling axes, to inhibit Tgfbr1/Smad2/3-driven processes and promote Acvrl1/Smad1-driven signaling. By redirecting TGF-β signaling, glucocorticoids were demonstrated to potentiate fibroblast to myofibroblast differentiation. Taken together, our data indicate that glucocorticoids have a powerful effect on TGF-β signaling, and as such, glucocorticoids may *drive* or *inhibit* TGF-β signaling pathways that are relevant to disease pathogenesis.

EXPERIMENTAL PROCEDURES

Cells and Cell Lines—Primary human lung pulmonary microvascular endothelial cells (C0085C) and pulmonary artery smooth muscle cells (C0095C) were obtained from Invitrogen. Primary human lung fibroblasts were obtained from Lonza. Primary mouse lung fibroblasts were isolated as described previously (22). The NIH/3T3 mouse fibroblast-like cell line (CRL-1658™) and H441 human Clara cell-like airway epithelial cell line (HTB-174™) were obtained from the American Type Culture Collection. H441 cells formed polarized monolayers on membranes of Transwell inserts and were maintained on an air/liquid interface, as described previously (40). H441 cells were exposed to dexamethasone from the basolateral side, with TGF-β stimulation made from the basolateral side. The other three cell types were plated on plastic and maintained in liquid culture as recommended by the manufacturers.

Glucocorticoid and TGF-β Stimulation—Cells were stimulated with dexamethasone (20 nM), methylprednisolone (20 nM), budesonide (2 nM), or fluticasone (2 nM) (all from Sigma) for 18 h, where indicated. These concentrations represent the mean, circulating, clinically relevant doses when these agents are employed therapeutically (41, 42). When cells were intended for the analysis of Smad protein phosphorylation, cells were subsequently stimulated with TGF-β_1 (2 ng/ml; R&D Systems) for 30 min, after the 18-h incubation with glucocorticoids. When cells were intended for analysis of gene expression by real time RT-PCR after TGF-β_1 stimulation, cells were stimulated with TGF-β_1 (2 ng/ml) for 12 h, after the 18-h incubation with glucocorticoids (total, 30 h).

siRNA Knockdown of Gene Expression—Expression of components of the TGF-β signaling machinery was abrogated by siRNA-mediated knockdown. The siRNA were from Santa Cruz, and the optimal working concentration was assessed for each siRNA, as: mouse Tgfbr3 (sc-40225; 200 nM) and mouse

TABLE 1
Primers employed for real time RT-PCR

Gene	Forward primer	Reverse primer	Amplicon size	Number of cycles	Annealing temperature
			bp		°C
tgfbr3	5′-ATGGCAGTGACATCCCACCACAt-3′	5′-agaacggtgaagctctccatca-3′	152	45	60.0
acvrl1	5′-CACCTACATGTGGAGATCT-3′	5′-CGATATCCAGGTAATCGCTG-3′	160	45	60.0
smad1	5′-GCCTCTGGAATGCTGTGAGTTCCCA-3′	5′-GAGCCAGAAGGCTGTGCTGAGCA-3′	152	45	60.0
gapdh	5′-ATGGTGAAGGTCGGTGTGAA-3′	5′-TCATACTGGAACATGTAGACC-3′	143	45	60.0

Smad1 (sc-36507; 200 nM). In all cases, cells were treated with scrambled siRNA (Ambion; AM-4611; at the equivalent concentration) to serve as a negative control. The knockdown efficiency was assessed at the protein level by immunoblot for Tgfbr3 and Smad1. The siRNA transfections were performed with Lipofectamine™ 2000 (Invitrogen), followed by a 6-h transfection period in serum-free Opti-MEM® (Invitrogen), after which the medium was exchanged for DMEM supplemented with 10% FCS, and the cells were then stimulated with glucocorticoids and/or TGF-β_1 (or vehicle alone, where indicated).

Tgfbr3 Overexpression—Tgfbr3 was overexpressed in NIH/3T3 cells using an expression construct containing the mouse *tgfbr3* (43) gene that was obtained from Dr. Fernando Lopéz-Casillas (Universidad Nacional Autónoma de México). The human *TGFBR3* gene was cloned from human lung cDNA using forward (5′-AA **GAT ATC** ATG ACT TCC CAT TAT GTG AT-3′; containing an EcoRV site, in bold type) and reverse (5′-A **AGC GGC CGC** CTA GGC CGT GCT GCT GCT GG-3′; containing a NotI site, in bold type) primers, which generated a 2556-bp amplicon containing the complete *TGFBR3* coding sequence that was cloned into the EcoRV and NotI sites of pIRES hrGFPII (Agilent). Plasmids were transfected into NIH/3T3 cells using Lipofectamine™ 2000 (Invitrogen) as described above for siRNA. Overexpression was validated by immunoblot.

Immunoblotting—Proteins were prepared from cultured cells by scraping in lysis buffer: 20 mM Tris-Cl, 150 mM NaCl, 1 mM EDTA, 1 mM EGTA, 1% (v/v) Nonidet P-40, 1 mM sodium vanadate, and 1× Complete™ protease inhibitor mixture (Roche Applied Science). Proteins from mouse lung tissue were homogenized in lysis buffer (1 ml/0.1 g of wet tissue) by disruption in a Precellys® 24-Dual Homogenisator (PeqLab) using 1.4-mm ceramic beads (PeqLab) to disrupt tissue. Protein concentration was determined by Bradford assay. Proteins (25 μg/lane) were resolved by SDS-PAGE and transferred to nitrocellulose membranes, and immunoblots were probed as described previously (22), using the following antibodies: mouse anti-rabbit Tgfbr3 (Cell Signaling Technology; 2519; 1:1000), mouse anti-rabbit β-actin (Cell Signaling Technology; 4967; 1:1000), mouse anti-rabbit phospho-Smad1/5/8 (Cell Signaling Technology; 9511; 1:800), mouse anti-rabbit Smad1 (Cell Signaling Technology; 9743; 1:1000), mouse anti-rabbit phospho-Smad2 (Cell Signaling Technology; 3101; 1:1000), mouse anti-rabbit phospho-Smad3 (Cell Signaling Technology; 9520; 1:1000), mouse anti-mouse Smad2 (Cell Signaling Technology; 3103; 1:1000), mouse anti-rabbit Smad2/3 (Cell Signaling Technology; 3102; 1:1000), rabbit anti-bovine MYH11 (smooth muscle myosin heavy chain 11; Abcam, ab53219; 1:1000), and monoclonal mouse anti-rabbit ACTA2 (α-smooth muscle actin; Sigma, A-2547; 1:1000). Immune complexes were detected using peroxidase-conjugated secondary antibodies: anti-rabbit (ThermoFisher Scientific; rb:13460; 1:3000) and anti-mouse (ThermoFisher Scientific; ms:31450; 1:3000). Densitometric analysis of immunoblot bands was performed using the Multi Gauge MFC application version 3.0.0.0.

Real Time RT-PCR Analysis—Total RNA was harvested from cell cultures or mouse lung tissue, after homogenization as described for immunoblotting, using the PeqGold total RNA kit (Peqlab; 12–6834-01) and screened by quantitative real time RT-PCR with the primers listed in Table 1, as described previously (22, 44, 45). Changes in mRNA expression were assessed using the *gapdh* gene as a reference, as described previously (22, 44, 45). Changes in mRNA expression were reflected as fold change, using the formula: fold change = $2^{\Delta\Delta CT}$ values (22, 44, 45).

Dual Luciferase Assay—The Dual-Luciferase assay, using both the firefly luciferase and *Renilla* luciferase reporters was employed to assess TGF-β signaling. The $(CAGA)_9$-firefly luciferase (p$(CAGA)_9$-luc) (46) and the BRE-firefly luciferase (pBRE-luc) (47) constructs were obtained from Dr. Daizo Koinuma (University of Tokyo). NIH/3T3 cells or primary lung fibroblasts were co-transfected with both the appropriate firefly luciferase-expressing construct and pRL-SV40 (Promega; which constitutively expresses *Renilla* luciferase) using Lipofectamine™ 2000 (Invitrogen), followed by a 6-h transfection period in serum-free Opti-MEM® (Invitrogen). If cells were intended for subsequent siRNA transfection, the siRNA was also transfected with Lipofectamine™ 2000 (Invitrogen), and cells were incubated with siRNA in serum-free Opti-MEM® (Invitrogen) medium, after which medium was exchanged for DMEM supplemented with 10% FCS, and cells were then stimulated with glucocorticoids and/or TGF-β_1 (or vehicle alone, where indicated). The Dual-Luciferase ratio (DLR),[4] was calculated from luminescence units generated by firefly luciferase normalized for luminescence units generated by *Renilla* luciferase, as described previously (23).

Animal Studies—Animal experiments performed in Germany were approved by the Regierungspräsidium Darmstadt (housing the Institutional Animal Care and Use Committee equivalent in Germany) under approval number B2/331. To assess the impact of glucocorticoid administration on TGF-β signaling *in vivo* in the mouse lung, six female C57Bl/6J mice received an intraperitoneal injection (100 μl) of dexamethasone (10 mg/kg of body mass; from a dexamethasone sodium

[4] The abbreviations used are: DLR, Dual-Luciferase ratio; ANOVA, analysis of variance; BRE, BMP response element.

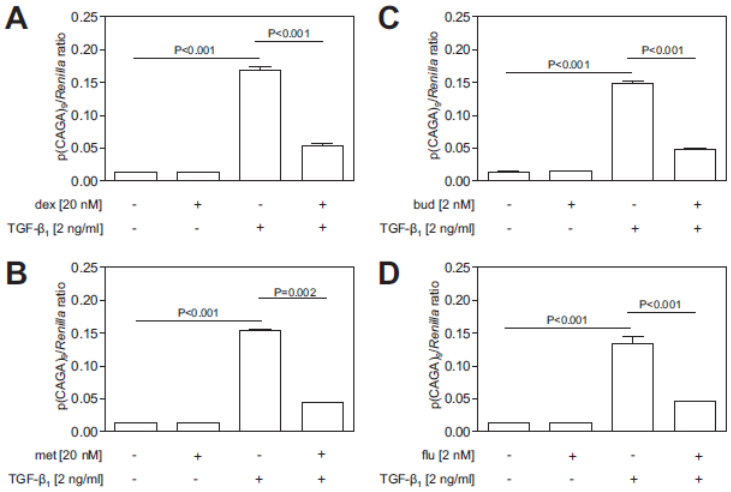

FIGURE 1. **Glucocorticoids inhibit canonical Tgfbr1/Smad2/3 TGF-β signaling in NIH/3T3 cells.** *A–D*, activation of the TGF-β-responsive $(CAGA)_9$ promoter element by TGF-β_1 (2 ng/ml), assessed by Dual-Luciferase reporter assay. NIH/3T3 cells were transfected with $p(CAGA)_9$-luc and pRL-SV40 constructs and, 6 h later, treated with dexamethasone (*A*, *dex*, 20 nM), methylprednisolone (*B*, *met*, 20 nM), budesonide (*C*, *bud*, 2 nM), or fluticasone (*D*, *flu*, 2 nM), or vehicle alone for 18 h, followed by TGF-β_1 (2 ng/ml) for an additional 12 h. The data indicate means ± S.D. ($n = 6$). The *p* values were assessed by one-way ANOVA followed by a Bonferroni post hoc test.

phosphate 4 mg/ml injection solution (JENAPHARM®, mibe GmbH), diluted in PBS], whereas six control mice received an intraperitoneal injection (100 μl) of vehicle (PBS) alone. Twenty-four hours later, the mice were sacrificed, and the lung, liver, heart, and kidneys were harvested for protein and RNA isolation. Organ homogenates were screened for changes in Tgfbr3, Smad1, phospho-Smad1/5/8, Smad2/3, and phospho-Smad2 expression by immunoblot and for changes in mRNA expression of *acvrl1*, *tgfbr3*, and *smad1* by real time RT-PCR.

Statistical Analyses—Data are indicated as means ± S.D. Statistical comparisons were made between two samples with an unpaired Student's *t* test and by one-way ANOVA followed by a Bonferroni post hoc test (for more than two samples), to evaluate changes between mean values.

RESULTS

Glucocorticoids Inhibit Classical TGF-β Signaling—The effect of glucocorticoids on TGF-β signaling was assessed by the activation of the $(CAGA)_9$ Smad3-binding element that is common to promoters of Tgfbr1/Smad2/3-regulated genes (46), which was assessed in a luminescence-based Dual-Luciferase assay. TGF-β activated the $(CAGA)_9$ element of the $p(CAGA)_9$-luc construct, which was evident by an increase in DLR from 0.014 ± 0.00007 (Fig. 1*A*, *first bar*) in the unstimulated condition to 0.168 ± 0.01 (Fig. 1*A*, *third bar*) after TGF-β_1 (2 ng/ml; 12 h) stimulation. The presence of dexamethasone (20 nM) did not impact the DLR, at 0.014 ± 0.0003 (Fig. 1*A*, *second bar*), relative to the unstimulated condition, where a DLR of 0.014 ± 0.00007 was attained (Fig. 1*A*, *first bar*). However, pretreatment of NIH/3T3 cells with dexamethasone (20 nM) for 18 h prior to stimulation with TGF-β_1 caused a decrease in DLR, from 0.168 ± 0.01 (Fig. 1*A*, *third bar*) in the absence of dexamethasone to 0.054 ± 0.005 (Fig. 1*A*, *fourth bar*) in the presence of dexamethasone. These data indicate that the activation of the $(CAGA)_9$ element by TGF-β_1 was inhibited by dexamethasone. Identical trends were also seen with another older generation synthetic glucocorticoid, methylprednisolone (20 nM; Fig. 1*B*), as well as with two newer generation synthetic glucocorticoids: budesonide (2 nM; Fig. 1*C*) and fluticasone (2 nM; Fig. 1*D*).

Glucocorticoids Alter Expression of Tgfbr3—Glucocorticoids blocked TGF-β signaling via the Tgfbr1/Smad2/3 axis, as assessed by activation of the $(CAGA)_9$ element (Fig. 1). One possible explanation for this was that glucocorticoids might alter the expression of components of the TGF-β signaling machinery. To address this possibility, the expression of key components of the Tgfbr1/Smad2/3 axis signaling machinery was assessed in NIH/3T3 cells by real time RT-PCR 18 h after dexamethasone (20 nM) treatment and also after 18 h dexamethasone (20 nM) treatment followed by 12 h of TGF-β_1 (2 ng/ml) stimulation (30 h total). Interestingly, the mRNA abundance of the gene accessory type III TGF-β receptor, Tgfbr3 (also called betaglycan (37–39)) was increased by dexamethasone 1.88 ± 0.35-fold ($p < 0.001$, relative to the unstimulated condition), hinting at a mechanism by which glucocorticoids might inhibit TGF-β signaling in fibroblasts. For this reason, a possible role for Tgfbr3 in regulating TGF-β signaling in NIH/3T3 cells was explored in detail.

Glucocorticoids Recruit Tgfbr3 to Shift TGF-β Signaling from Smad2/3 to Smad1—To examine the functional contribution of Tgfbr3 to the effects of dexamethasone on TGF-β signaling, the expression of *tgfbr3* was ablated by transfection of NIH/3T3 cells with siRNA directed against *tgfbr3*, with scrambled siRNA

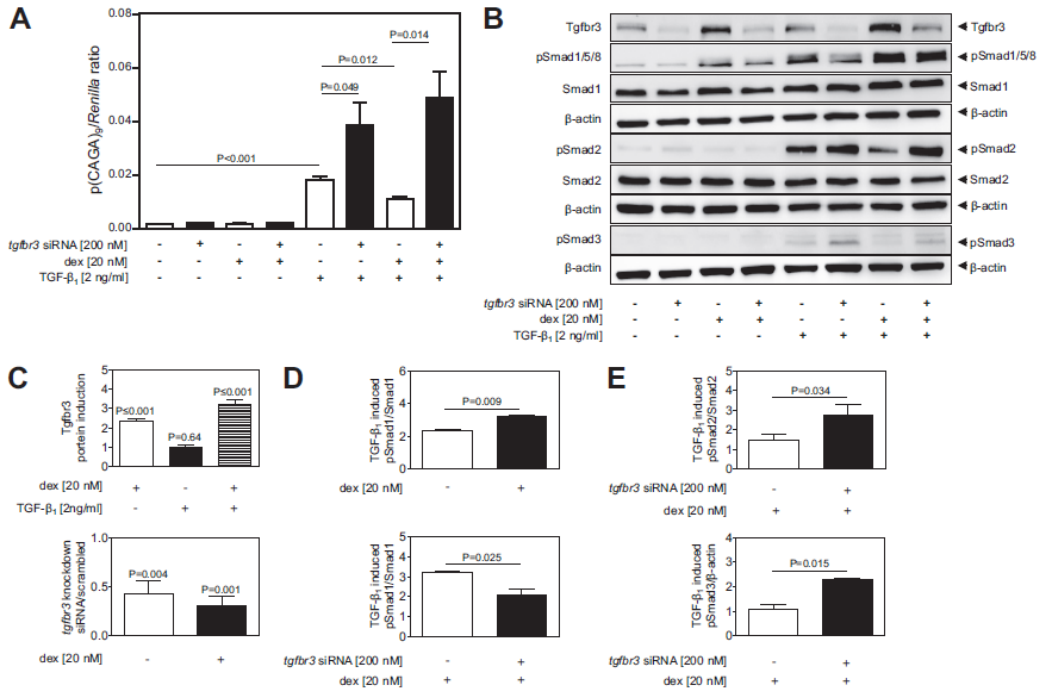

FIGURE 2. **Glucocorticoids recruit Tgfbr3 to shift TGF-β signaling from the Tgfbr1/Smad2/3 to the Acvrl1/Smad1 axis in NIH/3T3 cells.** *A*, Tgfbr3 expression was knocked down by siRNA transfection, and the effects of dexamethasone (*dex*; 20 nM) and TGF-β_1 (2 ng/ml), alone or in combination, were assessed in a luminescence-based Dual-Luciferase assay employing p(CAGA)$_9$-luc and pRL-SV40. The data represent means ± S.D. ($n = 6$), and *p* values were assessed by one-way ANOVA followed by a Bonferroni post hoc test (groups of four). *B*, the impact of reduced Tgfbr3 expression on the phosphorylation of Smad1, Smad2, and Smad3 induced by dexamethasone and TGF-β_1 stimulation (alone, or in combination), was assessed by immunoblot. *C*, densitometric analysis was employed to assess the impact of dexamethasone and/or TGF-β_1 on Tgfbr3 levels in NIH/3T3 cells treated with scrambled siRNA alone (*upper panel*) or with siRNA directed against *tgfbr3* (*lower panel*). *D*, densitometric analysis was employed to assess the impact of dexamethasone on TGF-β_1-induced Smad1 phosphorylation, in the presence of Tgfbr3 (*upper panel*) and after ablation of Tgfbr3 expression (*lower panel*). For *D*, *p* values compare mean values in the stimulated *versus* unstimulated condition. *E*, densitometric analysis was employed to assess the impact of ablation of Tgfbr3 expression on TGF-β_1-induced Smad2 (*upper panel*) and Smad3 (*lower panel*) phosphorylation. The data represent means ± S.D. ($n = 3$), and *p* values were assessed by unpaired Student's *t* test.

serving as a negative control. Using a luciferase-based DLR assay, TGF-β_1 induced activation of the TGF-β-responsive (CAGA)$_9$ element (Fig. 2*A*), and this effect was potentiated (*i.e.*, (CAGA)$_9$-driven luciferase production was increased) when *tgfbr3* expression was ablated by siRNA, confirming that Tgfbr3 was antagonistic to the Tgfbr1/Smad2/3 axis. Consistent with the data presented in Fig. 1*A*, dexamethasone blocked TGF-β induction of luciferase expression by the (CAGA)$_9$ element (Fig. 2*A*; compare the *seventh bar versus* the *fifth bar*). When *tgfbr3* expression was ablated, dexamethasone lost the ability to dampen (CAGA)$_9$ responsiveness to TGF-β (Fig. 2*A*, compare the *eighth bar versus* the *seventh bar*). These DLR data confirm that Tgfbr3 impacts both the responsiveness of the Tgfbr1/Smad2/3 (CAGA)$_9$ element to TGF-β_1 and that Tgfbr3 mediates the effect of glucocorticoids on TGF-β_1 induction of the (CAGA)$_9$ element.

To examine the mechanistic role of Tgfbr3 further, the more proximal aspects of the Tgfbr1/Smad2/3 and Acvrl1/Smad1 axes were examined, by assessing Smad2/3 phosphorylation, and Smad1 phosphorylation, respectively (Fig. 2*B*; quantified from three independent experiments in Fig. 2, *D* and *E*). In support of the increased *tgfbr3* mRNA levels observed in response to dexamethasone stimulation (reported above), increased Tgfbr3 protein expression in response to dexamethasone stimulation was also observed by immunoblot (Fig. 2*B*, compare the *third lane versus* the *first lane*; quantified in Fig. 2*C*, *upper panel*). In the case of Smad2/3, TGF-β stimulation drove phosphorylation of both Smad2 and Smad3 (Fig. 2*B*, *fifth lane*), and this effect was potentiated (*i.e.*, more Smad phosphorylation was seen) when *tgfbr3* expression was knocked down (Fig. 2*B*, *sixth lane*), with the knockdown of Tgfbr3 validated by immunoblot (Fig. 2*B*, compare *even versus odd lanes*; quantified in Fig. 2*C*, *lower panel*). In the presence of Tgfbr3, dexamethasone reduced Smad2/3 phosphorylation levels (Fig. 2*B*, compare the *seventh lane versus* the *fifth lane*; quantified in Fig. 2*E*), whereas after siRNA-mediated ablation of *tgfbr3* expression, the inhibitory effect of dexamethasone on TGF-β_1-induced phosphorylation of Smad2/3 was lost (Fig. 2*B*, compare the

eighth lane versus the *sixth lane*; quantified in Fig. 2*E*). These data clearly indicate that (i) Tgfbr3 is antagonistic to TGF-β-driven Smad2/3 phosphorylation in NIH/3T3 cells and (ii) dexamethasone requires Tgfbr3 to block phosphorylation of Smad2/3 induced by TGF-β.

Interestingly, an analysis of Smad1 phosphorylation, which lies in the alternative Acvrl1/Smad1 TGF-β signaling axis, was dramatically—and oppositely—impacted by dexamethasone (Fig. 2*B*). Indeed, dexamethasone alone was able to drive Smad1 phosphorylation (Fig. 2*B*, compare the *third lane versus* the *first lane*; quantified in Fig. 2*D*). Furthermore, TGF-β_1 stimulated Smad1 phosphorylation, and this effect was stronger in the presence of Tgfbr3 (Fig. 2*B*, compare the *sixth lane versus* the *fifth lane*), which is the opposite of what is seen for Smad2 phosphorylation in the presence of Tgfbr3. Most notably, Tgfbr3 had a pivotal effect on the ability of dexamethasone to impact the ability of TGF-β_1 to phosphorylate Smad1 (Fig. 2*B*, *sixth lane versus fifth lane*, compared with *eighth lane versus seventh lane*). This effect is highlighted in the densitometric analysis presented in Fig. 2*D*. Together, these data demonstrate two important facts: (i) that dexamethasone redirects TGF-β signaling in NIH/3T3 cells, blocking the Smad2/3 axis and favoring the Smad1 axis, and (ii) that Tgfbr3 is central to the ability of dexamethasone to redirect TGF-β signaling in this way.

The ability of Tgfbr3 to impact TGF-β signaling via the Acvrl1/Smad1 axis was validated by the overexpression of human TGFBR3 (which mimics the effect of dexamethasone on Tgfbr3 expression in NIH/3T3 cells) from plasmid pIRES::*TGFBR3*. Overexpression of TGFBR3 dose-dependently increased both base-line and TGF-β-stimulated Smad1/5/8 phosphorylation (Fig. 3*A*; quantified in Fig. 3*B*). Employing a DLR-based luciferase reporter system, where the Smad1-responsive BMP response element (BRE) drives luciferase production in plasmid pBRE-luc, co-transfection of pBRE-luc with p pIRES::*TGFBR3* increased base-line activity of the Smad1-responsive BRE (Fig. 3*C*). The impact of dexamethasone on TGF-β-driven BRE activity was not assessed, because dexamethasone alone drove pBRE-luc luciferase expression, suggesting the presence of a glucocorticoid response element in the pBRE-luc plasmid (data not shown). These data demonstrate that overexpression of Tgfbr3, as would be induced by dexamethasone, would drive signaling via the Acvrl1/Smad1 axis. It is important to note that the level of increased Tgfbr3 expression required to drive Smad1/5/8 phosphorylation (Fig. 3*B*) was below or equal to the levels of Tgfbr3 expression increased by dexamethasone (Fig. 2*C*, *upper panel*). As such, the levels of Tgfbr3 increased by dexamethasone are sufficient to drive increased Smad1/5/8 phosphorylation. These data also support the idea that dexamethasone-driven Tgfbr3 expression would shift the balance of TGF-β signaling from the Tgfbr1/Smad2/3 axis to the Acvrl1/Smad1 axis in NIH/3T3 cells.

Smad1 Functionally Contributes to the Effects of Dexamethasone on TGF-β Signaling—Both dexamethasone and Tgfbr3 impacted Smad1 phosphorylation in NIH/3T3 cells (Fig. 2*B*), suggesting a role for Smad1, which is the key mediator of the Acvrl1/Smad1 axis, in the effects of dexamethasone on TGF-β signaling. The Acvrl1/Smad1 axis, which is traditionally considered to be active primarily in the endothelium (29, 48–50), was demonstrated to be active in NIH/3T3 cells (results not shown) and in fibroblasts (51, 52). To examine the functional contribution of Smad1 to the effects of dexamethasone on TGF-β signaling, the expression of *smad1* was ablated by transfection of NIH/3T3 cells with siRNA directed against *smad1*, with scrambled siRNA serving as a negative control. Using a luciferase-based promoter reporter assay, TGF-β_1 could induce expression of the TGF-β-responsive $(CAGA)_9$ element (Fig. 4*A*), and this effect was potentiated when *smad1* expression was ablated by siRNA (Fig. 4*A*, compare the *sixth bar versus* the *fifth bar*). Consistent with the data presented in Fig. 1*A*, dexamethasone blocked TGF-β_1 induction of luciferase expression by the $(CAGA)_9$ element (Fig. 4*A*). These DLR data confirm that Smad1 impacts the responsiveness of the Tgfbr1/Smad2/3 $(CAGA)_9$ element to TGF-β, which is consistent with the Acvrl1/Smad1 axis being antagonistic to the Tgfbr1/Smad2/3 axis. Additionally, these data reveal that Smad1 is a central mediator of the effects of dexamethasone on Tgfbr1/Smad2/3-driven $(CAGA)_9$ activation, because when *smad1* expression was ablated, the inhibitory effects of dexamethasone on the responsiveness of the Tgfbr1/Smad2/3 $(CAGA)_9$ element to TGF-β were lost (Fig. 4*A*, compare the *eighth bar versus* the *sixth bar*). These data support the idea that increased Tgfbr3 expression would redirect TGF-β signaling by two separate but related mechanisms: increased Tgfbr3 expression would (i) drive the Acvrl1/Smad1 pathway directly by enhancing Smad1/5/8 phosphorylation and (ii) inhibit the Tgfbr1/Smad2/3 pathway through the antagonistic impact of increased Smad1 activity on Tgfbr1/Smad2/3 signaling.

TGF-β_1 stimulation drove Smad2 phosphorylation (Fig. 4*B*, compare the *fifth lane versus* the *first lane*), and this effect was potentiated (*i.e.*, more Smad2 phosphorylation was seen) when *smad1* expression was knocked down (Fig. 4*B*, compare the *sixth lane versus* the *fifth lane*). In the presence of Smad1, dexamethasone dramatically reduced Smad2 phosphorylation levels (Fig. 4*B*, compare the *seventh lane versus* the *fifth lane*), whereas after siRNA-mediated ablation of *smad1* expression, pretreatment with dexamethasone did not appreciably impact the ability of TGF-β to drive phosphorylation of Smad2 (Fig. 4*B*, compare the *eighth lane versus* the *sixth lane*). The Smad2 phosphorylation data are quantified in Fig. 4*C*, where Smad2 phosphorylation has been preferentially used as a proximal readout for TGF-β/Tgfbr1/Smad2/3 signaling, because the low abundance of Smad3 makes total Smad3 detection troublesome, and the phospho-Smad3 antibody yields high background. Together, these data confirm (i) that Smad1 is antagonistic to the Tgfbr1/Smad2/3 axis in NIH/3T3 cells and (ii) that dexamethasone requires Smad1 to dampen the activity of the Tgfbr1/Smad2/3 axis.

Glucocorticoids Have Comparable Effects in Primary Lung Fibroblasts—Because the NIH/3T3 cell line essentially serves as a model for fibroblasts, the effects of glucocorticoids on TGF-β signaling were also assessed in primary lung fibroblasts. Indeed, responses were seen in primary lung fibroblasts comparable to those observed in the preceding data obtained with NIH/3T3 cells, where exposure to dexamethasone dampened activation of the Tgfbr1/Smad2/3-responsive $(CAGA)_9$ element in

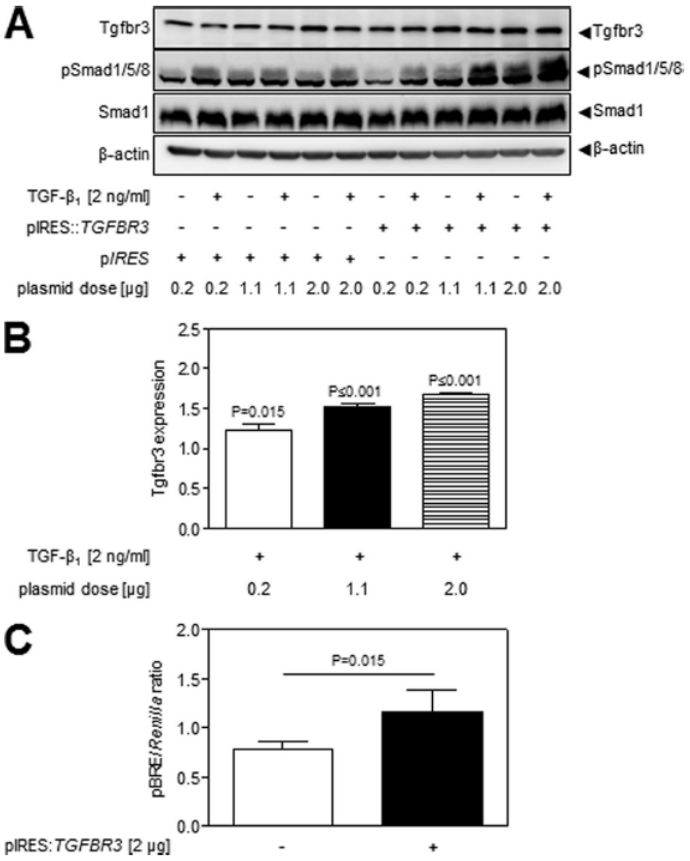

FIGURE 3. **Overexpression of TGFBR3 drove the Acvrl1/Smad1 axis.** *A*, the impact of the overexpression of human TGFBR3 in NIH/3T3 cells in Smad1/5/8 phosphorylation was assessed by immunoblot, employing pIRES::*TGFBR3* for TGFBR3 overexpression or pIRES as empty vector. Identical data were obtained with the mouse Tgfbr3-expressing construct; however, the increased expression of human *TGFBR3* over the background, endogenous mouse Tgfbr3 was more evident, and hence, these data are presented here. *B*, expression changes in Tgfbr3 in the TGF-β-stimulated groups were assessed by densitometry, where *p* values compare mean values in the pIRES-transfected *versus* pIRES::*TGFBR3*-transfected cells. *C*, to validate that the expression of TGFBR3 can (in the absence of TGF-β stimulation) drive Acvrl1/Smad1 signaling, the expression of the Smad1-responsive "BMP-responsive element" in pBRE-luc was assessed by Dual-Luciferase assay, in the presence of either pIRES::*TGFBR3* or pIRES as empty vector. The data represent means ± S.D. ($n = 6$), and *p* values were assessed by unpaired Student's *t* test.

$p(CAGA)_9$-luc after TGF-β stimulation (Fig. 5*A*). Furthermore, exposure of primary fibroblasts potentiated Smad1 phosphorylation and dampened Smad3 phosphorylation in primary lung fibroblasts in response to TGF-β stimulation (Fig. 5*B*), which is comparable to the effects of dexamethasone on NIH/3T3 cells. However, dexamethasone did not impact Smad2 phosphorylation in primary lung fibroblasts (Fig. 5*B*), which contrasts with observations made in NIH/3T3 cells (Fig. 2*B*).

The impact of dexamethasone on Smad phosphorylation was also assessed in other cells that represent the constituent cell types of the lung, including H441 cells, which are a human airway epithelial cell line that polarizes in culture and are similar to Clara cells (Fig. 5*D*); primary human lung microvascular endothelial cells (Fig. 5*C*); and primary human pulmonary artery smooth muscle cells (Fig. 5). In all of these cell types, TGF-β-driven Smad1 phosphorylation and, thus, activation of the Acvrl1/Smad1 axis, were potentiated by dexamethasone. Thus, the impact of dexamethasone on the Acvr1/Smad1 axis appears to be a mechanism common to many lung (and perhaps other) cell types. As with lung fibroblasts and NIH/3T3 cells, dexamethasone dampened the phosphorylation of Smad3 in response to TGF-β_1, in both primary pulmonary artery endothelial cells (Fig. 5*C*) and primary lung pulmonary artery smooth muscle cells (Fig. 5*E*). Thus, dexamethasone was also antagonistic to Tgfbr1/Smad2/3 signaling in these cells, although no impact on Smad2 phosphorylation was noted for either cell type. Furthermore, dexamethasone had no appreciable impact on Smad2 or Smad3 phosphorylation in airway epithelial cells (Fig. 5*D*). Noteworthy among the observations

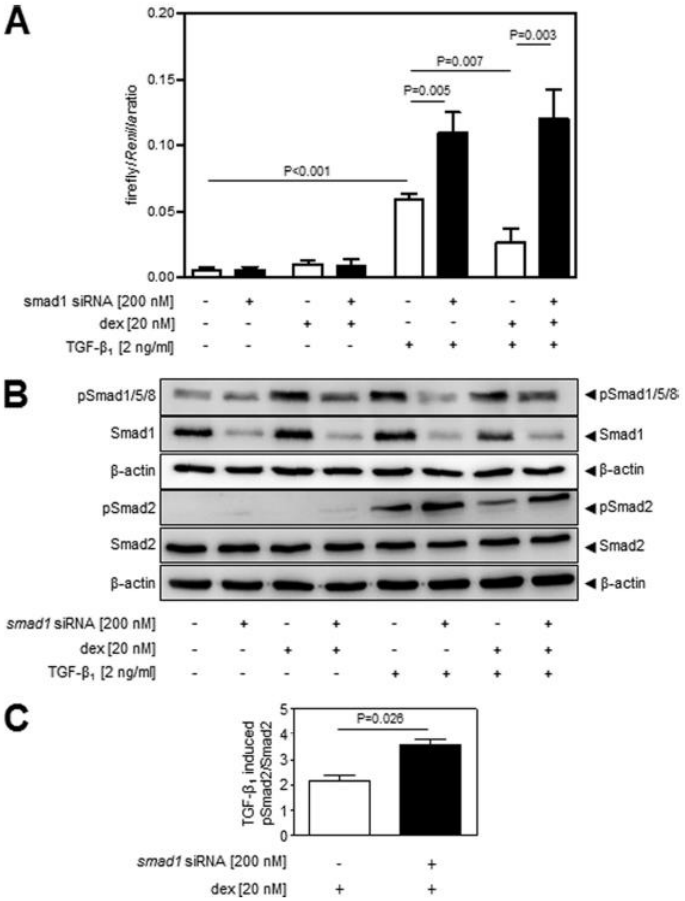

FIGURE 4. **Smad1 functionally contributes to the effects of glucocorticoids on Tgfbr1/Smad2 signaling in NIH/3T3 cells.** Smad2 was preferentially employed as a readout of Tgfbr1/Smad2/3 axis activation, because Smad2 is more abundant than Smad3, which made quantification and visualization easier. *A*, Smad1 expression was knocked down by siRNA transfection, and the effects of dexamethasone (*dex*) and TGF-β_1 (2 ng/ml), alone or in combination, were assessed in a luminescence-based Dual-Luciferase assay employing p(CAGA)$_9$-luc and pRL-SV40. The data represent means ± S.D. ($n = 6$), and p values were assessed by one-way ANOVA followed by a Bonferroni post hoc test. *B*, the impact of reduced Smad1 expression on the phosphorylation of Smad2 induced by dexamethasone and TGF-β_1 stimulation (alone, or in combination) was assessed by immunoblot. *C*, densitometric analysis was employed to assess the impact of *smad1* ablation on TGF-β_1-induced Smad2 phosphorylation in the presence or absence of dexamethasone. The data represent means ± S.D. ($n = 3$), and p values were assessed by unpaired Student's t test.

made here are (i) that dexamethasone has largely the same impact on primary lung fibroblasts as seen with NIH/3T3 cells and (ii) that dexamethasone has different effects on different lung cell types, although the ability of dexamethasone to potentiate TGF-β-driven Smad1 phosphorylation appears to be common to all lung cell types explored.

Glucocorticoids Functionally Impact TGF-β-regulated Physiological Processes—TGF-β regulates a broad spectrum of processes in lung fibroblasts. To assess the impact of glucocorticoids on some of these processes, the TGF-β-driven differentiation of primary human lung fibroblasts into myofibroblasts was selected to demonstrate proof of principle. This process is described to be driven by the Acvrl1/Smad1 axis (30–36) and thus should be enhanced in fibroblasts after exposure to dexamethasone. The acquisition of smooth muscle myosin (MYH11) and α-smooth muscle actin (ACTA2) markers are the hallmark characteristics of myofibroblast differentiation. No effect of TGF-β_1 alone or dexamethasone alone was evident on MYH11 expression (Fig. 6, *A* and *B*) but applied consecutively (18 h dexamethasone followed by 12 h TGF-β_1) increased MYH11 abundance. In contrast, both TGF-β_1 and dexamethasone applied alone drove ACTA2 expression, and this effect was potentiated by consecutive application (Fig. 6, *A* and *C*). This observation is consistent with the increased activation of the Acvrl1/Smad1 axis by dexamethasone that was observed in NIH/3T3 cells (Fig. 2*B*) and primary lung fibroblasts (Fig. 5*B*)

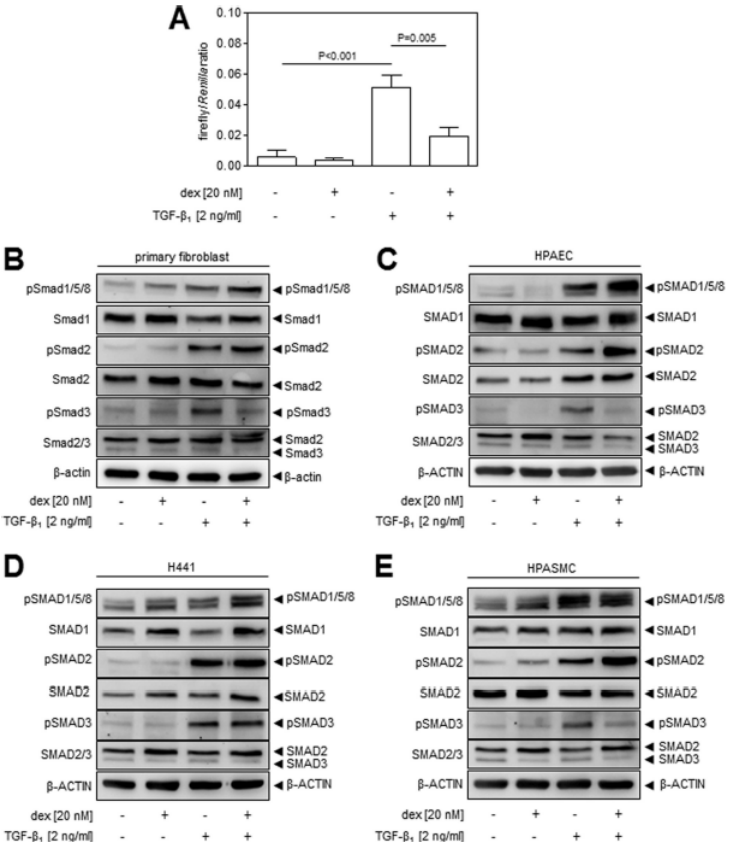

FIGURE 5. **The impact of glucocorticoids on the Acvrl1/Smad1 and Tgfbr1/Smad2/3 axes are paralleled in primary human lung fibroblasts and are evident in other constituent cell types of the lung.** *A*, activation of the TGF-β-responsive $(CAGA)_9$ promoter element by TGF-β_1 (2 ng/ml), assessed by Dual-Luciferase reporter assay. Primary adult human lung fibroblasts were transfected with $p(CAGA)_9$-luc and pRL-SV40 constructs and, 6 h later, treated with dexamethasone (*dex*; 20 nM) or vehicle alone for 18 h, followed by TGF-β_1 (2 ng/ml) for an additional 12 h. The data indicate means ± S.D. ($n = 6$), where *p* values were assessed by one-way ANOVA followed by a Bonferroni post hoc test. The impact of dexamethasone on Smad1, Smad2, and Smad3 phosphorylation was also assessed by immunoblot in primary adult human lung fibroblasts (*B*), primary adult human pulmonary artery endothelial cells (*C*), the human lung H441 cell line (*D*), and primary adult human pulmonary artery smooth muscle cells (*E*). In each case, cells were treated with dexamethasone (20 nM) for 18 h, followed by TGF-β_1 (2 ng/ml) for 30 min, prior to assessing Smad expression and phosphorylation by immunoblot.

and supports the idea that the impact of glucocorticoids on TGF-β signaling may be of physiological and pathophysiological importance.

Glucocorticoids Modulate Tgfbr3, Acvrl1, and Smad1 Expression in Vivo—Intraperitoneal administration of dexamethasone (10 mg/kg) for 24 h to living mice resulted in increased mRNA abundance of *tgfbr3*, *smad1*, and *acvrl1* in the lungs, but not generally in the extrapulmonary organs, of live mice (Fig. 7*A*). Interestingly, these changes were confined largely to the lung, with down-regulation of *smad1* expression in the heart and liver and down-regulation of *acvrl1* expression in the liver being the only changes observed in the three extrapulmonary organs examined. The basis for the lung-selective effect of dexamethasone is not known. In support of the gene expression data, the protein expression of Tgfbr3 and Smad1 was increased in the lungs of dexamethasone-treated live mice (Fig. 7*B*). These data are consistent with the trends observed in NIH/3T3 cells (Fig. 2*B*) and in primary lung fibroblasts (Fig. 5*B*). Additionally, an increased abundance of Smad1 was observed in the lungs from dexamethasone-treated *versus* vehicle-treated mice (Fig. 7*B*). In contrast, the abundance of phospho-Smad2 was unchanged comparing lungs from dexamethasone-treated mice *versus* lungs from vehicle-treated mice (Fig. 7*B*), which is also consistent with the data from primary lung fibroblasts (Fig. 5*B*). Unfortunately, neither phospho-Smad3 nor total Smad3 could be reliably detected in mouse lung homogenates (data not shown). Together, these data suggest that dexamethasone can drive TGF-β/Acvrl1/Smad1 signaling in the lungs of live mice, lending credence to our suggestion that this phenomenon may be physiologically relevant.

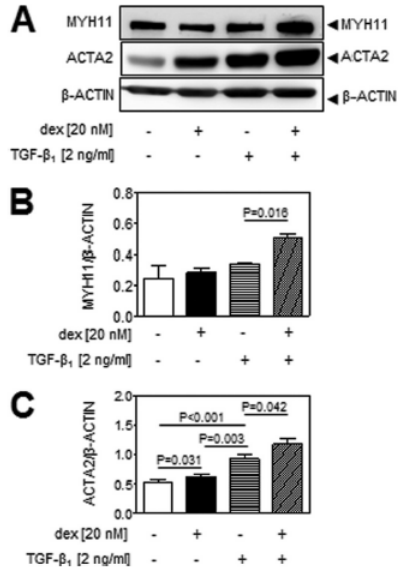

FIGURE 6. **Glucocorticoids act synergistically with TGF-β_1 to drive the differentiation of primary adult human lung fibroblasts to myofibroblasts.** *A*, primary adult human lung fibroblasts were stimulated with TGF-β_1 (2 ng/ml; 30 min) after prestimulation with dexamethasone (*dex*; 20 nM; 18 h) or PBS (as vehicle), prior to the assessment of acquisition of markers of myofibroblast differentiation: smooth muscle myosin (MYH11) and smooth muscle actin (ACTA2) by immunoblot. *B* and *C*, densitometric analysis was employed to assess changes in MYH11 (*B*) and ACTA2 (*C*) abundance. The data represent means ± S.D. ($n = 3$), and p values were assessed by one-way ANOVA followed by a Bonferroni post hoc test.

DISCUSSION

The data presented here demonstrate that glucocorticosteroids impact TGF-β signaling in lung fibroblasts, as well as in other constituent cell types of the lung. This was demonstrated for four synthetic glucocorticoids used in clinical practice: dexamethasone, methylprednisolone, budesonide, and fluticasone. These data are important because (i) TGF-β is recognized as a key mediator of both normal physiological processes that take place in the lung and pathological processes that underlie a broad spectrum of lung diseases; (ii) lung fibroblasts are a key disease-mediating cell type in several lung diseases and are an important regulator of organogenesis and tissue repair; and (iii) glucocorticoids are a mainstay therapy for several lung diseases. The possible interaction between glucocorticoids and the TGF-β signaling system should be considered when glucocorticoids are used to treat lung disease.

The primary impact of glucocorticoids on TGF-β signaling in fibroblasts was to shift TGF-β signaling away from the Tgfbr1/Smad2/Smad3 axis and in favor of the Acvrl1/Smad1/Smad5/Smad8 axis. This was achieved primarily by glucocorticoid-driven expression of Tgfbr3, where Tgfbr3 acted as a redirecting "switch." In this study, the effects of glucocorticoids on Tgfbr3 expression have been demonstrated to be a functionally relevant mechanism by which glucocorticoids dampen Tgfbr1/Smad2/3 signaling and, at the same time, enhance Acvrl1/Smad1 signaling in fibroblasts.

In the endothelium, the presence of functional Tgfbr1/Smad2/3 and Acvrl1/Smad1 TGF-β signaling axes has been described (28, 29), although no role for Tgfbr3 has ever been implicated in the balance of activity of these two axes. In the endothelium, the balance between these two signaling axes has been credited with profound effects on vascular homeostasis, where the Tgfbr1/Smad2/3 pathway leads to inhibition of endothelial cell migration and proliferation, and the Acvrl1/Smad1 pathway induces endothelial cell migration and proliferation (28, 29). Specifically in the pulmonary arteries, reduced Acvrl1/Smad1 signaling in the endothelium plays a role in the aberrant pulmonary vascular remodeling seen in pulmonary arterial hypertension and hereditary hemorrhagic telangiectasia, where Smad1 signaling is blocked, because of dysfunctional Acvrl1 caused by *ACVRL1* mutations (53). Diminished Smad1 phosphorylation is also seen in the monocrotaline-based rat model of pulmonary hypertension (44). In other (nonhereditary) forms of telangiectasia, such as radiation-induced telangiectasia, a similar pattern emerges, where ionizing radiation shifts the balance from Tgfbr1/Smad2/3 to Acvrl1/Smad1 signaling in human dermal and lung microvascular endothelial cells, driving pathological activation of Notch signaling (54). In addition, blunted Acvrl1/Smad1 signaling is associated with the development of pulmonary arterial hypertension (44, 55–57), and Smad1-driven endothelial cell migration and proliferation are associated with pulmonary vascular development (58).

This highlights the importance of proper Acvrl1/Smad1 signaling in normal vascular homeostasis, as well as in pathology. It is tempting to speculate, based on the data presented here, that glucocorticoids may be employed to correct this defect by driving Smad1 signaling in endothelial cells, particularly considering that both Tgfbr3 and Smad1 mRNA expression is also down-regulated in patients with idiopathic pulmonary arterial hypertension (59). To date, the value of glucocorticoids in patients with pulmonary arterial hypertension has not been evaluated in a randomized controlled clinical trial; however, dexamethasone has been reported to reverse monocrotaline-induced pulmonary hypertension in rats (60), but Smad1 signaling was not assessed in that study. Pathological consequences caused by disturbances to the balance between the Tgfbr1/Smad2/3 and the Acvrl1/Smad1 axes are not limited to the vascular endothelium, where a shift in favor of the Acvrl1/Smad1 axis has been reported in chondrocytes in osteoarthritis. This pro-Acvrl1/Smad1 shift is regarded as pathogenic, because Acvrl1/Smad1 signaling promotes the pathological terminal differentiation of chondrocytes, driving cartilage destruction and osteoarthritis (61), which is interesting, given the widespread use of intra-articular injections of glucocorticoids to manage inflammatory flares associated with osteoarthritis (62).

Our observations that glucocorticoids modulate TGF-β signaling by promoting Acvrl1/Smad1-driven processes and suppressing Tgfbr1/Smad2/3-driven processes in lung fibroblasts are interesting when seen in the background of glucocorticoid use in lung disease. Indeed, these data may explain some observations recently reported in the literature. In a chorioamnion-

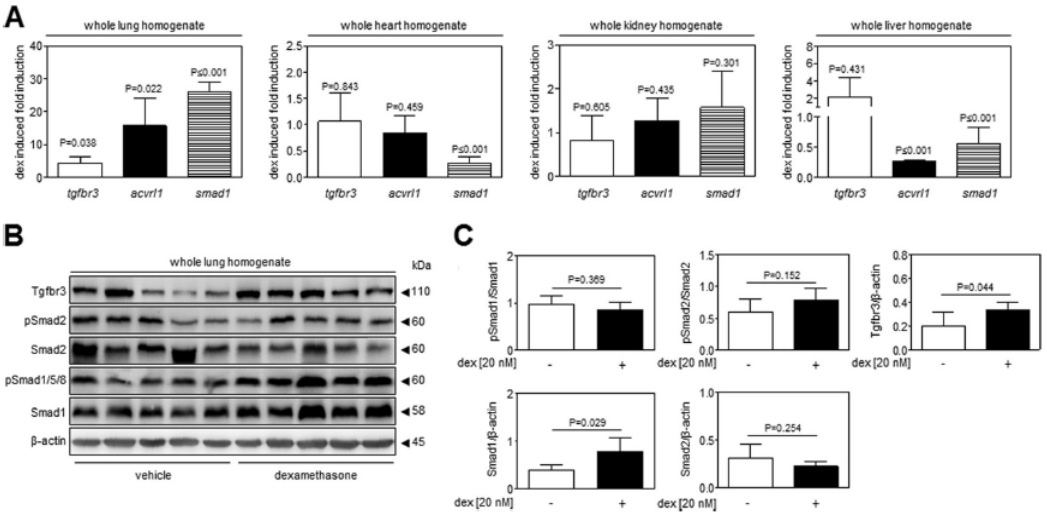

FIGURE 7. **Glucocorticoids modulate expression of the TGF-β signaling machinery in the lungs of living mice.** To assess whether the effects observed in NIH/3T3 cells and primary human lung fibroblasts were applicable *in vivo* in living mice, six adult female C57Bl/6J mice received an intraperitoneal injection of dexamethasone (10 mg/kg body mass), whereas six control adult female C57Bl/6J mice received an intraperitoneal injection of vehicle alone (PBS, 200 μl). 24 h later, mouse tissues were harvested for analysis. *A*, assessment of *tgfbr3*, *acvrl1*, and *smad1* expression by real time RT-PCR in the lungs, heart, kidney, and liver of dexamethasone (*dex*)- and vehicle-treated mice. The data represent means ± S.D. ($n = 6$), and p values were assessed by unpaired Student's t test and compare gene expression in dexamethasone-treated *versus* vehicle-treated mice. *B*, the expression of Tgfbr3 and total and phosphorylated Smad1 and Smad2 were assessed by immunoblot in mouse lung tissues. *C*, data were quantified by densitometric analysis, where data represent mean ± S.D. ($n = 5$/group), and p values were assessed by unpaired Student's t test.

itis preterm lamb model, administration of the glucocorticoid betamethasone to pregnant sheep, in which intrauterine inflammation had been induced by intra-amniotic injection of *Escherichia coli* lipopolysaccharide, caused a decrease in Tgfbr1-dependent Smad2 phosphorylation in fetal lungs (63). This is consistent with the data we present here, where we propose that glucocorticoids dampen the activity of the Tgfbr1/Smad2/3 axis. In further support of this idea, in another study, antenatal betamethasone dampened lung elastin and collagen deposition (64). Because the deposition of elastin and collagen is Tgfbr1/Smad2/Smad3-dependent, the reduced elastin and collagen deposition would be expected, given the impact of glucocorticoids on Tgfbr1/Smad2/Smad3 signaling reported here.

Glucocorticoids exhibited different effects on TGF-β signaling in the primary constituent cell types of the lung. Consistent across all four primary lung cell types was the ability of dexamethasone to promote increased base-line Smad1/5/8 phosphorylation. Additionally, dexamethasone acted synergistically with TGF-β to drive Smad1/5/8 phosphorylation in H441, fibroblast, and endothelial cells, although not in vascular smooth muscle cells. Thus, dexamethasone generally promoted Smad1/5/8 activation in multiple lung cell types. The opposite was seen with the Tgfbr1/Smad2/3 axis, where dexamethasone blunted TGF-β-induced Smad3 phosphorylation in lung fibroblasts, endothelial, and smooth muscle cells, but not H441 cells. In primary fibroblasts and H441 cells, dexamethasone did not impact TGF-β-induced Smad2 phosphorylation and acted synergistically with TGF-β to increase TGF-β-driven Smad2 phosphorylation in endothelial and smooth muscle cells. In general, the Tgfbr1/Smad2/Smad3 axis in H441 cells appeared relatively resistant to the effects of dexamethasone, although it has been suggested that in human fetal lung epithelial cells, dexamethasone, and TGF-β antagonize one another (65). Thus, in sum, although dexamethasone generally drove the Acvrl1/Smad1 pathway, the impact of dexamethasone on the Tgfbr1/Smad2/3 (and Smad2) pathway was variable and cell type-dependent.

The impact of glucocorticoids on TGF-β signaling in primary adult human lung fibroblasts was physiologically relevant, because dexamethasone and TGF-β acted synergistically to drive fibroblast to myofibroblast differentiation, as assessed by the acquisition of MYH11 (smooth muscle myosin) and ACTA2 (α-smooth muscle actin) markers. These contentions are supported by the observations of others that dexamethasone and TGF-β act synergistically to drive the differentiation of primary fetal human lung fibroblasts to myofibroblasts, as monitored by the acquisition of ACTA2 (66). The myofibroblast is a key pathogenic mediator of asthma, chronic obstructive pulmonary disease, bronchopulmonary dysplasia, and acute respiratory distress syndrome (67), and the data presented here indicate that glucocorticoids may drive myofibroblast differentiation in the background of glucocorticoid use in these pathologies. Although not addressed in this study, our data suggest a mechanism by which TGF-β signaling may also be modulated by endogenous glucocorticoids, such as cortisol, which are active in lung and airway diseases such as asthma (68, 69). Indeed, Smad1 signaling is reported to be activated (and proposed to drive pathology) in airway epithelial cells during experimental allergic airway inflammation (70), and it would be

interesting to assess whether increased Smad1 activation might be due to or exacerbated by glucocorticoids, either endogenous or applied exogenously, because budesonide and fluticasone are the mainstay of asthma therapy today (3, 4). When dexamethasone and TGF-β were applied in the reverse sequence (first TGF-β, then dexamethasone), no impact on TGF-β signaling was observed (results not shown); however, no impact was anticipated, because the effects of dexamethasone on TGF-β signaling are attributed here to dexamethasone-induced changes in the expression of Tgfbr3, a component of the TGF-β signaling machinery. The idea we present here is likely to be of disease relevance, because in a patient that is chronically treated with glucocorticoids, the expression of Tgfbr3 is likely to be increased. At the same time, TGF-β is generated continuously over the course of disease, and lung fibroblasts (and other lung cells) are likely to become more (through Acvrl1/Smad1) and less (through Tgfbr1/Smad2/3) responsive to TGF-β over time.

Used *in vivo* in mice, glucocorticoids influenced TGF-β signaling, and most notably, dexamethasone drove Tgfbr3 expression, as well as Smad1 expression (leading to an overall increase of phospho-Smad1 levels) in the lung. Unfortunately, neither Smad3 nor pSmad3 could be reliably detected in whole lung homogenates from mice. However, these data document that the two key effects of dexamethasone: increased Tgfbr3 and Smad1 expression, also occur *in vivo*. Although examined in the context of the respiratory system, the impact of glucocorticoids on TGF-β signaling almost certainly occurs in other cell types (and organs) as well, and as such, the data presented here are of broad general interest, in systems other than the respiratory system. Although, we also report here that when administered via the intraperitoneal route, the impact of dexamethasone on the expression of the TGF-β signaling machinery was seen predominantly in the lung, with little or no changes observed in the heart, kidney, or liver. The reasons for this are currently not apparent and should form the basis of future work exploring systemic glucocorticoid use to treat lung disease.

Acknowledgments—We thank Peter Rauschkolb (Max Planck Institute for Heart and Lung Research) for assistance with the isolation of primary fibroblasts from mouse lungs, Dr. Ardeshir Ghofrani (University Hospital Giessen) for helpful discussions regarding glucocorticoid use in patients with pulmonary arterial hypertension, Dr. Fernando Lopéz-Casillas (Universidad Nacional Autónoma de México) for providing the Tgfbr3 expression construct, and Dr. Daizo Koinuma (University of Tokyo) for providing the p(CAGA)$_9$-luc and pBRE-luc reporter constructs.

REFERENCES

1. Rhen, T., and Cidlowski, J. A. (2005) Antiinflammatory action of glucocorticoids. New mechanisms for old drugs. *N. Engl. J. Med.* **353,** 1711–1723
2. Barnes, P. J. (2006) Corticosteroid effects on cell signalling. *Eur. Respir. J.* **27,** 413–426
3. Barnes, P. J. (2011) Biochemical basis of asthma therapy. *J. Biol. Chem.* **286,** 32899–32905
4. Barnes, P. J. (2011) Pathophysiology of allergic inflammation. *Immunol. Rev.* **242,** 31–50
5. Wapner, R., and Jobe, A. H. (2011) Controversy. Antenatal steroids. *Clin. Perinatol.* **38,** 529–545
6. Barnes, P. J. (2011) Glucocorticosteroids. Current and future directions. *Br J. Pharmacol.* **163,** 29–43
7. Barnes, P. J. (2010) Inhaled corticosteroids in COPD. A controversy. *Respiration* **80,** 89–95
8. Steinberg, K. P., Hudson, L. D., Goodman, R. B., Hough, C. L., Lanken, P. N., Hyzy, R., Thompson, B. T., and Ancukiewicz, M. (2006) Efficacy and safety of corticosteroids for persistent acute respiratory distress syndrome. *N. Engl. J. Med.* **354,** 1671–1684
9. Thompson, B. T. (2010) Corticosteroids for ARDS. *Minerva Anestesiol.* **76,** 441–447
10. Walter, N., Collard, H. R., and King, T. E., Jr. (2006) Current perspectives on the treatment of idiopathic pulmonary fibrosis. *Proc. Am. Thorac. Soc.* **3,** 330–338
11. Doyle, L. W., Ehrenkranz, R. A., and Halliday, H. L. (2010) Dexamethasone treatment in the first week of life for preventing bronchopulmonary dysplasia in preterm infants. A systematic review. *Neonatology* **98,** 217–224
12. Watterberg, K. (2012) Evidence-based neonatal pharmacotherapy. Postnatal corticosteroids. *Clin. Perinatol.* **39,** 47–59
13. de Benedictis, F. M., and Bush, A. (2012) Corticosteroids in respiratory diseases in children. *Am. J. Respir. Crit. Care. Med.* **185,** 12–23
14. Madurga, A., Mizíková, I., Ruiz-Camp, J., and Morty, R. E. (2013) Recent advances in late lung development and the pathogenesis of bronchopulmonary dysplasia. *Am. J. Physiol. Lung Cell. Mol. Physiol.* **305,** L893–L905
15. Sanjabi, S., Zenewicz, L. A., Kamanaka, M., and Flavell, R. A. (2009) Anti-inflammatory and pro-inflammatory roles of TGF-β, IL-10, and IL-22 in immunity and autoimmunity. *Curr. Opin. Pharmacol.* **9,** 447–453
16. Wynn, T. A., and Ramalingam, T. R. (2012) Mechanisms of fibrosis. Therapeutic translation for fibrotic disease. *Nat. Med.* **18,** 1028–1040
17. Warburton, D., Shi, W., and Xu, B. (2013) TGF-β-Smad3 signaling in emphysema and pulmonary fibrosis. An epigenetic aberration of normal development? *Am. J. Physiol. Lung. Cell Mol. Physiol.* **304,** L83–L85
18. Farkas, L., Farkas, D., Warburton, D., Gauldie, J., Shi, W., Stampfli, M. R., Voelkel, N. F., and Kolb, M. (2011) Cigarette smoke exposure aggravates air space enlargement and alveolar cell apoptosis in Smad3 knockout mice. *Am. J. Physiol. Lung Cell. Mol. Physiol.* **301,** L391–L401
19. Xu, B., Chen, H., Xu, W., Zhang, W., Buckley, S., Zheng, S. G., Warburton, D., Kolb, M., Gauldie, J., and Shi, W. (2012) Molecular mechanisms of MMP9 overexpression and its role in emphysema pathogenesis of Smad3-deficient mice. *Am. J. Physiol. Lung Cell. Mol. Physiol.* **303,** L89–L96
20. Tarantal, A. F., Chen, H., Shi, T. T., Lu, C. H., Fang, A. B., Buckley, S., Kolb, M., Gauldie, J., Warburton, D., and Shi, W. (2010) Overexpression of transforming growth factor-β1 in fetal monkey lung results in prenatal pulmonary fibrosis. *Eur. Respir. J.* **36,** 907–914
21. Jain, M., Budinger, G. R., Lo, A., Urich, D., Rivera, S. E., Ghosh, A. K., Gonzalez, A., Chiarella, S. E., Marks, K., Donnelly, H. K., Soberanes, S., Varga, J., Radigan, K. A., Chandel, N. S., and Mutlu, G. M. (2011) Leptin promotes fibroproliferative acute respiratory distress syndrome by inhibiting peroxisome proliferator-activated receptor-γ. *Am. J. Respir. Crit. Care Med.* **183,** 1490–1498
22. Alejandre-Alcázar, M. A., Kwapiszewska, G., Reiss, I., Amarie, O. V., Marsh, L. M., Sevilla-Pérez, J., Wygrecka, M., Eul, B., Köbrich, S., Hesse, M., Schermuly, R. T., Seeger, W., Eickelberg, O., and Morty, R. E. (2007) Hyperoxia modulates TGF-β/BMP signaling in a mouse model of bronchopulmonary dysplasia. *Am. J. Physiol. Lung Cell. Mol. Physiol.* **292,** L537–L549
23. Kumarasamy, A., Schmitt, I., Nave, A. H., Reiss, I., van der Horst, I., Dony, E., Roberts, J. D., Jr., de Krijger, R. R., Tibboel, D., Seeger, W., Schermuly, R. T., Eickelberg, O., and Morty, R. E. (2009) Lysyl oxidase activity is dysregulated during impaired alveolarization of mouse and human lungs. *Am. J. Respir Crit Care Med.* **180,** 1239–1252
24. Miyazawa, K., Shinozaki, M., Hara, T., Furuya, T., and Miyazono, K. (2002) Two major Smad pathways in TGF-β superfamily signalling. *Genes Cells* **7,** 1191–1204
25. Massagué, J. (2012) TGFβ signalling in context. *Nat. Rev. Mol. Cell Biol.* **13,** 616–630
26. Feng, X. H., and Derynck, R. (2005) Specificity and versatility in TGF-β signaling through Smads. *Annu. Rev. Cell Dev. Biol.* **21,** 659–693

27. Eickelberg, O., and Morty, R. E. (2007) Transforming growth factor β/bone morphogenic protein signaling in pulmonary arterial hypertension. Remodeling revisited. *Trends Cardiovasc. Med.* **17,** 263–269
28. Goumans, M. J., Lebrin, F., and Valdimarsdottir, G. (2003) Controlling the angiogenic switch. A balance between two distinct TGF-b receptor signaling pathways. *Trends Cardiovasc. Med.* **13,** 301–307
29. Goumans, M. J., Valdimarsdottir, G., Itoh, S., Rosendahl, A., Sideras, P., and ten Dijke, P. (2002) Balancing the activation state of the endothelium via two distinct TGF-β type I receptors. *EMBO J.* **21,** 1743–1753
30. Araoka, T., Abe, H., Tominaga, T., Mima, A., Matsubara, T., Murakami, T., Kishi, S., Nagai, K., and Doi, T. (2010) Transcription factor 7-like 2 (TCF7L2) regulates activin receptor-like kinase 1 (ALK1)/Smad1 pathway for development of diabetic nephropathy. *Mol. Cells* **30,** 209–218
31. Chen, W., Guo, Y., Walker, E. J., Shen, F., Jun, K., Oh, S. P., Degos, V., Lawton, M. T., Tihan, T., Davalos, D., Akassoglou, K., Nelson, J., Pile-Spellman, J., Su, H., and Young, W. L. (2013) Reduced mural cell coverage and impaired vessel integrity after angiogenic stimulation in the Alk1-deficient brain. *Arterioscler. Thromb. Vasc. Biol.* **33,** 305–310
32. Islam, S. S., Mokhtari, R. B., Kumar, S., Maalouf, J., Arab, S., Yeger, H., and Farhat, W. A. (2013) Spatio-temporal distribution of Smads and role of Smads/TGF-β/BMP-4 in the regulation of mouse bladder organogenesis. *PLoS One* **8,** e61340
33. Abe, H., Tominaga, T., Matsubara, T., Abe, N., Kishi, S., Nagai, K., Murakami, T., Araoka, T., and Doi, T. (2012) Scleraxis modulates bone morphogenetic protein 4 (BMP4)-Smad1 protein-smooth muscle α-actin (SMA) signal transduction in diabetic nephropathy. *J. Biol. Chem.* **287,** 20430–20442
34. Mima, A., Abe, H., Nagai, K., Arai, H., Matsubara, T., Araki, M., Torikoshi, K., Tominaga, T., Iehara, N., Fukatsu, A., Kita, T., and Doi, T. (2011) Activation of Src mediates PDGF-induced Smad1 phosphorylation and contributes to the progression of glomerulosclerosis in glomerulonephritis. *PLoS One* **6,** e17929
35. Jeffery, T. K., Upton, P. D., Trembath, R. C., and Morrell, N. W. (2005) BMP4 inhibits proliferation and promotes myocyte differentiation of lung fibroblasts via Smad1 and JNK pathways. *Am. J. Physiol. Lung Cell. Mol. Physiol.* **288,** L370–L378
36. Matsubara, T., Abe, H., Arai, H., Nagai, K., Mima, A., Kanamori, H., Sumi, E., Takahashi, T., Matsuura, M., Iehara, N., Fukatsu, A., Kita, T., and Doi, T. (2006) Expression of Smad1 is directly associated with mesangial matrix expansion in rat diabetic nephropathy. *Lab. Invest.* **86,** 357–368
37. López-Casillas, F., Cheifetz, S., Doody, J., Andres, J. L., Lane, W. S., and Massagué, J. (1991) Structure and expression of the membrane proteoglycan betaglycan, a component of the TGF-β receptor system. *Cell* **67,** 785–795
38. Dong, M., How, T., Kirkbride, K. C., Gordon, K. J., Lee, J. D., Hempel, N., Kelly, P., Moeller, B. J., Marks, J. R., and Blobe, G. C. (2007) The type III TGF-β receptor suppresses breast cancer progression. *J. Clin. Invest.* **117,** 206–217
39. Gordon, K. J., Dong, M., Chislock, E. M., Fields, T. A., and Blobe, G. C. (2008) Loss of type III transforming growth factor β receptor expression increases motility and invasiveness associated with epithelial to mesenchymal transition during pancreatic cancer progression. *Carcinogenesis* **29,** 252–262
40. Althaus, M., Pichl, A., Clauss, W. G., Seeger, W., Fronius, M., and Morty, R. E. (2011) Nitric oxide inhibits highly selective sodium channels and the Na^+/K^+-ATPase in H441 cells. *Am. J. Respir. Cell Mol. Biol.* **44,** 53–65
41. Czock, D., Keller, F., Rasche, F. M., and Häussler, U. (2005) Pharmacokinetics and pharmacodynamics of systemically administered glucocorticoids. *Clin. Pharmacokinet.* **44,** 61–98
42. Hübner, M., Hochhaus, G., and Derendorf, H. (2005) Comparative pharmacology, bioavailability, pharmacokinetics, and pharmacodynamics of inhaled glucocorticosteroids. *Immunol Allergy Clin. North Am.* **25,** 469–488
43. Ponce-Castañeda, M. V., Esparza-López, J., Vilchis-Landeros, M. M., Mendoza, V., and López-Casillas, F. (1998) Murine betaglycan primary structure, expression and glycosaminoglycan attachment sites. *Biochim. Biophys. Acta* **1384,** 189–196
44. Morty, R. E., Nejman, B., Kwapiszewska, G., Hecker, M., Zakrzewicz, A., Kouri, F. M., Peters, D. M., Dumitrascu, R., Seeger, W., Knaus, P., Schermuly, R. T., and Eickelberg, O. (2007) Dysregulated bone morphogenetic protein signaling in monocrotaline-induced pulmonary arterial hypertension. *Arterioscler. Thromb. Vasc. Biol.* **27,** 1072–1078
45. Zakrzewicz, A., Kouri, F. M., Nejman, B., Kwapiszewska, G., Hecker, M., Sandu, R., Dony, E., Seeger, W., Schermuly, R. T., Eickelberg, O., and Morty, R. E. (2007) The transforming growth factor-β/Smad2,3 signalling axis is impaired in experimental pulmonary hypertension. *Eur. Respir J.* **29,** 1094–1104
46. Dennler, S., Itoh, S., Vivien, D., ten Dijke, P., Huet, S., and Gauthier, J. M. (1998) Direct binding of Smad3 and Smad4 to critical TGF β-inducible elements in the promoter of human plasminogen activator inhibitor-type 1 gene. *EMBO J.* **17,** 3091–3100
47. Korchynskyi, O., and ten Dijke, P. (2002) Identification and functional characterization of distinct critically important bone morphogenetic protein-specific response elements in the Id1 promoter. *J. Biol. Chem.* **277,** 4883–4891
48. Goumans, M. J., Valdimarsdottir, G., Itoh, S., Lebrin, F., Larsson, J., Mummery, C., Karlsson, S., and ten Dijke, P. (2003) Activin receptor-like kinase (ALK)1 is an antagonistic mediator of lateral TGFβ/ALK5 signaling. *Mol. Cell* **12,** 817–828
49. Lebrin, F., Goumans, M. J., Jonker, L., Carvalho, R. L., Valdimarsdottir, G., Thorikay, M., Mummery, C., Arthur, H. M., and ten Dijke, P. (2004) Endoglin promotes endothelial cell proliferation and TGF-β/ALK1 signal transduction. *EMBO J.* **23,** 4018–4028
50. Oh, S. P., Seki, T., Goss, K. A., Imamura, T., Yi, Y., Donahoe, P. K., Li, L., Miyazono, K., ten Dijke, P., Kim, S., and Li, E. (2000) Activin receptor-like kinase 1 modulates transforming growth factor-β 1 signaling in the regulation of angiogenesis. *Proc. Natl. Acad. Sci. U.S.A.* **97,** 2626–2631
51. Alejandre-Alcázar, M. A., Michiels-Corsten, M., Vicencio, A. G., Reiss, I., Ryu, J., de Krijger, R. R., Haddad, G. G., Tibboel, D., Seeger, W., Eickelberg, O., and Morty, R. E. (2008) TGF-β signaling is dynamically regulated during the alveolarization of rodent and human lungs. *Dev. Dyn.* **237,** 259–269
52. Morris, E., Chrobak, I., Bujor, A., Hant, F., Mummery, C., Ten Dijke, P., and Trojanowska, M. (2011) Endoglin promotes TGF-β/Smad1 signaling in scleroderma fibroblasts. *J. Cell. Physiol.* **226,** 3340–3348
53. Upton, P. D., Davies, R. J., Trembath, R. C., and Morrell, N. W. (2009) Bone morphogenetic protein (BMP) and activin type II receptors balance BMP9 signals mediated by activin receptor-like kinase-1 in human pulmonary artery endothelial cells. *J. Biol. Chem.* **284,** 15794–15804
54. Scharpfenecker, M., Kruse, J. J., Sprong, D., Russell, N. S., Ten Dijke, P., and Stewart, F. A. (2009) Ionizing radiation shifts the PAI-1/ID-1 balance and activates notch signaling in endothelial cells. *Int. J. Radiat Oncol. Biol. Phys.* **73,** 506–513
55. Girerd, B., Montani, D., Coulet, F., Sztrymf, B., Yaici, A., Jaïs, X., Tregouet, D., Reis, A., Drouin-Garraud, V., Fraisse, A., Sitbon, O., O'Callaghan, D. S., Simonneau, G., Soubrier, F., and Humbert, M. (2010) Clinical outcomes of pulmonary arterial hypertension in patients carrying an ACVRL1 (ALK1) mutation. *Am. J. Respir Crit. Care Med.* **181,** 851–861
56. Long, L., Crosby, A., Yang, X., Southwood, M., Upton, P. D., Kim, D. K., and Morrell, N. W. (2009) Altered bone morphogenetic protein and transforming growth factor-β signaling in rat models of pulmonary hypertension. Potential for activin receptor-like kinase-5 inhibition in prevention and progression of disease. *Circulation* **119,** 566–576
57. Yang, X., Long, L., Southwood, M., Rudarakanchana, N., Upton, P. D., Jeffery, T. K., Atkinson, C., Chen, H., Trembath, R. C., and Morrell, N. W. (2005) Dysfunctional Smad signaling contributes to abnormal smooth muscle cell proliferation in familial pulmonary arterial hypertension. *Circ. Res.* **96,** 1053–1063
58. Southwood, M., Jeffery, T. K., Yang, X., Upton, P. D., Hall, S. M., Atkinson, C., Haworth, S. G., Stewart, S., Reynolds, P. N., Long, L., Trembath, R. C., and Morrell, N. W. (2008) Regulation of bone morphogenetic protein signalling in human pulmonary vascular development. *J. Pathol.* **214,** 85–95
59. Geraci, M. W., Moore, M., Gesell, T., Yeager, M. E., Alger, L., Golpon, H., Gao, B., Loyd, J. E., Tuder, R. M., and Voelkel, N. F. (2001) Gene expression patterns in the lungs of patients with primary pulmonary hypertension. A

gene microarray analysis. *Circ. Res.* **88,** 555–562
60. Price, L. C., Montani, D., Tcherakian, C., Dorfmüller, P., Souza, R., Gambaryan, N., Chaumais, M. C., Shao, D. M., Simonneau, G., Howard, L. S., Adcock, I. M., Wort, S. J., Humbert, M., and Perros, F. (2011) Dexamethasone reverses monocrotaline-induced pulmonary arterial hypertension in rats. *Eur. Respir. J.* **37,** 813–822
61. Blaney Davidson, E. N., Remst, D. F., Vitters, E. L., van Beuningen, H. M., Blom, A. B., Goumans, M. J., van den Berg, W. B., and van der Kraan, P. M. (2009) Increase in ALK1/ALK5 ratio as a cause for elevated MMP-13 expression in osteoarthritis in humans and mice. *J. Immunol.* **182,** 7937–7945
62. Bijlsma, J. W., Berenbaum, F., and Lafeber, F. P. (2011) Osteoarthritis. An update with relevance for clinical practice. *Lancet* **377,** 2115–2126
63. Collins, J. J., Kunzmann, S., Kuypers, E., Kemp, M. W., Speer, C. P., Newnham, J. P., Kallapur, S. G., Jobe, A. H., and Kramer, B. W. (2013) Antenatal glucocorticoids counteract LPS changes in TGF-β pathway and caveolin-1 in ovine fetal lung. *Am. J. Physiol. Lung. Cell Mol. Physiol.* **304,** L438–L444
64. Collins, J. J., Kuypers, E., Nitsos, I., Jane Pillow, J., Polglase, G. R., Kemp, M. W., Newnham, J. P., Cleutjens, J. P., Frints, S. G., Kallapur, S. G., Jobe, A. H., and Kramer, B. W. (2012) LPS-induced chorioamnionitis and antenatal corticosteroids modulate Shh signaling in the ovine fetal lung. *Am. J. Physiol. Lung Cell. Mol. Physiol.* **303,** L778–L787
65. McDevitt, T. M., Gonzales, L. W., Savani, R. C., and Ballard, P. L. (2007) Role of endogenous TGF-β in glucocorticoid-induced lung type II cell differentiation. *Am. J. Physiol. Lung. Cell Mol. Physiol.* **292,** L249–L257
66. Gu, L., Zhu, Y. J., Guo, Z. J., Xu, X. X., and Xu, W. B. (2004) Effect of IFN-γ and dexamethasone on TGF-β1-induced human fetal lung fibroblast-myofibroblast differentiation. *Acta Pharmacol. Sin.* **25,** 1479–1488
67. Phan, S. H. (2012) Genesis of the myofibroblast in lung injury and fibrosis. *Proc. Am. Thorac. Soc.* **9,** 148–152
68. Josephson, M. B., Jiao, J., Xu, S., Hu, A., Paranjape, C., Grunstein, J. S., Grumbach, Y., Nino, G., Kreiger, P. A., McDonough, J., and Grunstein, M. M. (2012) IL-13-induced changes in endogenous glucocorticoid metabolism in the lung regulate the proasthmatic response. *Am. J. Physiol. Lung. Cell Mol. Physiol.* **303,** L382–L390
69. Yao, H., and Rahman, I. (2012) Role of histone deacetylase 2 in epigenetics and cellular senescence. Implications in lung inflammaging and COPD. *Am. J. Physiol. Lung Cell. Mol. Physiol.* **303,** L557–L566
70. Rosendahl, A., Pardali, E., Speletas, M., Ten Dijke, P., Heldin, C. H., and Sideras, P. (2002) Activation of bone morphogenetic protein/Smad signaling in bronchial epithelial cells during airway inflammation. *Am. J. Respir. Cell Mol. Biol.* **27,** 160–169

9. Acknowledgements

In this last part of my thesis I want to sincerely thank all those who supported and encouraged me throughout this scientific project, especially, the whole “Morty Laboratory” (Simone Becker, Gero Niess, Łukasz Wujak, and Elpidoforos Sakkas) for sharing their deep scientific insights into molecular pulmonary biology and pathology.

I want to thank Prof. Dr. med. Werner Seeger for his support and giving insights into his unique approach to translational pulmonary medicine. I believe he has managed to create a unique pulmonary research center in which basic pulmonary research and patient care coexist in a very friendly and productive relationship.

I want to thank my direct supervisor Rory E. Morty, MD, for all the coffees during which we had endless discussions about “Smad-binding here and there” and showing great support throughout the whole project. I would also like to thank Rory for making it possible for me to present this project at two major international conferences which further encouraged me to develop a deep interest into basic science.

I want to thank Peter Rauschkolb for sharing his knowledge on how to isolate primary adult mouse fibroblasts from mouse lungs.

I want to thank Fritz and Maja who live in Zurich and let me write part of this thesis in their flat!

I want to thank Alexander Nave without whom I would never have started this project in Rory’s Lab and without whom all of this would only have been half as much fun!

Finally, I want to thank my whole family, especially both my parents, who always gave their full support during the whole time of my thesis. Without them, all of this would not have been possible!

THANK YOU ALL!

10. Appendix

Table 10.1 List of primary mouse/human antibodies

Primary	Host	Dilution	Company	Catalog number
anti-phospho Smad1/5/8	rabbit	1:800	Cell Signaling Technology	#9511
anti-phospho Smad2	rabbit	1:1000	Cell Signaling Technology	#3101
anti-phospho Smad3	rabbit	1:1000	Cell Signaling Technology	#9520
anti-total Smad1	rabbit	1:1000	Cell Signaling Technology	#9743
anti-total Smad2	mouse	1:1000	Cell Signaling Technology	#3103
anti-total Smad2/3	rabbit	1:1000	Cell Signaling Technology	#3102
anti-Tgfbr3	rabbit	1:1000	Cell Signaling Technology	#2519
anti-β-actin	rabbit	1:1000	Cell Signaling Technology	#4967
anti-smooth muscle myosin (MYH11)	rabbit	1:1000	Abcam	ab53219
anti-α-smooth muscle actin (ACTA2)	rabbit	1:1000	Sigma	A-2547

Table 10.2 List of secondary antibodies

Secondary	Host	Dilution	Company	Catalog number
Peroxidase-conjugated anti-rabbit IgG	goat	1:3000	Thermofisher Scientific	rb:31640
Peroxidase-conjugated anti-mouse IgG	goat	1:3000	Thermofisher Scientific	ms:31450

Table 10.3 List of mouse primers for quantitative real-time PCR

Gene name	Forward primer [5′-3′]	Reverse Primer [5′-3′]	Amplification size [bp]	Number of cycles	Annealing temperature [°C]
tgfbr3	ATGGCAGTGACATCCCACCACAT	AGAACGGTGAAGCTCTCCATCA	152	45	60.0
acvrl1	CACCTACATGTGGAGATCT	CGATATCCAGGTAATCGCTG	160	45	60.0
smad1	GCCTCTGGAATGCTGTGAGTTCCCA	GAGCCAGAAGGCTGTGCTGAGCA	152	45	60.0
gapdh	ATGGTGAAGGTCGGTGTGAA	TCATACTGGAACATGTAGACC	143	45	60.0

Table 10.4 List of mouse small interfering RNA

Gene name	Company	Catalog number
tgfbr3	Santa Cruz Biotechnology, Inc., USA	sc-40225
smad1	Santa Cruz Biotechnology, Inc., USA	sc-40213
scrambled siRNA	Ambion® Life Technologies™, USA	AM-4611